Structure-Function Studies of the Sodium-Calcium Exchanger Isoforms, NCX1 and NCX2

By

Danielle de Moissac

A thesis submitted to the Faculty of Graduate Studies,
in partial fulfillment of the requirements for the Degree of

DOCTOR OF PHILOSOPHY

Department of Physiology

Faculty of Medicine

University of Manitoba

June 2009

© Danielle de Moissac

TABLE OF CONTENTS

Page

Dédicace……...……...iv

Acknowledgements…….....v

List of Figures and Tables……vi

List of abbreviations……...viii

Abstract……..1

1. Review of the literature

1.1 Introduction…….....4

1.2 NCX transport and ionic regulation……...5

1.3 NCX topology and transmembrane domains……7

1.4 NCX1 regulatory domains

1.4.1 The XIP region…… 13

1.4.2 The Ca^{2+}- binding domains ……..16

1.4.3 Phosphorylation……21

1.5 NCX isoforms and splice variants

1.5.1 NCX genes……22

1.5.2 Unique regulatory profiles……24

1.5.3 NCX localization…… 25

1.5.4 NCX2 …….. 27

1.5.5 NCX3 …….. 29

1.5.6 CALX……30

1.6 NCX in the heart

1.6.1 Physiological function…… 31

1.6.2 NCX1.1 knock-out mice……...……33

1.6.3 NCX overexpression…… 35

1.6.4 NCX and cardiovascular disease…….. ……35

1.7 NCX in neuronal and muscular tissues

1.7.1 Physiological function…….....38

1.7.2 NCX and neurological conditions…… 40

1.8 NCX in the kidney and the vasculature……41
1.9 Inhibition of NCX
1.9.1 Cations…… 42
1.9.2 KB-R7943…… 43
1.9.3 SEA0400…….. 44
1.9.4 New NCX inhibitors…… 45
1.10 Rationale for this study…… 46

2. Hypothesis……..48

3. Materials and methods
3.1 Construction of chimaeric exchangers……..49
3.2 Site-directed mutagenesis……..……. 52
3.3 cRNA synthesis……...…53
3.4 Preparation and injection of *Xenopus laevis* oocytes…….....53
3.5 Measurement of NCX exchange activity using
giant, excised patch clamp technique…….....54
3.6 Inhibition of NCX by SEA0400……...…55
3.7 Analysis of data……55

4. Results……57
4.1 Comparison of the mutually exclusive exon region in NCX1
and NCX2…… 58
4.2 Stability of Na^+-dependent inactive state at high Ca^{2+}_i
concentrations in NCX2.1……62
4.3 The role of the region corresponding to the mutually
exclusive exon on Na^+-dependent inactivation in NCX2.1……..65
4.4 Interaction between the mutually exclusive exon
and the XIP region from NCX1……69
4.5 Characterization of the XIP region from NCX2.1……74
4.6 Recovery from Na^+-dependent inactivation……80

5. Discussion……..85

5.1 Similarities between NCX2.1 and NCX1.3 regulatory profiles conferred by residues in the region corresponding to the mutually exclusive exon……....90

5.2 Role of the region corresponding to the mutually exclusive exon in NCX2.1 in maintaining Na^+-dependent inactivation……..93

5.3 Interaction between the XIP region and the region corresponding to the mutually exclusive exon in NCX1 required for Na^+-dependent inactivation……...94

5.4 The XIP region and Na^+-dependent inactivation in NCX2.1……...96

5.5 NCX2.1 regulatory profile confers neuroprotective properties……98

6. Future Studies…...……100

7. Conclusions……..102

8. References……103

DÉDICACE

Je dédie cette thèse et tous les travaux qui y sont associés à ma famille,

qui a partagé avec moi les hauts et les bas de la recherche et des études doctorales.

A Richard, merci pour ton appui moral tout au long de ce parcours. Tu as su

m'encourager à persévérer, à croire en moi-même et à surmonter ce défi.

Je n'aurais pu y arriver sans toi, et j'en suis très reconnaissante.

A Luc, Eric et Myriam, merci de votre amour et humour,

qui m'ont bien diverti quand j'en avais besoin

et qui m'ont rappelé que les choses

les plus importantes dans la vie

sont aussi les plus simples.

Je vous aime.

ACKNOWLEDGEMENTS

This thesis would not have been possible without the support of my supervisor, Dr. Larry Hryshko, and colleagues in his lab. To Larry, thank you for believing in me and supporting me throughout my studies. I have greatly appreciated your understanding and compassion as I struggled to manage work, studies and family life. To Mark, Alex and Hoa, your willingness to guide and assist me in my research has been essential to the success of this project, and I am very grateful. To Kristy, thank you for the many hours spent working together at the bench, your friendship has made it enjoyable and memorable. To Catherine, Daron, Raissa and Heather, I hope your time in the lab as students will benefit you in your personal endeavours. To my committee members, Dr. Dixon, Dr. Kardami, and Dr. Pierce, thank you for your encouragement and constructive suggestions which have made this such a learning experience.

Je tiens à remercier le Collège universitaire de Saint-Boniface pour l'appui financier lors de mon congé d'étude, ce qui m'a permis de faire mes recherches à temps plein. A mes collègues de travail, merci pour le soutien moral tout au long de cette démarche. C'est un plaisir de travailler parmi vous.

I am also grateful for the funding received from the Canadian Institute of Health Research, which has allowed me to focus on my studies and fully appreciate the world of research.

LIST OF FIGURES AND TABLE

Page

Figure 1. Topological model of the Na^+-Ca^{2+} exchanger……..9

Figure 2. Models of NCX1 helix packing and dimerization……...12

Figure 3. Model of the intact NCX exchanger based on high resolution NMR spectroscopy in the Ca^{2+} bound form……18

Figure 4. Structure of the CBD2 Ca^{2+}-binding site…….19

Figure 5. Na^+-Ca^{2+} exchange and excitation-contraction coupling…….31

Figure 6. Representation of splicing protocol for chimaeric construction……..50

Figure 7. Sequence comparison and nomenclature for chimaeric constructs….59

Figure 8. Ca^{2+}_i-dependence of NCX1-mediated outward currents…….61

Figure 9. Ca^{2+}_i-dependence of NCX2-mediated outward currents…….64

Figure 10. Ca^{2+}_i-dependence of NCX2.1 chimaera-mediated outward currents..66

Figure 11. Inhibition of outward exchange currents in the presence of SEA0400…….68

Figure 12. Ca^{2+}_i-dependence of NCX2 double chimaeras for outward exchange currents……..72

Figure 13. Ca^{2+}_i-dependence of Fss for NCX2 double chimaeras……73

Figure 14. Ca^{2+}_i-dependence of NCX1.4 and its XIP2 chimaera for outward exchange currents and Fss……...75

Figure 15. Ca^{2+}_i-dependence of NCX1.3 and its XIP2 chimaera for outward exchange currents and Fss…….. 77

Figure 16. Ca^{2+}_i-dependence of NCX1-2A and N1-2A-XIP2 chimaeras for outward exchange currents and Fss……...79

Figure 17. Rate of recovery from Na^+-dependent inactivation…….82

Figure 18. Comparison of recovery rates from inactivation for NCX1.3 chimaeric and point mutation constructs…… 83

Table I. Values for fractional steady state (Fss) and rate of recovery for NCX isoforms, NCX1 chimaeric and point mutation constructs……83

LIST OF ABBREVIATIONS

-/-	knockout
α	alpha
AD	anoxic depolarization
AKAP	a kinase anchoring protein
AMPA	α-amino-3-hydroxyl-5-methyl-4-isoxazole-propionate
Asn	asparagine
ATG	adenine-tyrosine-guanine
ATP	adenosine triphosphate
ATPase	adenosine triphosphatase
β	beta
Ba^{2+}	barium
BHK	baby hamster kidney cells
BSA	bovine serum albumin
c-AMP	cyclic adenosine monophosphate
C-terminal	carboxy terminal
$Ca^{2+}{}_i$	intracellular calcium
CaCA	Ca^{2+}/cation antiporter
$CaCl_2$	calcium chloride
$CaCO_3$	calcium carbonate
CALX	Na^+-Ca^{2+} exchanger in *Drosophila melanogaster*
CamKII	Ca^{2+}/calmodulin-dependent protein kinases
$Ca(NO_3)_2$	calcium nitrate
CAP	5' cap nucleotide
CBD1/2	Ca^{2+} binding domain 1 and 2
Cd^{2+}	cadmium
CICR	calcium induced calcium release
CLD	catenin-like domain
Co^{2+}	cobalt
Cre/loxP	cyclization recombination/ locus of X-over P1
cRNA	complementary ribonucleic acid
DHPR	dihydropyridine receptor
DNA	deoxyribonucleic acid
DNase	deoxyribonuclease
ECC	excitation-contraction coupling
EGTA	ethylene glycol tetraacetic acid
FRET	fluorescence resonance energy transfer
Fss	fractional steady state
GC	guanine-cytosine
H^+	hydrogen ion
HEPES	4-(2-hydroxyethyl)-1-piperazineethanesulfonic acid
I_1	Na^+-dependent inactivation
I_2	Ca^{2+}-dependent inactivation
I_{Ca}	calcium current
I_{k1}	inward rectifier potassium current

I_{ko}	outward potassium current
JSR	junctional sarcoplasmic reticulum
K^+	potassium
K_2HPO_4	potassium phosphate
KB-R7943	2-(2-[4-(4-nitrobenzyloxy)phenyl]ethyl)-isothiourea methane-sulphonate
KCl	potassium chloride
kDa	kilo Daltons
KOH	potassium hydroxide
La^{3+}	lanthanum
Li^+	lithium
LiOH	lithium hydroxide
MES	2-(N-morpholino) ethanesulfonic acid
Mg^{2+}	magnesium
$MgCl_2$	magnesium chloride
$Mg(OH)_2$	magnesium hydroxide
$MgSO_4$	magnesium sulphate
mM	millimolar
mmol/L	millimoles/ litre
Mn^{2+}	manganese
mRNA	messenger ribonucleic acid
ms	millisecond
mV	millivolts
N-linked	asparagine linked
N-terminal	amino terminal
Na^+_i	intracellular sodium
NaCl	sodium chloride
Na^+/H^+	sodium-hydrogen
$NaHCO_3$	sodium bicarbonate
Na^+/K^+	sodium-potassium
NCKX	sodium-calcium-potassium exchanger
NCX	sodium-calcium exchanger
Nd^{3+}	neodymium
Ni^{2+}	nickel
NMDA	N-methyl-D-aspartic acid
NMR	nuclear magnetic resonance
NTP	nucleoside triphosphate
P	statistical probability
PCR	polymerase chain reaction
PIP_2	phosphatidylinositol 4, 5-bisphosphate
PKA	protein kinase A
PKC	protein kinase C
PMCA	plasma membrane calcium adenosine triphosphatase
pMCAO	permanent middle cerebral artery occlusion
PP1	protein phosphatase 1
PP2A	protein phosphatase 2A

RT	room temperature
RYR	ryanodine receptor
s	seconds
SDS-PAGE	sodium dodecyl sulphate polyacrylamide gel electrophoresis
SEA0400	2-(-4-[(2,5-difluorophenyl)methoxy]phenoxy)-5-ethoxyaniline
sec^{-1}	per second
SEM	standard error of measurement
SERCA	sarcoplasmic reticulum calcium adenosine triphosphatase
shRNA	short hairpin ribonucleic acid
SR	sarcoplasmic reticulum
Sr^{2+}	strontium
TEA	Tris/ethylenediaminetetraacetic acid/acetic acid
Thr	threonine
Tm^{3+}	thulium
TMS	transmembrane segment
μM	micromolar
XIP	eXchanger inhibitory peptide

ABSTRACT

The sodium-calcium exchanger (NCX) is a countertransporter of Na^+ and Ca^{2+} across membranes of most cell types. It has been identified as an essential component of Ca^{2+} homeostasis in physiological and disease conditions in both cardiovascular and neurological settings. The exchanger not only transports Na^+ and Ca^{2+}, but is also regulated by these ions. Although ionic regulatory profiles differ between NCX isoforms, similar regulatory domains have been identified in the large cytoplasmic loop of the exchangers. Previous structure-function studies have determined key residues within these domains, particularly in the eXchanger Inhibitory Peptide region (XIP) and the Ca^{2+} binding domains (CBD1/2), which have a direct impact on ionic regulation of the outward exchange currents, mediating Ca^{2+} flux. Recent structural studies of the Ca^{2+} binding domains of NCX1 suggest a mechanism by which Ca^{2+} binding would not only be essential for activation of current but may also influence Na^+-dependent inactivation. The alternative splice region is located within the Ca^{2+} binding domain and may play a role in mediating these regulatory phenotypes. Alternatively spliced variants of NCX1 are often expressed in a tissue-specific manner and differ according to the level of development. Previous studies have demonstrated that specific combinations of the mutually-exclusive and cassette exons are associated with profound effects on ionic regulation in NCX1. While no alternative splicing has been identified for NCX2, the region corresponding to the alternative splice region may be a critical determinant of the unique ionic regulatory profile exhibited by this exchanger. This study focuses on examining the mechanisms by which specific regulatory domains modulate exchange activity in two isoforms, NCX1 and NCX2.

To investigate the role of the mutually exclusive exons in NCX1 (A and B), their analogous counterpart in NCX2, and their association with the XIP region, chimeric exchangers were constructed with single-exon and combination interchanges with the XIP regions from NCX1 and NCX2. Single and double amino acid substitutions were also done to determine the role of specific residues within these two regions. Chimaeric and mutant constructs were expressed in *Xenopus* oocytes and outward Na^+-Ca^{2+} exchange activity was assessed using the giant, excised patch clamp technique. The Ca^{2+} dependance of Na^+-dependent inactivation was analyzed, as well as rate of recovery from inactivation. Substitution of the region corresponding to the mutually exclusive exon from NCX2 with either exons A or B from NCX1 greatly reduced the rate and extent of Na^+-dependent inactivation, independently of intracellular Ca^{2+} concentrations. However, replacement of both the region corresponding to the mutually exclusive exon and the XIP region from NCX2 with the analogous regions from NCX1.4 re-establishes a wild-type NCX2 profile. Moreover, this construct gains an additional phenotype of NCX1.4, that of alleviation of Na^+-dependent inactivation at higher $[Ca^{2+}_i]$. The first mutually exclusive exon is therefore critical in determining Na^+ and Ca^{2+}-dependent regulatory properties in NCXs and appears to interact with other regulatory regions of the cytoplasmic loop (i.e. the XIP region) to achieve distinctive regulatory phenotypes.

Chimaeric exchangers substituting the XIP region of NCX1.4 with the corresponding region from NCX2.1 caused an apparent loss of Na^+-dependent inactivation, whereas a reduction in the extent of inactivation and a 15-fold increase in the rate of recovery from this inactivation were observed in the NCX1.3–XIP2 chimaera. Similarly, substitution of charged amino acids within the XIP region in NCX1.3 caused a

slight increase in the rate of recovery, equivalent to that observed for NCX2.1. Thus non-conserved residues in the XIP region may be essential in maintaining the structural stability of the Na^+-dependent inactive state of NCX1. Furthermore, the XIP region may interact with other regulatory domains of the protein, such as the mutually exclusive exon, thereby contributing to the structure-function relationship as well as the regulatory phenotype of each Na^+-Ca^{2+} exchanger variant and isoform. As NCX1 and NCX2 are expressed in a cell and tissue specific manner, examination of their ionic regulatory domains may help to elucidate the mechanisms by which NCX exchange activity is modulated in response to specific cellular environments, both physiologically and pathophysiologically, and may provide an explanation for the requirement of specifically regulated NCX variants in mammalian systems.

1. REVIEW OF THE LITERATURE

1.1 Introduction

Sodium-calcium exchangers (NCX) are members of the large Ca^{2+}/cation (CaCA) antiporter superfamily, whose main function is Ca^{2+} transport across membranes. These counter-transporters have been identified in a variety of organisms, ranging from bacteria and yeast to plant and animal species. NCX has been cloned in invertebrates such as the common fruit fly and squid as well as members of most classes of vertebrates, such as trout, frog, chicken and 16 mammalian species (23; 134; 137). Although sodium-calcium transport was first described in the heart (208) and in the squid axon (10) in the late 1960's, the actual NCX1 protein was cloned two decades later from canine heart (160). The exchanger's function was initially shown to be in transsarcolemmal Ca^{2+} efflux, allowing for rapid Ca^{2+} transport during excitation-contraction coupling and restoration of cellular Ca^{2+} homeostasis (22; 66; 116).

NCX is present in the plasma membrane of most cells and exchanges three Na^+ for one Ca^{2+}, making this an electrogenic process (15; 72; 179; 197). The physiological role of NCX is primarily Ca^{2+} efflux from the cell, but as this process is driven by the cellular Na^+ gradient produced by the Na^+/K^+ pump, NCX-mediated transport is directly affected by changes in the intracellular ionic environment. According to the proposed consecutive model for NCX transport under physiological conditions, extracellular Na^+ binds to the transport site, is internalized and released inside the cell. Ca^{2+} then binds to the same translocation site, is internalized into the membrane and released to the extracellular space (63). However, when intracellular Na^+ levels increase, as observed under pathophysiological conditions such as hypoxia, ischemia/reperfusion injury and

heart failure (16; 106; 152; 153; 215; 240), NCX functions more frequently in its reverse mode, causing Ca^{2+} influx. This inward flow of Ca^{2+} can contribute to calcium overload, which may ultimately lead to myocardial damage resulting from arrhythmogenesis (187), cellular ultrastructural changes, disruption of membrane integrity and mitochondrial dysfunction (13). Dysregulation of cellular Ca^{2+} homeostasis is also a common feature in a variety of neurological disorders, including stroke, epilepsy and trauma, where activation of Ca^{2+}-dependent proteases, such as calpains, and activation of nitric oxide production lead to excitotoxic neuronal death (6; 106). Inhibition of the reverse mode of action of NCX may be useful in maintaining physiological levels of Ca^{2+} in the cell and protecting it from death (118; 136; 138). Investigative efforts have focused on the structure, function and regulation of NCX, as it has become a potential therapeutic target in cardiovascular and neurological diseases. Herein, the latest findings pertaining to NCX transport and ionic regulation, the proposed topological model, the regulatory domains, the differences between the three mammalian isoforms and their splice variants, the role of NCX in physiological and pathophysiological conditions in both cardiovascular and neurological settings, as well as the cardio and neuro-protective effects of NCX inhibition will be reviewed.

1.2 NCX transport and ionic regulation

NCX has the ability to function in two transport modes (66). The primary mode is the forward or inward mode, where Na^{+} enters the cell in exchange for Ca^{2+} efflux. This mode is essential for the restoration of baseline Ca^{2+} levels following a muscular contraction or neuronal activation. The second mode of transport is the reverse or

outward mode, where Ca^{2+} enters the cell as a consequence of Na^{+} efflux. The activation of a specific mode of exchange is dependent on the membrane potential and on the existing Na^{+} and Ca^{2+} gradients across the membrane, and therefore is intimately regulated by cellular ionic conditions. Furthermore, although NCX's function is Na^{+} and Ca^{2+} transport, the exchanger is also regulated by these ions (61; 73; 142; 143). Na^{+}-dependent inactivation (I_1) is a partial inactivation of outward exchange current and occurs when Na^{+} is applied to the intracellular surface of the cell membrane (65). Initially, outward currents rapidly achieve a peak level, but a transition to the inactive state may occur when the Na^{+}-binding sites on the cytoplasmic side of the protein become fully loaded, potentially causing a conformational change rendering the exchanger inactive. Although the physiological importance of Na^{+}-dependent inactivation is not well understood, it could provide a natural defence mechanism minimizing Ca^{2+} entry via the reverse mode when intracellular Na^{+} levels are high, as seen during ischemia.

Calcium-dependent regulation (I_2) also plays an important role in the regulation of NCX, as it is not only required for activation of exchange activity but also modulation of Na^{+}-dependent inactivation (64; 121; 143). I_2 inactivation occurs in the absence of cytoplasmic Ca^{2+}, but can be reversed by the addition of submicromolar concentrations of free Ca^{2+} intracellularly, as occurs physiologically following depolarization in muscle and neural tissues. The binding of regulatory Ca^{2+} causes a conformational rearrangement, allowing for exchange activity and efficient extrusion of Ca^{2+} (163). High levels of cytoplasmic Ca^{2+} have a secondary effect on outward mode currents, where a decrease in the extent of Na^{+}-dependent inactivation is observed in NCX1 variants expressed in

excitable tissues (38). For example, at regulatory Ca^{2+} concentrations ranging from 1-3 μM, Na^{+}-dependent inactivation causes a significant decrease in outward currents, limiting exchange activity and Ca^{2+} influx. Therefore, at low intracellular Ca^{2+} concentrations, Ca^{2+}-dependent regulation may play a role in reducing unnecessary ion transport by limiting Ca^{2+} binding and efflux via the Ca^{2+} transport site, but also reducing Ca^{+2} influx via the reverse mode of action by promoting Na^{+}-dependent inactivation (143). However, when intracellular Ca^{2+} concentrations increase to 10-30 μM, peak outward currents do not degrade significantly and outward flow of Na^{+} is maintained, leading to further Ca^{2+} influx. This may contribute to Ca^{2+} overload and therefore would be detrimental to the cell. A physiological role for this particular regulatory phenotype in excitable tissues has yet to be determined and may be a consequence of prolonged imbalance in the homeostatic cellular environment.

1.3 NCX topology and transmembrane domains

Initial molecular studies of NCX1, performed when the exchanger was first cloned, suggested an open reading frame of 2910 bases encoding for a 970 amino acid protein with a molecular size of 108 kDa (160). Conserved membrane topology, as determined by amino acid sequence comparison between NCX isoforms as well as with other members of the CaCA superfamily, demonstrate two clusters of transmembrane helices joined by a cytoplasmic loop (23). The current topological model, based on further hydropathy analysis, cysteine susceptibility analysis, sulfhydryl modification experiments, immunolocalization and functional measurements (34; 90; 94; 161; 196), proposes a 938 amino acid protein consisting of nine transmembrane segments (TMS)

and a large intracellular loop connecting TMS 5 and TMS 6 (Figure 1). Several regulatory domains have been identified in the cytoplasmic loop (144) and will be discussed in the following sections.

The C-terminal end of the protein is located intracellularly, whereas the N-terminal is located in the extracellular space and appears to be glycosylated at Asn 9 (75). Five other possible *N*-linked glycosylation sites have been identified (160), but these do not appear to be involved in NCX function or regulation (75). NCX also encodes a cleaved signal sequence originally thought to ensure the correct topological orientation of the exchanger in the membrane (36). However, our laboratory and others have demonstrated that deletion of the signal sequence has no impact on NCX ability to integrate into the cellular membrane and mediate current (de Moissac, D. and Hryshko, L.V., unpublished data) (48; 131; 212). More recently, a deletion mutant lacking the last seven residues of the exchanger exhibited impaired targeting to the plasma membrane, suggesting a possible role for the C-terminal end of the protein in membrane integration (172).

The transmembrane domains of NCX are highly conserved amongst Ca^{2+} counter-transporters and appear to be sufficient to mediate the ion transport process in NCX. This has been demonstrated by chymotrypsin digestion or deletion of the large cytoplasmic loop by mutagenesis, which does not inhibit exchange activity but rather causes deregulation (61; 144). Sulfhydryl group modifications have demonstrated that proper folding of the transmembrane regions is also required for exchange activity (182). Amongst the nine transmembrane segments of NCX, two internal repeat sequences

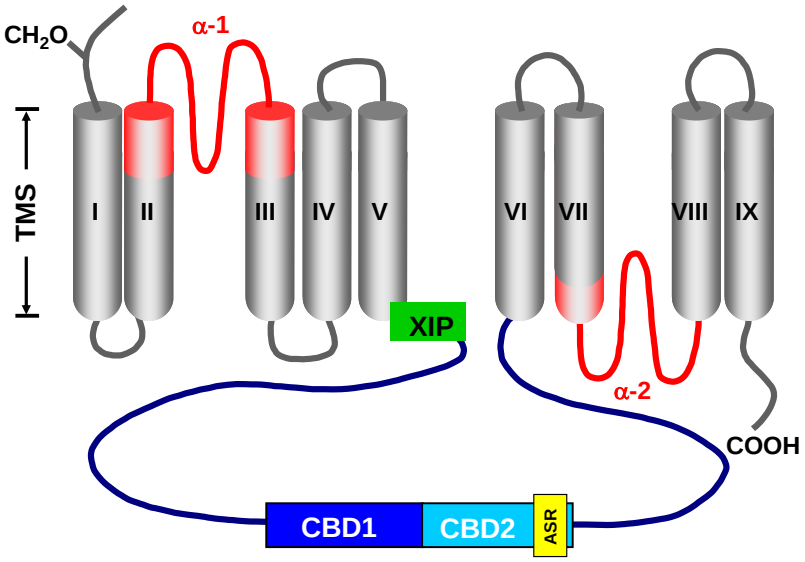


Figure 1. Topological model of the Na^{+}-Ca^{2+} exchanger. Schematic representation of NCX with 9 transmembrane segments (TMS), the α-repeats (red) and a large intracellular loop containing the regulatory domains such as the Ca^{2+} binding domains CBD1 and CBD2 (blue), the alternative splice region (yellow) and the endogenous exchange inhibitory peptide (XIP) region (green). (197), with modifications.

forming re-entrant loops have been identified (159) and labelled as α-repeats. Because of high homology between both α-repeat sequences, it is believed that they are a product of a gene duplication event (22).

The observation that the α-repeat sequences are conserved amongst all sodium-calcium exchangers and are the only regions of sequence conservation with NCKX and other members of the CaCA superfamily is indicative of their importance in exchange activity (158; 228). The α-1 repeat, consisting of TMS 2, the loop joining it to TMS 3 and the first half of TMS 3, faces the extracellular surface of the membrane, whereas the α-2 repeat, located between TMS 7-8, is accessible from the cytoplasmic side (94). Initial site-directed mutagenesis studies of the α-1 repeat demonstrated that it was highly involved in ion transport activity, as mutations at 10 of 19 sites resulted in non-functional exchangers (159). Furthermore, exchange activity was especially sensitive to mutation of hydroxyl-containing residues, suggesting that the ion conduction pathway may be lined with acidic and hydroxyl-containing residues which neutralize the charges of the transported ions (159). Key residues located within the re-entrant loops have also been linked to differential sensitivity of exchanger isoforms to inhibition by Ni^{2+}, a competitive inhibitor for transport Ca^{2+} (95). Although some studies have demonstrated that highly conserved aspartic residues within the α-repeats may influence Ca^{2+}_o affinity (94), this is currently under debate (163; 173). Mutational analysis of TMS2 and TMS3 demonstrate rather that both transmembrane regions are involved in the ion translocation process, with specific residues having an impact on Na^+ affinity, cooperativity of Na^+-binding, or creation of an ideal environment for ion translocation (34; 159; 173).

Association between the two α-repeat segments has been elucidated by electrophoretic analysis of NCX1 protein (214) and cysteine cross-linking experiments (163). Electrophoresis of purified NCX1 protein displays three distinct bands with molecular masses of 160, 120, and 70 kDa. The 70-kDa band is likely a proteolytic fragment (36; 178), whereas the upper bands are evidence for an intramolecular disulfide bond between cysteine residues in different transmembrane segments. Cross-linking between the N-terminal and C-terminal halves of the exchanger, resulting in decreased mobility on SDS-PAGE (196), has also been determined by mutagenesis and biochemical analysis (214).

A model for the secondary structure of the intact exchanger with respect to transmembrane segment positions has recently been proposed, according to cysteine cross-linking studies (Figure 2) (163). It is believed that TMS 1, 2 and 6 are in close proximity (202; 203), with associations between TMS 1-6, 2-6, 2-7, 2-8 and 3-7 (163). This allows for proximity between the α-repeats, which together may form the hydrophilic ion conduction pathway as seen in the aquaporin family of proteins (47; 90; 163; 196).

Recent findings based on intermolecular cysteine cross-linking are suggestive of a higher order oligomerization of NCX (Figure 2) (201). Dimerization may occur along a face of the protein that includes the α-1 and α-2 repeats, along with TMS 1 and 2, and may be involved not only in proper targeting of the protein to the membrane but also formation of a multimeric complex (172). Residues thought to be involved in dimerization would be located in the α-1 repeat and modelled to be at the extracellular surface of TMS2 (94). It has been proposed that these residues exhibit substrate-

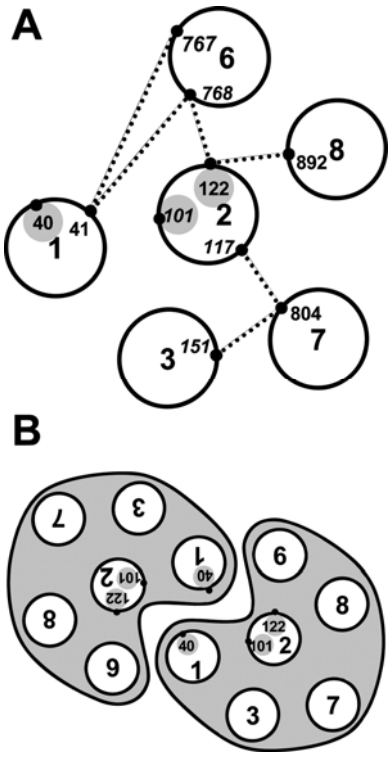


Figure 2. Models of NCX1 helix packing and dimerization. (A) Helix packing model allowing for dimerization between NCX1 monomers at residues 40, 101, or 122. Intramolecular cross-links are shown with dotted lines. Residues capable of forming intermolecular cross-links are highlighted with gray circles. (B) Dimerization model between NCX1 monomers. (201), with permission.

dependent changes in accessibility and could interact with residues in TMS 8 in the presence of transport Na^+, but become more accessible to a nearby NCX molecule in the absence of Na^+ (201). Although the importance of dimerization has yet to be determined, the weak interaction between NCX proteins appears to depend on the conformational state of the exchanger, and could therefore contribute to regulation of NCX transport activity.

1.4 NCX1 regulatory domains

1.4.1 The XIP region

The eXchanger Inhibitory Peptide (XIP) region is a highly basic and aromatic region of 20 amino acids located at the N-terminus of the cytoplasmic loop, immediately following TMS 5. Initial studies suggested that this site, distinct from the Na^+ transport site, was involved in the Na^+-dependent inactivation process but not Ca^{2+}-dependent regulation (144). Its auto-inhibitory properties characteristic of calmodulin binding sites (40; 124; 165) were thought to be through interactions with other regions of the exchanger, as intracellular application of a synthetic peptide, with a sequence identical to the endogenous XIP region, caused inhibition of NCX function (124; 144). Sodium gradient-dependent $^{45}Ca^{2+}$ uptake experiments in the presence of truncated NCX1 XIP peptides demonstrate that very few residues from either end of the peptide can be removed without influencing inhibition, implying that the conformation of the entire peptide is important for inhibitory function (56). Key residues in both the XIP peptide and the endogenous XIP region of NCX1 have been identified by mutational analysis as essential for the inhibitory properties of the exchanger, specifically affecting the rate and

extent of Na^+-dependent inactivation (56; 142; 144). The residues which appear to have a greater influence are either positively charged or aromatic, suggesting that the XIP binding site of the exchanger may have hydrophobic and anionic components. Mutations at specific residues within the endogenous XIP region of NCX1 have been shown to either accelerate the rate of inactivation (F223E, K225Q, Y226T) or completely inhibit inactivation (K229Q, Δ229-232) (142). Furthermore, mutants with an increased rate of inactivation also exhibit a decrease in regulatory Ca^{2+} affinity for activation of outward currents and a reduced suppression of Na^+-dependent inactivation by Ca^{2+}, whereas effects on Ca^{2+} regulation are minimal in mutants causing loss of inactivation (142). This suggests that although the regulatory domains mediating Na^+-dependent inactivation are distinct from Ca^{2+}-dependent regulatory regions, they nonetheless influence each other functionally.

The XIP region is in close proximity to the plasma membrane, and numerous studies have demonstrated that NCX is highly dependent on its immediate membrane environment. Treatment with phospholipases C and D and exposure to unsaturated fatty acids and cholesterol all stimulate NCX exchange activity (114; 177; 180; 181). Initially, it was proposed that the increased anionic surface charge and local lipid disorder may be responsible for the observed decrease in Ca^{2+} affinity under these conditions (181). More recently, it has been suggested that the XIP region associates with membrane phosphatidylinositol 4,5-bisphosphate (PIP_2) through electrostatic interactions and thereby influences NCX activity by preventing formation of the Na^+-dependent inactive state (55; 225). Evidence supporting this hypothesis is that elevated ATP levels, causing an increase in membrane PIP2 content, lead to activation of NCX exchange activity (62).

Binding of the XIP region to PIP_2 may therefore activate the exchanger by preventing XIP interaction with its binding site. In contrast, binding of Na^+ to the transport site may induce a conformational change provoking dissociation of XIP from PIP_2, allowing binding of XIP to its inhibitory site located within the cytoplasmic loop and causing inactivation (62). This is supported by findings that exchangers with mutations in the XIP region which accelerate the rate of inactivation bind poorly to PIP_2 (55). Recently, studies of insulin effects on NCX currents have also implicated XIP interaction with PIP_2 (246), but the precise mechanism by which this occurs has yet to be determined.

The inhibitory binding site of XIP has not been precisely identified, but a few regions of the cytoplasmic loop have been proposed. Initial analysis of the inhibitory effects of XIP on currents mediated by various deletion mutants have shown that deletion of amino acids 240-679 or 562-685, which are located within the cytoplasmic loop, cause loss of Na^+-dependent inactivation (144). Fluorescence titration binding studies initially suggested that the XIP region, being positively charged, could associate with a negatively charged region from amino acid 445-455 (52). This region has since been identified as a Ca^{2+}-binding site in the Ca^{2+} binding domain 1 and is essential for activation of exchange current. According to the proposed 3D model of the CBD1, the negatively charged residues are required for direct binding of Ca^{2+}, and therefore it is unlikely that they would have the capacity of binding both Ca^{2+} and the XIP region simultaneously (58). More recently, areas within the regulatory Ca^{2+} binding domains, such as residues 440-456, 498-510 and 680-685, have demonstrated no effect on XIP-mediated regulation of NCX current (135). Stronger evidence supports the proposition that the XIP binding site is located in the region corresponding to amino acids 562-679, as deletion of these

residues eliminate the XIP-induced inhibition of NCX currents in heterologous expression systems and in cardiac myocytes (135; 144). As well, deletion of these residues abrogates the insulin effect on NCX currents, as measured by $^{45}Ca^{2+}$ uptake experiments (246). The alternative splice region is located within the area corresponding to amino acids 562-679, and further investigations may demonstrate potential interactions between the splice region and the XIP region.

1.4.2 The Ca^{2+}- binding domains

The regulatory Ca^{2+}-binding domains, initially identified as the β-repeats, are located between residues 371-508 within the intracellular loop and are distinct from the Ca^{2+} transport site (121; 144). Regulatory Ca^{2+} binds to two highly acidic sequences characterized by three consecutive aspartic acid residues located in both Ca^{2+} binding domains, CBD1 and CBD2. Single point mutations at residues D447, D448 and D498 in CBD1 cause drastic loss of Ca^{2+} binding with a direct impact on regulatory Ca^{2+} affinity (143). The Ca^{2+} binding site mutant which demonstrates the lowest affinity for regulatory Ca^{2+} binding (D447V/D498I) also influences the extent of Na^{+}-dependent inactivation, and although there are conflicting reports as to whether Na^{+}-dependent inactivation is enhanced or suppressed, these data support the hypothesis that Na^{+}-dependent and Ca^{2+}-dependent regulation are linked (143; 175).

Regulatory Ca^{2+} binding to the exchanger appears to be a coordinated process. Both Ca^{2+} binding domains are believed to have two separate Ca^{2+}-binding sites which demonstrate cooperativity, suggesting that Ca^{2+} binding to one site causes a conformational change, allowing binding of Ca^{2+} to the second site. These

conformational changes were observed using a non-invasive FRET-based technique on NCX1 constructs with fluorescent probes flanking the CBD1/2 domains only (174) or incorporated into the cytoplasmic loop of an otherwise intact exchanger (172). Binding of Ca^{2+} to the Ca^{2+} binding domains caused a reduction in FRET efficiency, suggestive of an increased distance between the fluorescent probes due to a change in protein conformation. Point mutations of the aforementioned critical aspartate residues within the Ca^{2+}-binding sites prevented a change in FRET, supporting the role of these negatively charged residues in Ca^{2+} binding. Furthermore, these changes were observed within physiological Ca^{2+} concentrations in actively contracting neonatal myocytes, demonstrating that NCX is regulated by Ca^{2+} on a beat-to-beat basis during excitation-contraction coupling (174).

Recent structural studies of the two Ca^{2+} binding domains of NCX1, using NMR and crystallography, have been instrumental in identifying the secondary structure within these domains and the key amino acids determining both structure and ionic regulatory properties of the exchanger (17; 35; 59; 99; 164). Hypothetical three dimensional models for the intact NCX1 exchanger and for the Ca^{2+} binding domains specifically have been proposed, as illustrated in Figures 3 and 4, respectively. The model for the complete exchanger (Figure 3) depicts the Ca^{2+} binding domains linked via a catenin-like domain to the transmembrane region, where ion transport occurs (59). The mutually exclusive exon is located within the Ca^{2+} binding domain 2, and the remaining cassette exons forming the alternative splice region are exposed within the cytoplasm. According to this model, changes in conformation at high Ca^{2+} concentrations

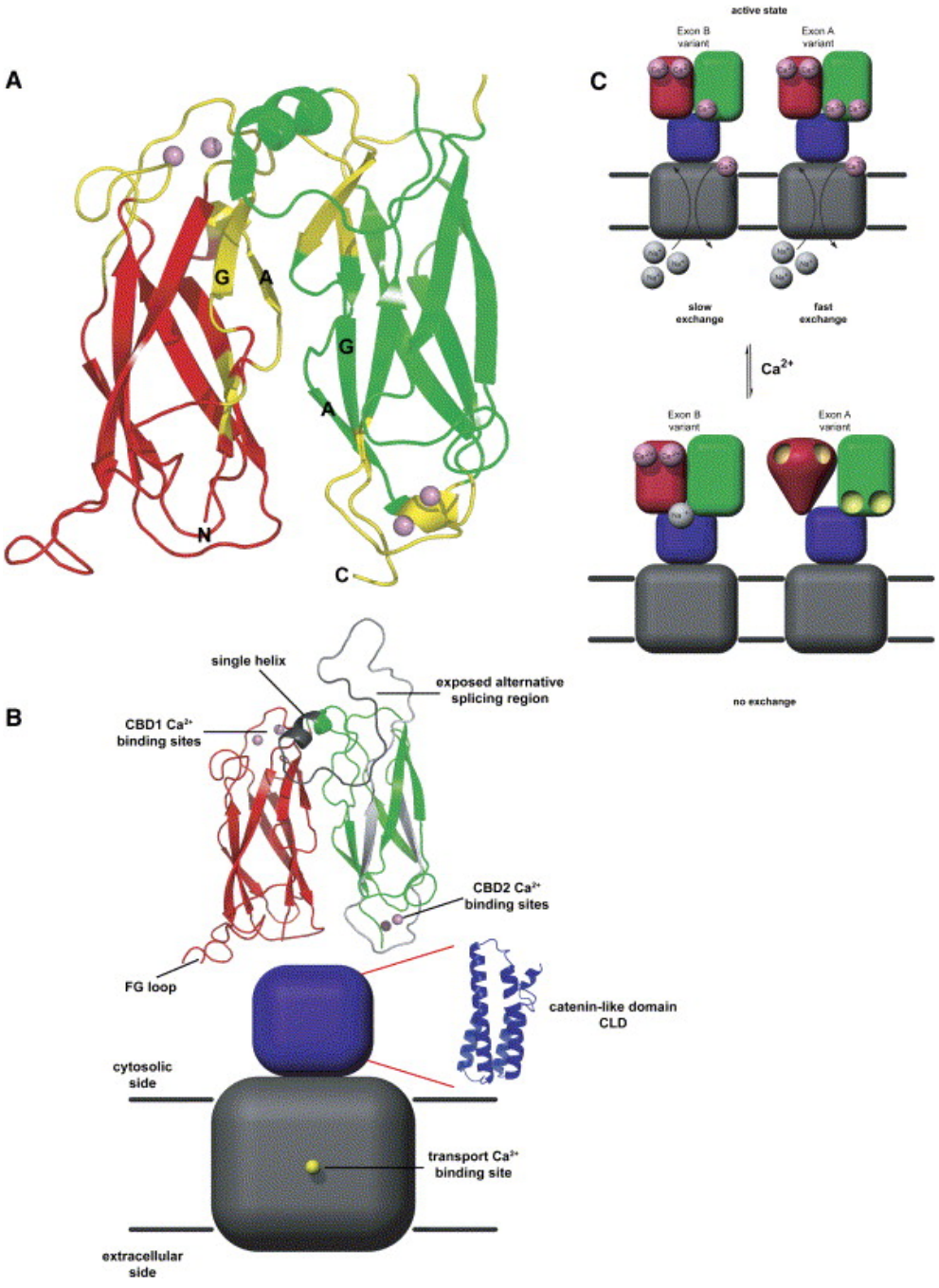


Figure 3. Model of the intact NCX exchanger based on high resolution NMR spectroscopy in the Ca^{2+} bound form. CBD1, in red and CBD2, in green, form an interface dependent on calcium binding to CBD1. Calcium binding sites are in pink. B. This hypothetical model of the intact exchanger consists of CBD1 and CBD2 with a catenin-like domain linking them to the transmembrane region where binding of transport Ca^{2+} and Na^{+} occurs. The exposed alternative splicing region is in gray, with exon A in light gray and exon D in dark gray. C. Schematic outline of exchanger operation, demonstrating the differences between exon A and exon B expressing splice variants. (59), with permission.

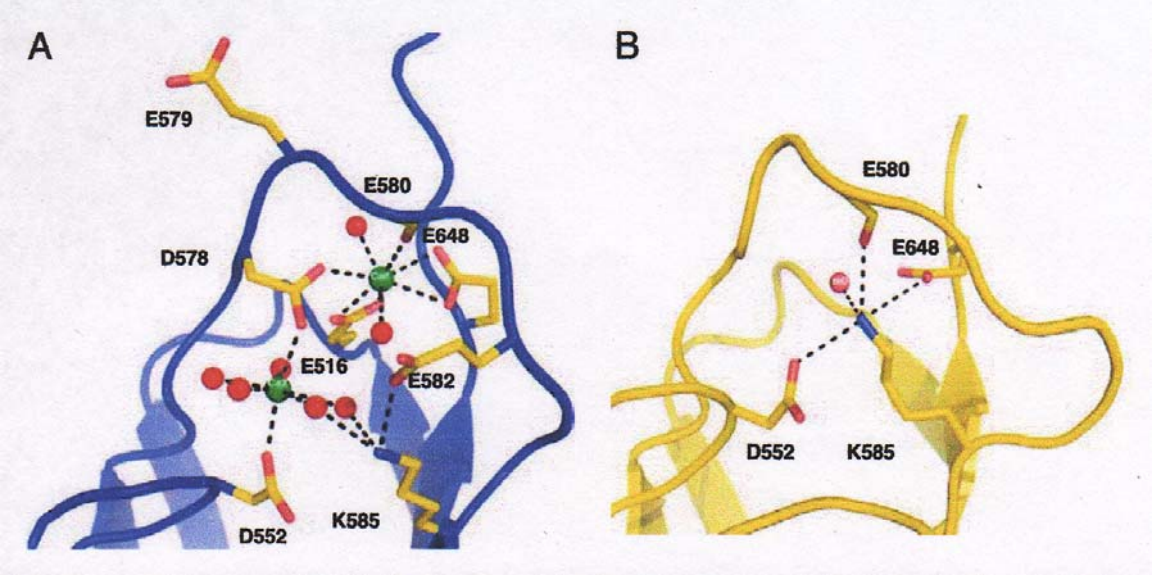


Figure 4. Structure of the CBD2 Ca^{2+}-binding site. A. The green spheres represent Ca ions and red molecules represent water molecules. Key residues involved in binding of the ions are linked to the ions by black dashed lines. B. Ca^{2+}-free structure demonstrating possible role for K585 in stabilizing the negatively charged area in the absence of bound Ca^{2+}. (17), with permission.

differ according to which mutually exclusive exon is expressed (Figure 3C). This will obviously have an impact on the NCX regulation and will be discussed shortly.

The hypothetical model for the Ca^{2+} binding domains (Figure 4) proposes that the main residues required for Ca^{2+} binding are the highly acidic residues between D446-E454 in CBD1 and their analogues D577-E648 in CBD2, with coordination of the two Ca^{2+} binding sites achieved by residues D578 and K585 (17). CBD1, with its higher affinity, is the primary Ca^{2+} sensor which elicits significant structural changes upon binding of two Ca^{2+} ions at its Ca^{2+} binding sites. In the absence of Ca^{2+}, CBD1 is highly unstructured, and prevents ion transport. CBD2, however, has limited structural alterations and only binds Ca^{2+} at elevated concentrations. Together, these two domains enable the exchanger to function over a wide range of Ca^{2+} concentrations.

The first Ca^{2+} binding site of CBD2 (residues D577-E582) is located within the mutually exclusive exon and is conserved amongst isoforms. Two key residues in the mutually exclusive exon A of NCX1 (D578 and K585) have been identified as critical in mediating distinct ionic regulatory properties in NCX1 splice variants expressing this exon (35). These residues have also been implicated in the secondary structure of the Ca^{2+} binding domains (59). Briefly, it is believed that D578 coordinates Ca^{2+} ions in both binding sites of CBD2 whereas K585 forms a salt bridge with D552, thus stabilizing the surrounding negatively charged residues and preventing the unfolding of CBD2 in the absence of bound Ca^{2+}. A possible mechanism of regulation of NCX by the Ca^{2+} binding domains has been proposed, where subsequently to the regulatory Ca^{2+} binding to CBD1, Ca^{2+} binds to site I of CBD2 by disrupting the salt bridge between K585 and E648, thus decreasing accessibility to site II. The salt bridge between K585 and D552 is then broken

and the second Ca^{2+} is free to bind (17). Binding of Ca^{2+} to CBD2 causes a conformational change disrupting the Na^{+}-dependent inactive state, hence outward exchange current is no longer inhibited and Ca^{2+} influx prevails. This demonstrates that residues located within the mutually exclusive exon play an essential role in the regulation of outward exchange currents mediated by NCX. Differences observed in splice variant phenotypes may be linked to specific residues in the alternative splice region.

1.4.3 Phosphorylation

Phosphorylation of NCX by different protein kinases, including the c-AMP-dependent kinase, PKA (53; 126; 162), PKC (92), CaMKII (78) and tyrosine kinase (151; 162) has been demonstrated in the heart (92; 126), in neural tissues (33) and in smooth muscle (96). Despite identification of several phosphorylation consensus sites in several NCX isoforms (162), the role of phosphorylation in NCX function and regulation remains controversial. Whereas some studies (92; 96) demonstrate activation of both forward and reverse mode of action of NCX in response to phosphorylation, others have failed to observe these effects (27; 64; 141; 162). This may be explained by activation via phosphorylation of associated proteins, whereby intermediate signals may mediate NCX activation independently of direct phosphorylation (91; 211; 221). The intracellular loop of NCX has been shown to associate with other proteins in the cytoplasm, such as kinases (PKA and PKC subunits), phosphatases (PP1 and PP2A) and a kinase anchoring protein (AKAP) (221). This macromolecular complex would facilitate regulation of NCX by

phosphorylation and/or dephosphorylation, as the key players would be in close proximity and could provide a specific and subtle control of NCX function.

Several studies suggest that the effects of phosphorylation may be isoform dependent. For example, ATP depletion appears to inhibit NCX1 and NCX2 but not NCX3 function (126), whereas phosphorylation by PKA and PKC has been shown to upregulate NCX1 and NCX3 but not NCX2 (54; 91). A potential PKC or cAMP-dependent kinase site has been identified in the XIP region of NCX2 and NCX3, but not NCX1. Also, a tyrosine kinase site has been identified in CBD2, as well as a PKC site in the mutually exclusive exon of certain NCX splice variants (162). This suggests that phosphorylation may be implicated in mediating differential Na^+ and Ca^{2+}-dependent regulation of NCX isoforms and splice variants.

New studies propose regulation of NCX by phosphorylation in pathophysiological settings. Phosphorylation of NCX was shown to activate NCX currents under β-adrenergic stimulation in failing pig myocytes (254), and calcineurin was shown to inhibit NCX activity in PKC-dependent and independent pathways in hypertrophic cardiomyocytes (103; 227). These data suggest that phosphorylation of NCX may not be essential physiologically, but rather may be involved in disease conditions.

1.5 NCX isoforms and splice variants

1.5.1 NCX genes

Three mammalian NCX isoforms have been cloned to date: NCX1 (160), ubiquitously expressed with higher levels in heart, brain, kidney and lung (108; 110), NCX2 (123), expressed in neural tissues, and NCX3 (162), expressed in skeletal muscle

and neuronal tissues. The NCX1 gene is located on the human chromosome 2p21-23 (226), whereas NCX2 is located on chromosome 19 and NCX3 on chromosome 14q21-31 (162). The fact that the three exchangers are encoded by three separate genes on different chromosomes allows for independent expression of all three isoforms. It should be noted that the genes encoding NCX1 and NCX3 are relatively short (316 kb and 126 kb respectively), whereas NCX2 is encoded by very compact genomic DNA (36 kb) (137). Recently, NCX4 has been cloned in zebrafish, with a sequence most similar to NCX1 (137). NCX4 appears to regulate left-right patterning in embryological zebrafish development (45).

NCX1 and NCX3 transcripts undergo alternative splicing, giving rise to several splice variants, of which 12 and 3 have been identified, respectively (109; 117; 120; 198). The alternative splicing region consists of a variable sequence of 110 amino acids located within CBD2 in the C-terminal portion of the intracellular loop (109) and contains one of the mutually exclusive exons A or B, followed by a combination of one or more of the cassette exons C, D, E and F. NCX1 splice variants expressing the A exon, such as NCX1.1 and NCX1.4, are present in excitable tissues such as heart and brain, respectively (198). Splice variants containing exon B are expressed in all other tissues, such as kidney, endocrine organs, digestive organs and reproductive organs (120; 198). NCX1.3, the most studied exchanger in this latter group, is expressed in the kidney and in vascular smooth muscle cells (80; 85; 120; 233). All NCX1 variants express exon D, suggesting that this region may be constitutively expressed and is not an authentic cassette exon (198). Both NCX2 and NCX3 have a 37 amino acid deletion in the area of exons D, E, and F (162).

1.5.2 Unique regulatory profiles

NCX isoforms and splice variants are not only expressed in different tissues but they display unique ionic regulatory profiles (2; 38; 169; 171; 222). For example, differential sensitivities to inhibitory agents and divalent cations (93) and to fatty acids (2) have been observed between isoforms. Also, NCX1.1 is ubiquitously expressed throughout the body. The additional splice variants are restricted to a few tissues, such as NCX1.4 in the brain and NCX1.3 in the kidney and the vasculature. This suggests that NCX1.1 may play more of a "housekeeping" role and the variants, a more specialized function in distinct tissues or cell types (198). Thus, NCX function may be specifically tailored to the different cellular environments of the tissues in which it is expressed. Unique regulatory and functional properties enable the NCX isoforms to fulfill their distinct physiological roles in Ca^{2+} homeostasis in a tissue specific manner.

Interplay between the regulatory regions located within the cytoplasmic loop, including the alternative splice region, may have a potential role in modulating the distinct phenotypes observed for each exchanger. For example, NCX1.4 and NCX1.3 differ only in the presence of the mutually exclusive exon, which encodes the first acidic segment of the Ca^{2+} binding site of CBD2. NCX1.4, expressing exon A, exhibits robust Na^{+}-dependent inactivation of outward exchange currents at low micromolar concentrations of Ca^{2+}_{i}, which can be alleviated at higher levels of Ca^{2+}_{i} (38). In contrast, NCX1.3, containing exon B, also exhibits strong Na^{+}-dependent inactivation, but increasing Ca^{2+}_{i} concentrations do not significantly modify the rate or the extent of inactivation. Mutational analysis and structural studies of CBD1/2 of NCX1 suggest that two key residues (D578 and K585) located within the mutually exclusive exon sequence

and involved in stabilization and coordination of Ca^{+2} ions in the Ca^{2+}-binding sites of CBD2, are critical determinants of the distinct phenotypes exhibited by these splice variants (35; 59). Exon A contains both aforementioned residues and has the capacity to bind Ca^{2+} at the Ca^{2+}-binding sites of CBD2 when high intracellular Ca^{2+} concentrations occur. This appears to disrupt the secondary structure required for stabilisation of the Na^{+}-dependent inactive state. Thus, high Ca^{2+}_{i} concentrations cause alleviation of Na^{+}-dependent inactivation of outward exchange currents mediated by exon A expressing variants. In contrast, exon B containing splice variants do not express D578 and K585 and do not appear to bind Ca^{2+} at the Ca^{2+}-binding sites of CBD2. Consequently, Na^{+}-dependent inactivation is maintained, independently of elevated intracellular Ca^{2+} levels. This unique mechanism could limit Ca^{2+} influx under conditions of high intracellular Na^{+}, thereby preventing excessive Ca^{2+} overload in tissues expressing exon B splice variants. This suggests that certain exchangers may have protective properties dependent on the ionic regulatory phenotype conferred by the alternative splice region.

1.5.3 NCX localization

NCX1 has been most extensively studied in cardiac myocytes (160), where it appears to be localized in the T-tubules (259). It has been shown that NCX1 is linked to the spectrin-actin cytoskeletal network via ankyrin, which may be critical for T-tubular targeting of NCX (25; 125; 154). It has also been suggested that NCX1 is in close proximity to the ryanodine receptor and L-type channels, ensuring efficient control of Ca^{2+} transport and signalling between the proteins involved in Ca^{2+}-induced Ca^{2+} release (CICR), which is critical in this tissue (28). A sodium-calcium exchange system has also

been localized to the mitochondrial membrane, where its role in intramitochondrial Ca^{2+} homeostasis is essential for regulating key enzymes involved in energy metabolism (24).

Although NCX1.1 is predominantly expressed in myocytes, it is also present in other cell types within the heart. NCX is expressed in ventricular myofibroblasts, where it is involved in motility, contraction and proliferation, thus contributing to post myocardial infarct wound healing (199). NCX is also expressed in arterial smooth muscle cells (261), in vascular smooth muscle and endothelial cells (30; 237), where its role in regulation of coronary tone has been described.

The brain is the only tissue where all three isoforms are expressed. Differential expression of NCX mRNA and proteins has been described for neuronal and glial cells in rat cerebral cortex, hippocampus and cerebellum (49; 150; 176; 242). The NCX isoforms appear to be selectively expressed, suggesting different functional roles in different parts of the central nervous system. Conflicting evidence as to protein expression has been noted, possibly due to observations made in cultured and *in vivo* cell preparations. NCX1 appears to be expressed in neuronal cell bodies and dendrites, whereas NCX2 appears to be more highly expressed in glial cells, and NCX3, in a restricted subpopulation of neurons (242). NCX has also been studied in the developing rat brain, where NCX2 transcripts in the cortex are believed to increase during postnatal development whereas NCX1 and NCX3 transcripts decrease (190; 213).

NCX expression is evident in skeletal muscle, where its role in Ca^{2+} transport would be minimal for contraction, as skeletal muscle does not rely on trans-sarcolemmal Ca^{2+} influx during an action potential and requirements for a high level of Ca^{2+} extrusion have not been described (50; 162). NCX1 mRNA and protein levels peak shortly after

birth. Mature protein is expressed as clusters in T-tubular membranes of adult muscle, predominantly in oxidative (type 1 and 2A) fibres of both slow and fast twitch muscles (46). NCX3 is more uniformly distributed along the sarcolemma and inside the myoplasm in fast glycolytic (type 2B) fibers (46).

NCX1 is highly expressed in the vascular system. The splice variant present in this tissue is NCX1.3, which has been localized in the kidney cortex. It is predominantly expressed in the distal convoluted tubules of the nephron, where it is believed to play a role in Ca^{2+} reabsorption (120). NCX1.3 has also been localized in vascular smooth muscle cells and appears to be involved in arterial tone control (233).

1.5.4 NCX2

The second sodium-calcium exchanger to be discovered was cloned from rat brain (123). NCX2 has an open reading frame of 2763 nucleotides encoding for a 921 amino acid with 61 % homology with canine NCX1 with regards to the nucleotide sequence and 65 % homology on the amino acid level. The amino acid identity is particularly high (82 %) in the transmembrane regions involved in ion translocation. The first extracellular segment has a glycosylation site at Asn 34, with four other possible *N*-linked glycosylation sites. Several clusters of amino acids with high sequence identity have also been identified in the cytoplasmic loop, but overall, the loop showed sequence identity of only 60 %. However, the XIP region is well conserved. There are also potential phosphorylation sites, possibly for c-AMP and calmodulin-dependent kinases (123).

Characterization of NCX2 by our lab and others has demonstrated subtle regulatory differences in comparison to NCX1, although generally, both isoforms exhibit

similar transport and regulatory properties. These observations have been assessed by ion flux and giant excised patch clamp technique in transfected BHK cells, membrane vesicles and *Xenopus oocytes* (126; 171). Na^+-dependent inactivation of outward exchange currents is present for NCX2, but the extent of inactivation is moderate in comparison to what is observed in currents mediated by NCX1. At low Ca^{2+}_i concentrations (1 μM), peak outward currents do not decrease significantly in response to high Na^+_i levels; Na^+-dependent inactivation only becomes apparent at higher Ca^{2+}_i concentration, such as 3 or 10 μM Ca^{2+}_i. Unlike NCX1, high Ca^{2+}_i does not alleviate Na^+-dependent inactivation of outward currents in NCX2. As well, recovery from the Na^+-dependent inactive state is more rapid for NCX2.1 than for NCX1. These data suggest that although high levels of Ca^{2+} are unable to disrupt the Na^+-dependent inactive state of NCX2.1, the stability of the inactive state is not as strong as what is observed for NCX1 (171).

NCX2.1 is also regulated by non-transported, intracellular Ca^{2+}, although it exhibits a 5-fold decrease in Ca^{2+} affinity as compared to NCX1.1 (1.5 μM vs 0.3 μM, respectively). A decline in outward exchange currents upon removal of regulatory Ca^{2+} is approximately 6 times more rapid for NCX2.1 than NCX1.1, suggesting that NCX2.1 has a faster dissociation rate for regulatory Ca^{2+} than NCX1.1 (171). Non-conserved residues located in the regulatory domains of NCX2.1 may be responsible for these phenotypes.

1.5.5 NCX3

The third sodium-calcium exchanger to be cloned is NCX3, primarily expressed in brain and skeletal muscle (162). NCX3 contains an open reading frame of

2784 nucleotides which encode for a 927 amino acid protein. The 5' untranslated region is extremely GC rich (80 %) and has 17 ATG triplets in the region upstream of the initiating methionine, suggesting that its translation is highly regulated. Its signal peptide appears to be cleaved at amino acid 30. NCX3 has five potential *N*-linked glycosylation sites, although like NCX1, only the first is thought to be glycosylated (Asn45). Overall protein sequence identity has been evaluated at 73% with NCX1 and 75% with NCX2, but this identity is more prominent in the transmembrane segments. Topologically, NCX3 is similar to NCX1, with a high homology in the Ca^{2+} binding sites. However, only the first 14 residues of the XIP region are highly conserved (162). Phosphorylation sites have been identified for a variety of kinases, such as Ca^{+2}/calmodulin dependent kinase, cAMP-dependent kinase, protein kinase C and tyrosine kinase. Potential roles for phosphorylation have been proposed, such as residue Thr 113, located near the α-1 repeat, which could be involved in regulating ion transport (159). Furthermore, NCX3 does not appear to require ATP to be functional, and may therefore play a greater role in ATP-depleted situations (126).

Although currents mediated by NCX3 in oocytes are difficult to measure, preliminary data demonstrate that peak outward currents are rapidly achieved in the presence of regulatory Ca^{2+}, but appear to be almost completely inactivated subsequently (140). This suggests that regulatory Ca^{2+} has both Ca^{2+}-induced activation and inactivation properties unique to NCX3.

1.5.6 CALX

The CALX exchanger, expressed in *Drosophila melanogaster*, has a unique regulatory phenotype: it does not require regulatory Ca^{2+} to mediate outward exchange currents. Rather, the presence of micromolar Ca^{2+} concentrations inhibits exchange activity (37; 74). Differences in regulatory regions of the exchanger, predominantly the Ca^{2+} binding domains, are responsible for these phenotypic variations, as demonstrated by chimaeric constructs exchanging CBD between CALX1.1 and NCX1.1 as well as site directed mutagenesis (37). These results demonstrate that substitution of entire regulatory regions between different Na^{+}-Ca^{2+} exchangers can generate functional chimaeric constructs with regulatory properties transferred from both the parent and donor exchanger. Hence, this technique can be used to compare regulatory domains between NCX isoforms, as proposed in this study and described shortly.

CALX undergoes alternative splicing, and functional differences in ionic regulation have been observed in the splice variants (169). CALX1.1 and CALX1.2 differ by only five amino acids in the same region where alternative splicing occurs in NCX1 (210; 223). Increased extent of Na^{+}-dependent inactivation, alleviation of I_1 in response to $Ca^{2+}{}_i$ and a 2-3 fold difference in recovery rates were observed for CALX1.2 as compared to CALX1.1 (169). Furthermore, although $Ca^{2+}{}_i$ has an inhibitory effect on both splice variants, the extent of these effects is greatly reduced for CALX1.2, with only 20-40 % inhibition. Therefore, the alternative splice region plays a significant role in mediating the regulatory profile of CALX, similarly to what has been shown for NCX1 splice variants.

1.6 NCX in the heart

1.6.1 Physiological function

It is widely accepted that NCX function in cardiac myocytes is predominantly Ca^{2+} efflux on a beat-to-beat basis, removing the equivalent amount of Ca^{2+} that has entered the cell via the voltage dependent L-type Ca^{2+} channel upon depolarization of the sarcolemmal membrane (Figure 5) (13). This trans-sarcolemmal removal of Ca^{2+} via NCX and the plasma membrane Ca^{2+}-ATPase (PMCA), along with resequestering of Ca^{2+} in the sarcoplamic reticulum via the sarcoplasmic reticulum Ca^{2+}-ATPase (SERCA2), is essential for relaxation of the muscle prior to the next contraction. Ca^{2+} extrusion via NCX is ten times greater than by PMCA, as NCX is a low affinity, high capacity carrier of Ca^{2+}. PMCA has higher affinity but lower capacity for transport of Ca^{2+}, making it the "fine tuner" of intracellular Ca^{2+} concentrations (13).

It has been proposed that NCX current in myocytes is in its outward mode for less than 10 ms at the beginning of the action potential, but rapidly converts to its forward mode, transporting Ca^{2+} out of the cell (252). NCX exchange is activated by the high Ca^{2+}_i levels detected in the submembrane space, maintaining NCX is its forward mode for the majority of the action potential. In this mode, NCX has a depolarizing effect, as it maintains Na^+ entry into the cell. This contributes to the plateau phase of the action potential which is counterbalanced by other channels, such as I_{ki}. When the outward K^+ current mediated by the delayed rectifier is greater than the inward Ca^{2+} current mediated by the L-type channel, repolarization to the resting membrane potential occurs (7).

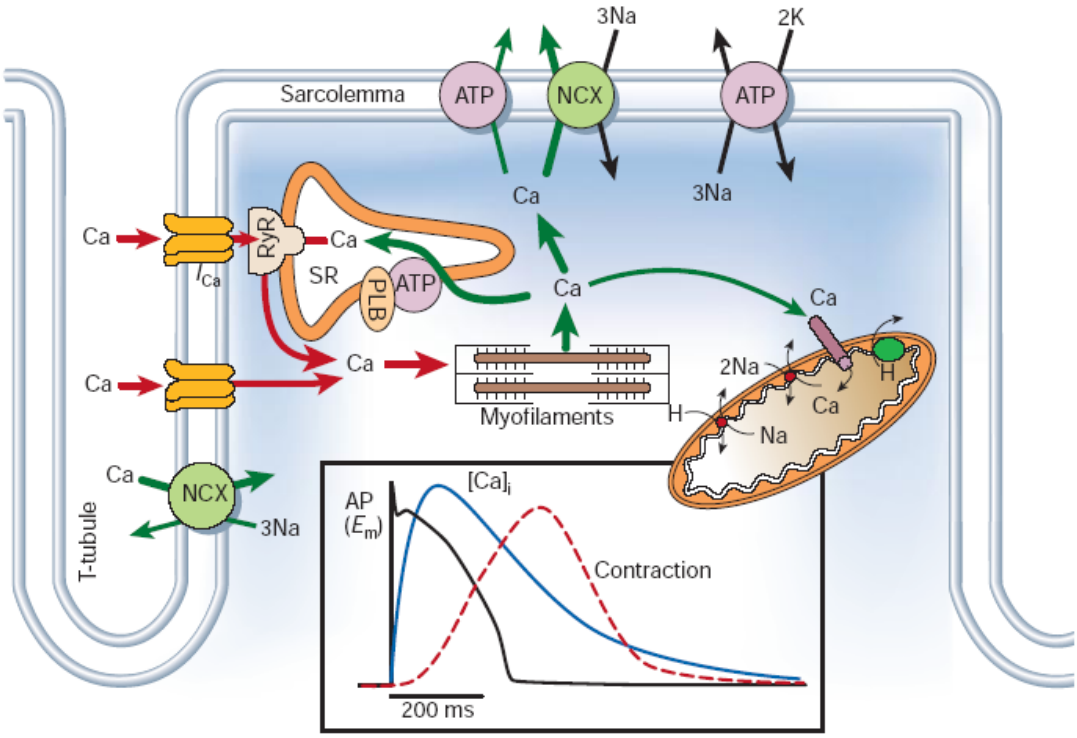


Figure 5. Na^+-Ca^{2+} exchange and excitation-contraction coupling. Proteins involved in Ca^{2+} signalling pathways during contraction of a ventricular myocyte are depicted. Briefly, Ca^{2+} enters the cell via the volgate-gated L-type channels (yellow) to initiate systole. This triggers Ca^{2+} release from the sarcoplasmic reticulum (SR) by the ryanodine receptor (RYR). Increased intracellular Ca^{2+} activates myofilament cross-bridge formation and contraction. For diastole, Ca^{2+} is transported back into the sarcoplasmic reticulum by the SR Ca^{2+} ATPase (SERCA) or is removed from the cytosol by NCX, the sarcolemmal Ca^{2+}-ATPase and the mitochondrial Ca^{2+} uniporter. (12), with permission.

Certain cellular conditions will cause NCX to function in its outward mode of exchange, causing Na^+ efflux. These situations include conditions when intracellular Na^+ concentrations increase, such as during ischemia, when a decrease in ATP levels and cellular pH cause inhibition of the Na^+/K^+ pump and a reversal of the Na^+/H^+ exchange activity (3; 101; 102; 184). Prolonged action potential duration observed during long QT syndrome (149) and lower peak Ca^{2+} concentrations occurring during heart failure due to a decrease in SERCA function also promote NCX outward mode of exchange and inward Na^+ flow (247). At Na^+ concentrations $\geq$ 10 mmol/L, outward NCX currents during the plateau phase of the action potential facilitate repolarization of the membrane and thus shortening of the action potential duration (7). This mode of exchange may also contribute to increasing cytoplasmic Ca^{2+} concentrations which, initially, may increase the sarcoplasmic reticulum Ca^{2+} load, the amplitude of systolic Ca^{2+} transients and hence, contractility (245). However, it may eventually lead to decreased Ca^{2+} entry into the cell via the L-type channel, as repolarization inactivates this transporter. This will decrease cell and sarcoplasmic reticulum Ca^{2+} content and thus affect contractility. Furthermore, the reverse mode of NCX, by causing Ca^{2+} influx, may activate the ryanodine receptor and contribute to Ca^{2+} waves or spontaneous release of Ca^{2+} from the sarcoplasmic reticulum, leading to arrhythmogenicity (236). We can therefore appreciate that NCX function is intimately linked to ionic concentrations in the cell, which vary according to the physiological events occurring and the interplay between the numerous proteins involved in Ca^{2+} transport and ionic homeostasis.

1.6.2 NCX1.1 knock-out mice

The critical role for NCX in cardiac myocytes is supported by studies of knock-out mice for NCX1.1, the splice variant highly expressed in this cell type. These mice are embryonically lethal at approximately 8.5 days post-conception, presumably due to a cardiac defect or apoptotic cell loss (26; 111; 249). The NCX1.1 deficient mice show severe disorganization of the myofibrils, with no Z lines and swelling of the mitochondria (249). Heterozygous mice grow normally, with no discernable phenotype.

At a later developmental stage, NCX function does not appear to be as critical. Conditional knock-out mice, created using the Cre/loxP technology, cause only a modest decrease in cardiac function, allowing these mice to survive to adulthood (57; 193; 206). These mice have normal Ca^{2+} transient magnitude and relaxation kinetics, with no evidence of increased protein or transcript levels of other myocardial proteins involved in excitation-contraction coupling (PMCA, DHPR, SERCA or calsequestrin) despite a decrease in contractility by 20-30 %, as assessed by measures of fractional shortening and ejection fraction. However, these animals can not withstand any stress, such as breeding or longevity, possibly due to heart failure.

To circumvent the absence of NCX and a compromised Ca^{2+} extrusion pathway in the adult mouse heart, it appears that the myocyte limits Ca^{2+} influx via the L-type channel, thus decreasing the need for transsarcolemmal Ca^{2+} efflux, which is now dependent on PMCA (57; 193; 206). The authors hypothesize that trigger Ca^{2+} is able to induce sarcoplasmic reticulum Ca^{2+} release more efficiently, thereby maintaining an equivalent Ca^{2+} transient despite an 80 % reduction in the flux of Ca^{2+} across the membrane. This represents a gain in the efficiency of excitation-contraction coupling

(ECC), as less Ca^{2+} influx from the extracellular space is required to maintain equivalent Ca^{2+} release from the sarcoplasmic reticulum. There appears, however, to be no increase in SR Ca^{2+} load in these knock-out mice. Possibly, a decrease in NCX protein in the dyadic cleft would cause an increase in local Ca^{2+} concentration, thus activating neighboring ryanodine receptors or causing Ca^{2+}-dependent inactivation of L-type channels (195).

To support these findings, observations were made on NCX-/- heart tubes from embryos at day 9.5 post-conception (206). Normal Ca^{2+} transients were measured, but these heart tubes could not withstand any form of stress, such as an increase in stimulation frequency, caffeine or isoproterenol. Action potential duration was shorter (plateau phase was absent) in NCX-/- heart tubes, with an accelerated repolarization, consistent with the concept that normally, L-type channel currents prolong action potential duration and the NCX inward currents prolong the plateau phase (219; 236). Also, this dramatic action potential shortening appeared to be due to upregulation of the outward K^+ current (I_{ko}) and an increase in expression of K^+ channel subunits (194). Inhibition of NCX expression by RNA interference using adenovirally delivered shRNA in cultured neonatal rat cardiomyocytes supports the observations that contractile function is maintained, but with lower frequency, depressed Ca^{2+} transient amplitude, elevated diastolic Ca^{2+} concentration and shorter action potentials (76). Furthermore, this study observed upregulation of PMCA protein expression, which may be an adaptive mechanism assuring adequate Ca^{2+} efflux.

1.6.3 NCX overexpression

Overexpression of NCX1.1 gives a mirror image of what is observed in knock-out mice (191; 204). In homozygous NCX1.1 overexpressing mice, Ca^{2+} influx via L-type channels increases and is compensated by an equivalent increase in Ca^{2+} extrusion via the exchanger (191). These animals have essentially normal cardiac function but a smaller Ca^{2+} transient and a decrease in ECC gain (191). An increase in NCX expression in the dyadic cleft rapidly removes Ca^{2+} from the microenvironment of L-type channels during depolarization, causing a decrease in Ca^{2+}-induced inactivation of I_{Ca} or reducing trigger Ca^{2+} flux before the ryanodine receptor senses that Ca^{2+} (51). This increase in I_{Ca} is also reflected in the prolonged AP duration due to a prolonged Ca^{2+} influx during the plateau phase (192). Furthermore, these transgenic animals displayed hypertrophic hearts and had an increased susceptibility to heart failure in response to stress, probably secondary to alterations in excitation-contraction coupling. A threefold increase in NCX expression not only caused an increase in forward mode but also reverse mode activity, thus contributing to Ca^{2+} influx and overload during depolarization, overfilling the sarcoplasmic reticulum and increasing oscillatory Ca^{2+} release and arrhythmias (204; 231).

1.6.4 NCX and cardiovascular disease

During ischemia reperfusion, NCX activity is perturbed by an ionic imbalance in the cell. A restriction in blood flow to the tissues during ischemia causes ATP levels to decrease, affecting normal Na^+/K^+ ATPase and SERCA function, as well as an accumulation of H^+ ions within the cell (3). This lowering of pH activates the Na^+/H^+ exchanger, leading to further influx of Na^+ (101; 102; 184). The increase in Na^+_i causes

NCX transport to be in the outward mode, and consequently, intracellular Ca^{2+} levels rise (128; 130; 132; 240). In the first few minutes of reoxygenation following reperfusion, NCX maintains transport in its outward mode, attempting to normalize Na^{+}_{i} concentrations. Entry of Ca^{2+} via this mode of NCX triggers Ca^{2+} release from the sarcoplasmic reticulum via the ryanodine receptor (127; 129). Resupply of energy to SERCA also activates uptake and release of Ca^{2+} from the sarcoplasmic reticulum. This can lead to oscillations of cytosolic Ca^{2+}, causing extrasystolic arrhythmias (156). Furthermore, reperfusion after ischemia can lead to a sudden development of hypercontraction of myocytes due to Ca^{2+} overload, which is a major cause of acute lethal cell injury (217). After a few minutes of reperfusion, NCX functions in its inward mode, driven by the re-established Na^{+} gradient and membrane potential, but with prolonged ischemic periods, considerable damage may have already compromised cardiac function. Activation of Ca^{2+}-dependent proteases may have influenced membrane integrity and specific signalling pathways, thereby not only influencing NCX activity directly (181) but also energy metabolism (43) and activation of cell death pathways (68).

Recent studies demonstrate that the ionic regulatory profile of the NCX isoform expressed in cardiac myocytes promotes Ca^{2+} overload in response to cardiac glycosides and ischemia (77). In contrast, the vascular isoform NCX1.3 exhibits strong Na^{+}-dependent inactivation of outward exchange mode, thus reducing Ca^{2+} influx and overload. This demonstrates the importance of ionic regulation in controlling NCX activity under conditions that enhance Ca^{2+} overload. Furthermore, as the ionic regulatory phenotype specific to the NCX isoform or variant expressed in the tissue undergoing ischemia may vary, the response to ischemia will be tissue-specific.

Deregulation of Ca^{2+} in the heart also contributes to impaired contractility and arrhythmias during heart failure and hypertrophy (146; 189; 218; 232), and although the role of NCX in such cases remains controversial, two views are held with respect to contractile dysfunction. NCX mRNA and protein expression are enhanced in heart failure, leading to a potentially two-fold increase in either inward or outward exchanger currents (42; 189). As NCX function is determined by intracellular Ca^{2+} and Na^{+} concentrations as well as membrane potential, its mode of action is modified in disease states where ionic homeostasis is compromised. Elevated Na^{+} levels in failing hearts cause NCX to function in its outward mode, promoting Ca^{2+} influx (31). The first view is that NCX-dependent Ca^{2+} influx contributes to sarcoplasmic reticulum Ca^{2+} load, but also increases susceptibility to overall cellular Ca^{2+} overload, causing diastolic dysfunction (32; 145). High Ca^{+2} content may subsequently increase NCX forward activity during diastole, causing Na^{+} influx, thus contributing to elongation of the action potential or depolarization and generation of extra action potential events (16; 230; 253).

The second view is that sarcoplasmic reticulum Ca^{2+} content is decreased in heart failure due to increased NCX function, decreased SERCA function and increased sarcoplasmic reticulum Ca^{2+} leak, facilitating the occurrence of early afterdepolarizations (247). Along with a decrease in SERCA function (147; 188) leading to unloading of the sarcoplasmic reticulum, NCX's enhanced expression would preserve diastolic function with normal relaxation but decrease systolic function, as demonstrated in heart failure in humans and dogs (166). Inhibition of NCX by adding the XIP peptide normalized sarcoplasmic reticulum Ca^{2+} release and re-uptake, demonstrating that NCX overexpression could be an important therapeutic target in heart failure (67). It is unsure

if up-regulation of NCX during cardiac hypertrophy and heart failure is an adaptive or maladaptive compensatory mechanism (157). This is dependent on which mode of action NCX functions. Most probably, NCX's activity is initially required to compensate for the increased contractile demands caused by the inability of the heart to contract fully, however the side effects of spontaneous Ca^{2+} release and prolongation of the action potential can be detrimental, as they may lead to arrhythmogenesis (229).

1.7 NCX in neuronal and muscular tissues

1.71 Physiological function

The physiological role of NCX in the brain is not well understood, but it has been proposed to be involved in removal of intracellular Ca^{2+} in parallel fibers (200), Purkinje fibers of the cerebellum (41) and synaptic sites of hippocampal neurons (207). Some studies suggest that NCX not only functions in reducing intracellular Ca^{2+} in pre-synaptic terminals after electrical stimulation, but also is involved in regulation of exocytosis of synaptic vesicles (207). In contrast, others propose that minor expression in presynaptic neurons would imply that NCX has little to do with neurotransmitter release but rather would contribute to rapid emptying of Ca^{2+} uptake organelles which serve as the main line of defence against high free Ca^{2+} (100). Minelli suggests that perisynaptic localization puts NCX in a favourable position for buffering Ca^{2+} exiting from postsynaptic sites, which could have a bearing on synaptic plasticity. An increase in $Ca^{2+}{}_i$ in postsynaptic neurons can occur due to increased neurotransmitter release from pre-synaptic terminals or delayed Ca^{2+} clearance from postsynaptic neurons, as seen in NCX2-/- mice. Mice deficient for NCX2 exhibit enhanced spatial learning and memory

secondary to delayed clearance of elevated Ca^{2+} following depolarization, favouring long term potentiation and enhanced synaptic plasticity (98) and supporting a role for Ca^{2+} removal from neurons. In addition, the presence of NCX in glial cells could also control Na^{+}_{i} concentrations, protecting neurons against Na^{+}-dependent glutamate-induced neurotoxicity (150).

NCX3, like NCX2, is expressed in the brain, but NCX3 knockout mice display features more closely related to neuromuscular transmission and muscular weakness. NCX3 is believed to maintain homeostatic levels of Ca^{2+} in the skeletal muscle in situations of fatigue or repetitive exercise, when high and sustained Ca^{2+} concentrations occur (133; 255). This is essential in preventing activation of Ca^{2+}-dependent necrotic pathways. Knockout of NCX3 causes impaired neuromuscular transmission, skeletal muscle fibre necrosis and cellular infiltrates, leading to muscle weakness and fatigability (235). Calcium clearance from motor nerve terminals appears to be dependent upon NCX3 and is necessary for timely neurotransmitter release during repetitive nerve stimulation.

Recently, NCX3 knock-out mice have been used to demonstrate that Ncx3 gene suppression leads to a worsening of brain damage after focal ischemia as well as massive neuronal death in hippocampal cell cultures and in cortical neurons exposed to oxygen and glucose deprivation followed by reoxygenation (155). Thus, suppression of NCX3 protein expression appears to have a detrimental effect in both neuronal and muscular tissues.

1.7.2 NCX and neurological conditions

During cerebral ischemia, increasing intracellular Na^+ levels in neurons and glial cells, in combination with cell membrane depolarization, cause NCX to function in its outward mode of exchange. This contributes to NMDA induced excitotoxicity by promoting Ca^{2+} influx (104; 105). Excitotoxicity refers to overactivation of the glutamate receptors, which are permeable to Na^+ and Ca^{2+}. The increase in cellular concentrations of these ions lead to neuronal death in a Ca^{2+} dependent manner, predominantly by activation of Ca^{2+}-dependent enzymes such as calpains and caspases (9). Excitotoxicity has been linked to several disease states, such as cerebral ischemia (70), traumatic brain injury (8), epilepsy (9), and Alzheimers's disease (148), among others. Therefore, NCX function may be involved in these neurological disorders by contributing to excitotoxicity.

Conflicting evidence of the neuroprotective effects of specific NCX isoforms is apparent and may be dependent on the experimental procedure used in the various studies. For example, following transient focal cerebral ischemia in rats, mRNA and protein levels of NCX1 appear to decrease, whereas NCX2 and NCX3 transcripts do not change significantly over time (122). In contrast, during permanent focal brain ischemia, NCX3 appears to be upregulated in the periinfarct regions as well as the nonischemic regions, whereas NCX2 is down regulated and NCX1 is only upregulated in nonischemic zones (18). The authors suggest that NCX1 and NCX3 may be neuroprotective, with NCX3 being more resistant than NCX1 following pMCAO. This is supported by studies using antisense oligodeoxynucleotides targeting NCX1 or NCX3, which increase the ischemic volume (183). Recently, it has been suggested that NCX1 and NCX3 may be

targets to the pro-survival Akt-mediated pathway, as NCX1 transcription and NCX3 translation appear to be induced by Akt activation during chemical hypoxia (44). Possibly, NCX3's neuroprotective properties are related to its ability to function in ATP-depleted conditions, in contrast to the other two isoforms. NCX3 could be neuroprotective in the ischemic core, where ATP levels are low, whereas in the peri-infarct area, where ATP is present, low intracellular Na^+ concentrations would cause NCX to function in its inward mode and prevent Ca^{2+} overload (4).

Recent studies suggest that overexpression of NCX2 may be neuroprotective during excitotoxicity, possibly linked to the inactivation of NCX3 by calpains (11). However, our laboratory has demonstrated that calpains cleave both NCX1 and NCX2 isoforms, deregulating the exchangers and rendering them constitutively active (170). NCX2 may be neuroprotective when functioning in its outward mode if indeed NCX2 is expressed in glial cells (242). NCX2 may cause Ca^{2+} to enter into the glial cells rather than into the neurons and thereby protect the functional cells for some time (243). It is evident that more studies are required to get a better understanding of the role each NCX isoforms plays with respect to normal brain function and survival during pathoneurological events.

1.8 NCX in the kidney and the vasculature

NCX1.3 is expressed in the kidney, predominantly in the distal convoluted tubules of the nephron, where it is believed to play a role in Ca^{2+} reabsorption (120). Ischemia-reperfusion-induced renal injury in heterozygous mice deficient in NCX exhibited less Ca^{2+} deposits in medullary epithelial cells and less epithelial cell necrosis as compared to

wild-type mice (257). Furthermore, KB-R7943, a specific inhibitor of outward exchange currents mediated by NCX1, was protective against this type of renal injury, suggesting that NCX outward-mode function, promoting Ca^{2+} overload during ischemia in the kidney, is involved in the pathological process leading to necrosis and acute renal failure (257; 258).

The NCX1.3 splice variant has been localized in vascular smooth muscle cells and appears to be involved in arterial tone control (233). In this tissue, NCX has been shown to contribute to Na^{+}-sensitive hypertension, as its pharmacological and genetic inhibition is protective, while its overexpression potentiates the effects of high Na^{+} on arterial tone and hypertension (80; 82). The presence of SEA0400, a potent and selective inhibitor of NCX, has been protective in salt-sensitive hypertension, vascular hypertrophy and renal dysfunction in animal models (89). SEA0400 inhibits NCX1.3 more potently than both the cardiac and the neuronal exchangers, possibly because NCX1.3 exhibits a greater extent of Na^{+} inactivation and SEA0400 stabilizes this conformation of the exchanger. It has also been demonstrated that angiotensin II significantly enhances NCX activity in vascular smooth muscle cells and therefore NCX may be involved in multiple pathways during the hypertensive state (241).

1.9 Inhibition of NCX

1.9.1 Cations

The first inhibitors of NCX function to be described were divalent cations such as Co^{2+}, Sr^{2+} and Mg^{2+} (248), Cd^{2+}, Ba^{2+} and Mn^{2+} and trivalent cations, such as La^{3+}, Nd^{3+}, Tm^{3+}, Y^{3+} (244). Nickel, a non-specific inhibitor of NCX, inhibits Na^{+}_{i}-dependent Ca^{2+}

uptake by competing against Ca^{2+} at the external transport site (71). Differences in Ni^{2+} sensitivities exist between NCX isoforms, with NCX1 and NCX2 having a ten-fold greater affinity than NCX3. It is believed that certain residues within the α-1 and α-2 repeats are predominantly responsible for these observed differences (95). As these inhibitors are not highly specific to NCX and are more effective when other ion transporters and ion channels are already blocked, they have limited value as experimental tools (79).

1.9.2 KB-R7943

The first isothiourea derivative exhibiting inhibitory effects on NCX was described in 1996 (97; 251). The 2-(2-[4-(4-nitrobenzyloxy)phenyl]ethyl)-isothiourea methane-sulphonate compound, better known as KB-R7943 and developed by Kanebo, is a non-competitive inhibitor with respect to Ca^{2+}_o which inhibits the exchanger from the external side of intact cells (71). Inhibition of the outward mode occurs at a potency of 0.3-2.4 μM, in contrast to the inward mode, which requires 10-50 times higher concentrations for similar effects (95). Inhibition of NCX by KB-R7943 has been shown to be protective in ischemia-reperfusion in the heart (118), with improved contractile function (216; 224), reduced propagation of cardiac hypercontracture (209), decreased enzyme release (115; 217), reduced infarct size (136; 139) and reduced incidence of arrhythmias (39; 216). KB-R7943's potential as a therapeutic agent has also been studied in the brain (21; 185; 220) and in the kidney (113; 256). However, KB-R7943 reportedly blocks ion channels, NMDA receptors and norepinephrine transporters at relatively low doses, and therefore may not be as specific as initially proposed (1; 5; 186; 205; 234).

1.9.3 SEA0400

In 2001, Taisho Pharmaceutical developed SEA0400 (2-(-4-[(2,5-difluorophenyl)methoxy]phenoxy)-5-ethoxyaniline), a novel isothiourea derivative, described as the most potent and selective inhibitor of NCX, with inhibitory potency for the outward mode of NCX in the nanomolar range (138). This potency is equivalent to thirty times that of KB-R7943 (87). SEA0400 preferentially inhibits the outward mode of NCX (86) by stabilizing the Na^+-dependent inactive state, as demonstrated by its effects on mutant exchangers with altered ionic regulatory properties (19; 87; 119). Its selective inhibitory effects for outward NCX currents appear to be strongly dependent on intracellular Na^+ concentrations (19; 119). This is an important observation, as SEA0400's effects would be minimal at physiological levels of Na^+_i, but would strongly inhibit NCX under pathophysiological conditions, when Na^+_i is high and the outward mode of action of NCX is more prominent. Furthermore, at nanomolar concentrations, SEA0400 had negligible effects on ion channels, norepinephrine transporters, a variety of receptors, the Na^+-H^+ exchanger, the Na^+-K^+ pump, Ca-ATPase and store-operated Ca^{2+} entry (138; 239). However, SEA0400 appears to have additional effects on other cellular components, as $NCX^{-/-}$ heart tubes exhibited depressed Ca^{2+} transients when subjected to low concentrations of SEA0400 (205), and therefore this compound should be used with caution. However, SEA0400 has demonstrated protective effects against *in vitro* and *in vivo* cerebral ischemia, with decreased infarct volume in the cerebral cortex (138). It has also proven to be cardioprotective (136; 238; 260) and protective against acute ischemic renal failure (84; 107; 167).

These inhibitors have differential sensitivities to the various NCX isoforms currently studied. Whereas KB-R7943 is three-fold more inhibitory for NCX3 than NCX1 or NCX2 (88), SEA0400 has maximal inhibitory effect on NCX1, moderate for NCX2 and minimal for NCX3 (87). It is believed that the difference in drug sensitivity between NCX1 and NCX3 is dependent on specific residues located in transmembrane segment 5, such as F213, which has the greatest impact on the formation of the SEA0400 receptor (87) and G833, located in the α-2 repeat and believed to be essential for KB-R7943-mediated inhibition (88). It has been proposed that both inhibitors interact with a specific receptor site, blocking ion pore formation and transport (79).

1.9.4 New NCX inhibitors

Recently, other inhibitors for NCX have been studied, such as CGP-37157, whose extent and potency of inhibition are less than those observed for SEA0400 and KB-R7943 (168). CGP-37157 has however been proposed as a selective mitochondrial NCX inhibitor (185). SN-6, a mode-selective inhibitor derived from KB-R7943, is believed to exert its inhibitory properties by its interaction with the XIP region (81) and also acts as an oxygen radical scavenger (69). SN-6 is known to be more inhibitory to NCX1 than to NCX2 and NCX3 (81). Most recently, YM-244769, a newly synthesized benzyloxyphenyl derivative with lower cell toxicity, has demonstrated cardioprotective capabilities, preventing ischemia/reperfusion-induced ventricular tachycardia and fibrillation (83; 112). Like SN-6, its inhibitory efficacy is dependent on the XIP region (250). However, it preferentially inhibits NCX3, and thus may be a potential therapeutic agent with neuromuscular protective properties.

1.10 Rationale for this study

Extensive studies of the Na^{+}-Ca^{2+} exchanger in the heart have demonstrated that while NCX is essential for maintaining homeostatic levels of Ca^{2+} in myocytes, it also has the potential to contribute to Ca^{2+} overload in cellular conditions when ionic imbalances occur. Overexpression of NCX in the heart, either experimentally or in disease conditions such as heart failure and hypertrophy, suggests that although normal cardiac function is possible, modifications in excitation-contraction coupling increase susceptibility to stressful events which can lead to death. Hypercontracture, arrhythmias and activation of cell death pathways are only a few of many consequences of Ca^{+2} overload, potentially aggravated by activation of NCX in its outward mode. Pharmacological inhibition of this specific mode of exchange has proven to be cardio-protective, rendering NCX a potential therapeutic target for cardiovascular disease. The outward mode of exchange is therefore critical and further investigation on its activation and regulation is warranted.

Mammalian species have the possibility of expressing over 20 different NCX variants, in distinct cell types and tissues and at different levels during development. Furthermore, these variants are regulated differently by the ions which they transport. Thus, as seen in the brain, a potential of three exchanger isoforms are expressed, and although their function is similar, their regulatory profiles confer unique roles for each one of them. Their distinct localization within the tissue, their response to changes in cellular environment and their regulatory profile as it pertains to Na^{+} and Ca^{2+} differ somewhat, potentially allowing for cell survival to occur in a cell specific manner. Structural domains influencing regulation have been identified and assist us in

determining the structural and molecular mechanisms mediating regulation and function of these exchangers.

The rationale for this study is to gain insight into the mechanisms regulating NCX exchange activity as modulated by the mutually exclusive exon in the alternative splice region, in conjunction with the XIP region. Along with previously characterized regulatory regions within the cytoplasmic loop of the exchanger, the alternative splice region appears to contribute to the ionic regulation of currents mediated by NCX. It has been demonstrated that specific residues in the mutually exclusive exon are involved in the structure-function relationship required for regulation of exchange activity for both NCX1 and CALX splice variants. I have chosen to investigate the region corresponding to the mutually exclusive exon in NCX2.1 to determine if this region has an equivalent impact on ionic regulation and if interactions with other regulatory domains are required to mediate these properties. Preliminary results suggested that Na^+-dependent regulation was involved, hence I chose to also investigate the XIP region of NCX2.1, comparing its role in Na^+-dependent inactivation with what has previously been shown for NCX1. Gaining insight into the role played by the mutually exclusive exon of the alternative splice region in the structure-function relationship of NCX1 and NCX2 may be beneficial in understanding the physiological role of NCX and ion transport mechanisms involved in Ca^{2+} homeostasis in different tissues.

2. HYPOTHESIS

The mutually exclusive exon in the alternative splice region of the Na^+-Ca^{2+} exchanger is a determinant of ionic regulation, either by direct or indirect association with other regulatory regions of the protein, such as the exchanger inhibitory peptide region (XIP) and the allosteric Ca^{2+} binding domains.

The main objective of this thesis is to investigate the mechanisms modulating ionic regulation of the Na^+-Ca^{2+} exchanger isoforms, NCX1 and NCX2, by examining:

1. the role of the mutually exclusive exons A and B in NCX1 and their analogous counterpart in NCX2 with respect to ionic regulation of the exchanger
2. whether contextual issues, such as the presence of other regulatory regions in the cytoplasmic loop, in combination with the mutually exclusive exons A or B in NCX1 or their analogous counterpart in NCX2, are needed to achieve the observed phenotypes
3. the XIP regions of NCX1 and NCX2 and how they affect NCX function and ionic regulation

3. MATERIALS AND METHODS

3.1 Construction of chimaeric exchangers

Chimaeric constructs were produced by PCR overlap extension, with NCX1.3, NCX1.4 and NCX2 as templates, using methods similar to those previously described (35). Three sets of primers were designed for each primer and synthesized by either Cortec Inc or Invitrogen. As illustrated in Figure 6, three DNA fragments were amplified: the first fragment (A) and the last fragment (C) coming from the parent exchanger, and the middle fragment (B) coming from the replacement exon. Fragment A was produced with a primer (P1) complementary with the nucleotide sequence slightly upstream of the restriction enzyme site which was used for subcloning and a random sequence allowing for further amplification of this fragment. The reverse primer (P2) matched the nucleotide sequence corresponding to the parent exchanger at the first site of chimerism with a 5' tail corresponding to the replacement exon sequence. Fragment B was produced using a primer (P3) with complementary sequence to P2 and a reverse primer (P4) with the nucleotide sequence coding for the 3' end of the exon of interest flanking a 5' overhang matching the parent exchanger at the second site of chimerism. Fragment C was produced using a primer (P5) complementary to P4 and an outermost reverse primer (P6) with sequence matching the parent exchanger at a site downstream of the subcloning site and a random sequence allowing for further amplification of the PCR-generated fragment. These fragments were amplified individually by PCR, using Deep Vent DNA Polymerase (New England Biolabs) and size and purity were assessed by gel electrophoresis. Following gel purification of the fragments A and B using Qiaquick PCR Cleaning kit

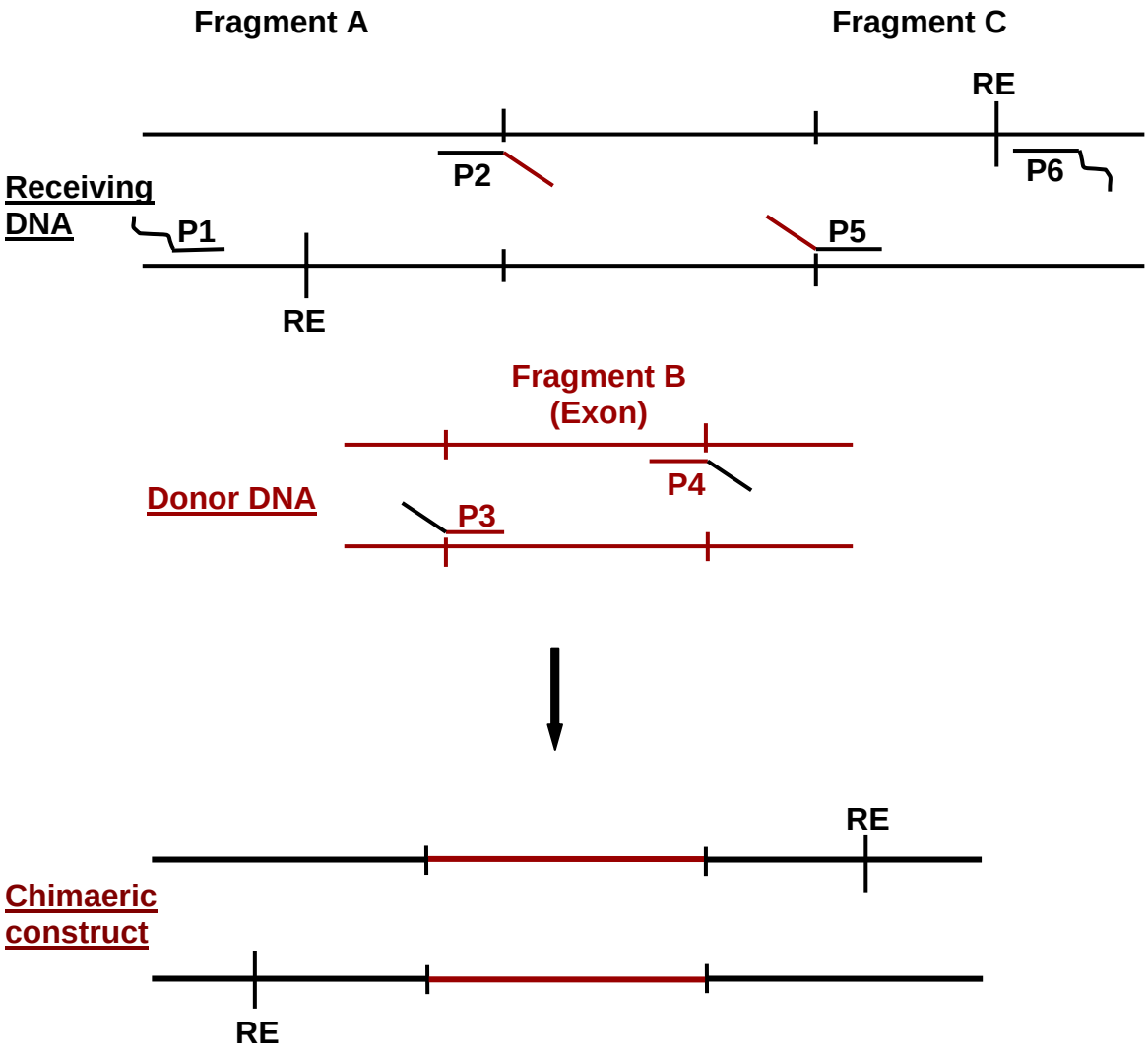


Figure 6. Representation of splicing protocol for chimaeric construction. Black lines represent sequences from receiving DNA, whereas red lines represent sequences from donor DNA. P1 to P6 represent primers designed for PCR amplification, and wavy ends on primers P1 and P6 represent non-complementary, random sequences. RE represents restriction enzyme site of digestion used for subsequent subcloning.

(Qiagen), these were annealed, extended and amplified by PCR using primers P1 and P4 and assessed for size and purity by gel electrophoresis. Following purification of the combined fragments A-B, the latter were annealed to fragment C, extended and amplified as done previously, using the two outermost primers (P1 and P6) mentioned above.

All constructs were subcloned into the parent NCX, which had been previously subcloned into the pBluescript II SK (+) plasmid, using *Bgl* II/*Eco*RI restriction sites (insert size 833bp) for NCX1.3 and NCX1.4 and *Xma* I/*Xho* I restriction sites (insert size 612 bp) for NCX2. All restriction enzymes were purchased from New England Biolabs. Briefly, both vector and insert were digested with the aforementioned restriction enzymes for 3 hours at 37°. The vector was subsequently dephosphorylated to prevent its recircularisation in the event of incomplete digestion. Following electrophoresis, both fragments were isolated from a 1 % agarose gel and purified using Qiaquick PCR Cleaning kit (Qiagen). Ligation of the insert containing the mutation and the wild-type vector was done using the Rapid DNA Ligation Kit (Roche). Following transformation into XL-1 Blue Ultra Competent Cells (Stratagene), DNA from six possible clones was purified and analysed for the presence of the subcloning sites. Two clones were selected and sequenced (Cortec) to assure correct nucleotide sequence at junction sites and throughout the insert created by PCR.

A similar protocol was followed to construct the XIP chimaeras in NCX1 and NCX2. These constructs were then subcloned into the parent NCX1 and the exon chimaera NCX1-2A using the *Age* I/ *Mfe* I restriction sites (insert size 740 bp). For NCX2.1 and its exon chimaeras NCX2-1A and NCX2-1B, the subcloning sites were the *Bam* I/*Xma* I restriction sites (insert size 1383 bp). The nomenclature used for these

constructs is depicted in Figure 7, with the first part of the name representing the parent exchanger and the second part representing the exchanger supplying the replacement exon and/or XIP region.

3.2 Site-directed mutagenesis

Single point mutations at residue 605 in the region corresponding to the mutually exclusive exon of NCX2.1 and at positions 233 to 237 in the XIP region of NCX1.3 were produced using the QuikChange Site-Directed Mutagenesis Kit (Stratagene). Complementary primers containing the mutation as well as an indicator restriction site, allowing detection of mutant transformants, were used to generate a mutated plasmid by PCR. The indicator sites were *Apo* I for NCX2.1 and loss of *NgoM* IV for NCX1.3. Following digestion of the parental dsDNA with *Dpn* I, the vector containing the desired mutation was transformed into XL-I Blue Ultra Competent Cells (Stratagene). A screening process, assessing the indicator restriction site as well as the preservation of the subcloning sites, was used to determine potential mutants. The subcloning sites for NCX2.1 were *Pml* I/*Xho* I, with insert size of 321 base pairs. For NCX1.3, the subcloning sites were *Age* I/ *Mfe* I, with insert size of 740 base pairs. Following subcloning of the mutant insert into the parent NCX2.1 or NCX1.3- pBluescript II SK (+), the constructs were confirmed by sequencing (Cortec Inc.) to ascertain the presence of the mutation and the absence of other changes in the upstream and downstream regions adjacent to the mutation.

3.3 cRNA synthesis

Complementary DNAs encoding for the various chimaeric constructs residing in pBluescript II SK (+) (Stratagene) were linearized with *Hin*dIII and purified using the Qiaquick PCR Cleaning kit (Qiagen). cRNA was synthesized using T3 mMessage mMachine in vitro transcription kit (Ambion) according to the manufacturer's instructions. More specifically, following a capped transcription reaction in the presence of RNA Polymerase Enzyme Mix and NTP/CAP mix at 37°C for 1 hour, template DNA was removed by DNase treatment before proceeding to RNA purification via lithium chloride precipitation and washing with 70 % ethanol. The RNA was resuspended in nuclease-free water (Ambion) and stored at -20°C.

3.4 Preparation and injection of *Xenopus laevis* oocytes

Xenopus laevis oocytes were prepared and stored as previously described (39). Briefly, *X. laevis* were anesthetized in 250 mg/l ethyl *p*-aminobenzoate (Sigma) in deionized ice water for 30 min. Oocytes were surgically removed and washed in *solution A*, containing (in mM) 88 NaCl, 15 HEPES, 2.4 $NaHCO_3$, 1.0 KCl, and 0.82 $MgSO_4$, pH 7.6 at room temperature (RT). The follicles were teased apart, and the oocytes were transferred to 5 ml of *solution A* containing ~3,500 U/ml collagenase (type II, Worthington) and incubated at RT for 45-60 min with gentle agitation. The oocytes were then washed several times in *solution B*, which contained (in mM) 88 NaCl, 15 HEPES, 2.4 $NaHCO_3$, 1.0 KCl, 0.82 $MgSO_4$, 0.41 mM $CaCl_2$, 0.3 mM $Ca(NO_3)_2$, and 1 mg/ml BSA (Fraction V, Sigma), pH 7.6 at RT, and were transferred to 5 ml of 100 mM K_2HPO_4, pH 6.5 at RT, containing 1 mg/ml BSA. After incubation at RT for 12 min with

gentle agitation, the oocytes were washed in *solution B* at RT. Defolliculated stage V-VI oocytes were selected and incubated at 18°C in *solution B* (without BSA) until injection the following day. Following injection with 25-30 ng of cRNA encoding NCX1 or NCX2 chimaeric or point mutation constructs, oocytes were maintained at 18°C and electrophysiological measurements were obtained from 4 to 14 days post-injection.

3.5 Measurement of Na^+/Ca^{2+} exchange activity using giant, excised patch clamp technique

Na^+-Ca^{2+} exchange current measurements were obtained using the giant, excised patch-clamp technique (60), as previously described (39). Briefly, borosilicate glass pipettes were pulled and polished to a final diameter of 20-30 μM and coated with a Parafilm^{TM}:mineral oil mixture to enhance patch stability and reduce electrical noise. The vitellin layer was removed by dissection and the oocytes were placed in a solution containing (in mM): 100 KOH, 100 MES, 20 HEPES, 5 EGTA, and 5-10 $MgCl_2$, pH 7.0 at room temperature (with MES). Gigaohm seals were formed by suction and membrane patches (inside-out configuration) were excised by progressive movements of the pipette tip. Rapid solution change was accomplished using a computer-controlled, 8-channel solution switcher.

For outward (reverse) Na^+-Ca^{2+} exchange current measurements, pipette (*i.e.*, extracellular) solutions contained (in mM): 100 *N*-methyl-D-glucamine-MES, 30 HEPES, 30 TEA-OH, 16 sulfamic acid, 8.0 $CaCO_3$, 6 KOH, 0.25 ouabain, 0.1 niflumic acid, and 0.1 flufenamic acid, pH 7.0 at room temperature (with MES). Outward currents were elicited by switching from Li^+- to Na^+-based bath solutions containing (in mM): 100 [Na^+

or Li^+]-aspartate, 20 CsOH, 20 HEPES , 20 TEA-OH, 10 EGTA, 0 to 9.91 $CaCO_3$, and 1.0-1.5 $Mg(OH)_2$, pH 7.0 at 30°C (with MES or LiOH). Solution changes were completed in ~200 ms and all experiments were conducted at 30°C. A holding potential of 0 mV was employed for all current measurements.

Paired-pulse experiments were performed to determine the rate of recovery from inactivation (65). Outward currents were measured for 32 secs, followed by a solution change removing Na^+_i from the intracellular side of the patch to terminate current. At timed intervals ranging from 400 ms to 32 s following the first pulse, a second pulse was activated by solution change to 100 mM Na^+_i. Rapid solution change was accomplished using a computer-controlled, 8-channel solution switcher.

3.6 Inhibition of NCX by SEA0400

SEA0400 (generously provided by Taisho Pharmaceutical Co., Ltd. (Tokyo, Japan)) was prepared as a 10 mM stock solution in dimethylsulfoxide and used at a final concentration of 0.1 μM. The final concentration of dimethylsulfoxide was therefore 0.01 % and did not influence our results. SEA0400 was applied to the cytoplasmic surface of the patch for all experiments. Outward currents were measured as described above.

3.7 Analysis of data

Axon Instruments hardware (Axopatch® 200A) and software (AxoTape®) were used for data acquisition and analysis, and Origin® software was used for curve-fitting and statistical analyses. The values of steady-state currents were obtained by curve-

fitting, whereas peak currents were determined by visual inspection. When peak was not clearly expressed, the value of the current monitored 1 s after the onset of current was acquired as a "peak" value. Fss, the fractional steady-state current, was calculated from the ratio of theoretical current level at infinite time, obtained from fitting current traces to a single exponential decay function, to the initial peak current. Rate of recovery was determined by calculating the ratio of the initial peak current with the peak current achieved on the second pulse. Pooled data is expressed in mean ± SEM format. Student's *t*-test was used to determine statistical significance, with $P \leq 0.05$ being considered statistically significant.

4. RESULTS

The main objective of this study is to investigate the mechanisms modulating ionic regulation of the Na^+-Ca^{2+} exchanger isoforms, NCX1 and NCX2.1. The regulatory domains of NCX are predominantly located within the large cytoplasmic loop of the protein, and are known to influence each other. This study focuses on the area corresponding to the mutually exclusive exon in the alternative splice region, specifically examining how this region influences distinct Na^+ and Ca^{2+}-dependent regulatory phenotypes, either independently or in concert with other regulatory domains of the exchanger.

Ionic regulatory profiles of NCX1 splice variants expressing either the mutually exclusive exon A or exon B have previously been described and demonstrate that this region is responsible for subtle differences in exchanger activity (38). Structural and site-directed mutational analysis studies have identified key residues within the mutually exclusive exon A which appear to be involved in coordination of regulatory Ca^{2+} binding and stabilization of the exchanger, allowing for activation of current (17; 35; 59; 99; 164). As structural studies have been limited to the Ca^{2+}-binding domains, which contain the alternative splice region but not the other regulatory or transport regions of the exchanger, it may be of interest to study the mutually exclusive exon in its usual conformation, within the complete protein. Thus, this study will assist us in gaining insight into possible molecular mechanisms by which the region corresponding to the mutually exclusive exon, in combination with other regulatory regions, mediates ionic regulation in the intact exchanger.

4.1 Comparison of the mutually exclusive exon region in NCX1 and NCX2

To date, NCX2.1 is believed to be the only mammalian isoform that does not undergo alternative splicing. However, the region corresponding to the mutually exclusive exon is maintained, with conservation of key residues involved in Ca^{2+} binding. Amino acid sequence comparison between exons A and B of NCX1 and the corresponding region in NCX2 is shown in Figure 7A (boxed letters). High variability is evident across the region, other than the small conserved acidic region and a few aromatic or charged residues. Although conserved glutamate residues have been shown to assist in structural stability of the Ca^{+2}-binding domain 2 (CBD2) in NCX1, other key residues essential for unique regulatory properties differentiating NCX1 exon A and exon B phenotypes, such as D578 and K585 (Figure 7A, underlined letters), are not thoroughly conserved in NCX2.1. The importance of non-conserved residues in mediating ionic regulation of the exchangers has been examined more closely by way of chimaeric constructs and site-directed mutational analysis.

Exchange of the region corresponding to the mutually exclusive exon between NCX1 splice variants expressing exon A (NCX1.4) and exon B (NCX1.3) and NCX2.1 created functional chimaeric constructs in all cases (the nomenclature used for the chimaeric constructs is explained in Figure 7C). To study the impact of these substitutions on ionic regulation, the giant, excised patch-clamp technique was used to measure currents mediated by these mutant constructs. As the ionic regulatory effects mediated by Ca^{2+} are more easily observed on outward exchange currents, where transport and regulatory Ca^{2+} are on opposite sides of the membrane, observations are limited to this mode of exchange. Ca^{2+}-dependence of outward peak and steady state

A

NCX 1.4	Exon A	569	K T I S V K V I D D E E Y E K N
NCX 1.3	Exon B	569	K I I T I R I F D R E E Y E K E
NCX 2.1	Equivalent	589	K T L Q V K I V D D E E Y E K K

585	K T F F L E I G E P R L V E M S E K K	
585	C S F S L V L E E P K W I R R G M K	
605	D N F F I E L G Q P Q W L K R G I S	

B

NCX 1	219	R R L L F Y K Y V Y K R Y R A G K Q R G
CX 2	248	K R L L F Y K Y V Y K R Y R T D P R S G



C

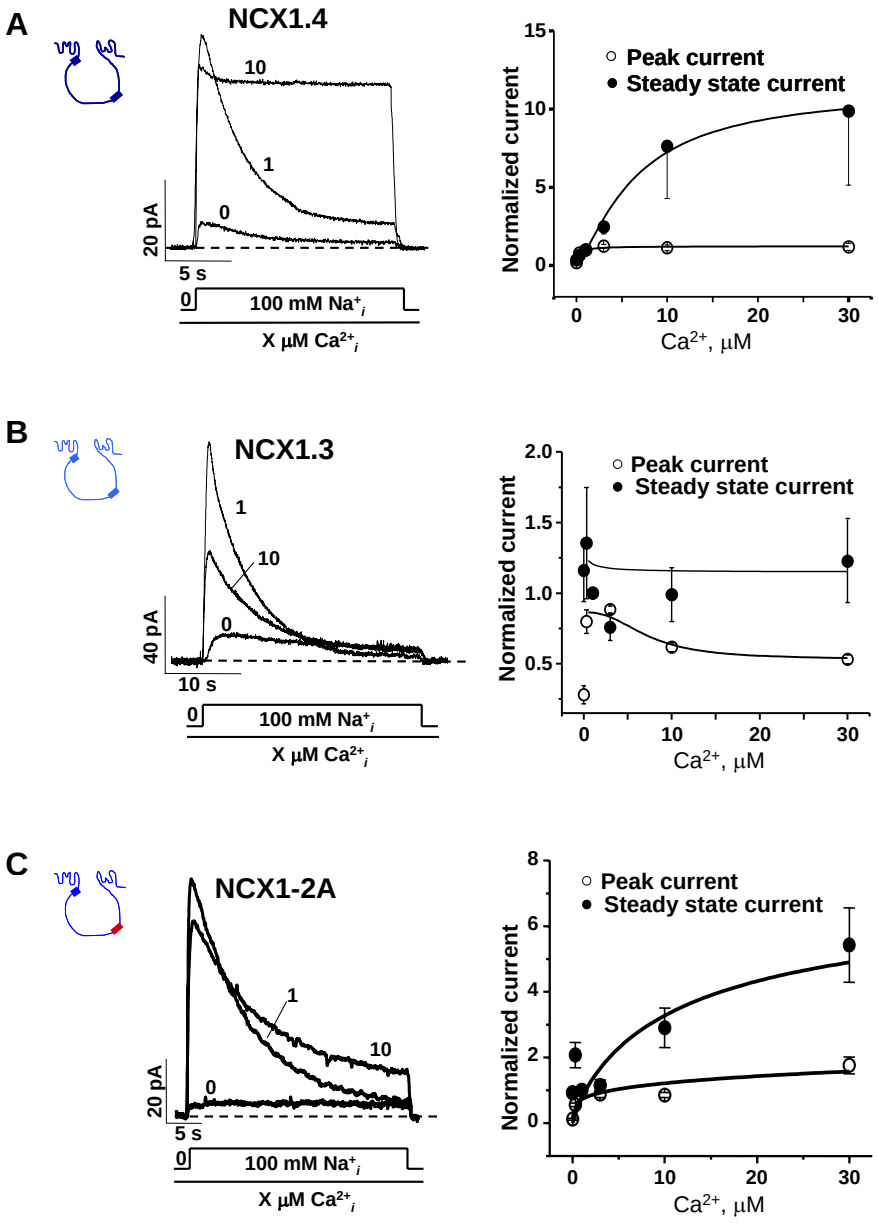
Chimaera	Parent exchanger	XIP region	Exon region
NCX1-2A	NCX1.4	NCX1	NCX2.1
NCX2-1A	NCX2.1	NCX2.1	NCX1.4 (A exon)
NCX2-1B	NCX2.1	NCX2.1	NCX1.3 (B exon)
NCX2-1A-XIP1	NCX2.1	NCX1	NCX1.4 (A exon)
NCX2-1B-XIP1	NCX2.1	NCX1	NCX1.3 (B exon)
NCX2-XIP1	NCX2.1	NCX1	NCX2.1
NCX1.4-XIP2	NCX1.4	NCX2.1	NCX1.4 (A exon)
NCX1.3-XIP2	NCX1.3	NCX2.1	NCX1.3 (B exon)

Figure 7. Sequence comparison and nomenclature for chimaeric constructs. A. Sequence comparison of the region corresponding to the mutually exclusive exons of NCX1.4, NCX1.3 and NCX2.1. Single-letter amino acid code is used and identities are boxed. Underlined residues illustrate the two critical residues distinguishing between NCX1 splice variant phenotypes. B. Sequence comparison of the XIP region of NCX1 and NCX2. C. Nomenclature used for chimaeric constructs, demonstrating origin of the regulatory regions for each construct.

currents were analyzed. Furthermore, the fractional steady state, a measure of the extent of Na^+-dependent inactivation of outward exchange currents, was measured for currents mediated by the chimaeric exchangers.

To appreciate subtle differences in ionic regulation of exchange currents mediated by the chimaeric constructs, it is essential that the regulatory phenotype for the parent exchanger be known. The unique regulatory profiles of outward exchange currents mediated by NCX1 splice variants expressing either exon A (NCX1.4) or exon B (NCX1.3) have previously been described by our lab (38) and are depicted by representative traces in Figures 8A and 8B. At 1 μM regulatory Ca^{2+}, outward exchange currents peak rapidly but gradually decline to a steady state level in response to high Na^+ on the intracellular side of the patch. This Na^+-dependent inactivation (I_1) at low $Ca^{2+}{}_i$ concentrations can be alleviated at higher levels of $Ca^{2+}{}_i$, such as observed with NCX1.4 (Figure 8A). At 10 μM $Ca^{2+}{}_i$, peak currents do not degrade significantly and little inactivation occurs. In contrast, NCX1.3 exhibits robust I_1, which is maintained independently of intracellular Ca^{2+} concentrations (Figure 8B). Normalized peak currents are at their highest level at 1 μM $Ca^{2+}{}_i$, and then decrease as $Ca^{2+}{}_i$ concentrations increase. Normalized steady state currents remain stable.

Substitution of the mutually exclusive exon of NCX1 with the corresponding region from NCX2.1 (chimaera NCX1-2A) appears to have minimal effects on outward exchange currents, as observed in Figure 8C. The rate and extent of Na^+-dependent inactivation are unchanged as compared to what is observed with native NCX1 currents. This phenotype is maintained independently of regulatory Ca^{2+} concentrations, as seen for NCX1.3-mediated outward currents (compare Figures 8B and 8C). The extent of



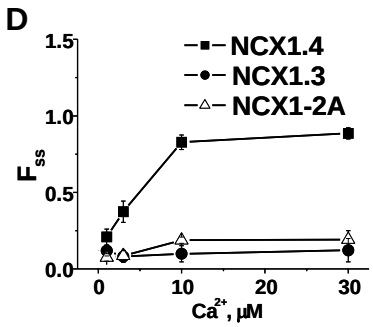


Figure 8. Ca^{2+}_i-dependence of NCX1-mediated outward currents. Overlapping representative outward exchange current transients at 0, 1 and 10 μM Ca^{2+}_i for A. NCX1.4, B.NCX1.3 and C. NCX1-2A, the NCX1 chimaeric construct with the mutually exclusive exon substituted with the corresponding region from NCX2.1. Outward currents were measured in the presence of 100 mM Na^+ and increasing μM levels of Ca^{2+} on the intracellular side of the patch. Pooled data for normalized peak and steady state currents are at the right, demonstrating activation of outward currents with increasing levels of Ca^{2+}. D. Comparison of extent of Na^+-dependent inactivation, exhibited as fractional steady state current (Fss) for NCX1.4, NCX1.3 and NCX1-2A (n≥4).

Na^+-dependent inactivation can be calculated by the ratio of steady state to peak outward currents, and is known as the fractional steady state current (Fss). In comparison to Fss values for both NCX1 splice variants, NCX1-2A chimaera behaves similarly to NCX1.3, maintaining Fss values lower than 0.25 at all Ca^{2+}_i concentrations assayed (Figure 8D). This reflects the stabilized inactive state of the exchanger, which is maintained at high Ca^{2+}_i concentrations.

Amino acid sequence variability between the mutually exclusive exons of NCX1 and the analogous region in NCX2.1 is high, yet conserved residues appear to be sufficient to maintain the Na^+- and Ca^{2+}-dependent regulatory phenotypes of NCX1 in the NCX1-2A chimaera. Similarities in the outward exchange currents mediated by the NCX1-2A chimaera and NCX1.3, pertaining to stabilization of the Na^+-dependent inactive state at high Ca^{2+}_i concentrations, are evident. This suggests that in contrast to exon A (NCX1.4), residues in exon B (NCX1.3) and the corresponding region in NCX2.1 are essential in mediating this property.

4.2 Stability of Na^+-dependent inactive state at high Ca^{2+}_i concentrations in NCX2.1

Examination of the amino acid sequence of the region corresponding to the mutually exclusive exon of NCX2.1, particularly around the conserved acidic cluster, reveals that the two residues previously identified by Dunn et al (35), primarily responsible for the phenotypic differences between NCX1.4 and NCX1.3, are not completely conserved (Figure 7A underlined letters): D578 is maintained in NCX1.4 and NCX2.1 whereas NCX1.3 expresses an arginine, and K585 in NCX1.4 corresponds to a

cysteine in NCX1.3 and an aspartate in NCX2.1. To determine if the presence of the two charged amino acids at positions 578 and 585 are required for alleviation of I_1 at high Ca^{2+} concentrations in NCX2.1, as seen with NCX1.4, site directed mutagenesis was performed. As the aspartate residue at position 578 in NCX1.4 is conserved in NCX2.1, only the negatively charged aspartate at position 605 in NCX2.1 was exchanged for a positively charged lysine, thus replicating the charge found at the corresponding position in NCX1.4 (K585).

Our data demonstrates that the presence of a charged residue at position 605 in NCX2.1 modifies its native ionic regulatory phenotype. Comparison of outward exchange current traces mediated by native NCX2.1 and its D605K mutant reveals differences in regulatory profile (Figures 9A and 9B). Wild type NCX2.1-mediated outward currents have minimal Na^+-dependent inactivation at low Ca^{2+}_i concentrations (1 μM). As Ca^{2+}_i concentrations increase into the 3 to 30 μM range, Na^+-dependent inactivation becomes moderate and remains stable (Figure 9A). NCX2.1 D605K has stronger I_1 at 3 μM Ca^{2+}, which decreases significantly at 30 μM Ca^{2+} (Figure 9B).

Comparison of fractional steady state currents (Fss) for NCX2.1, NCX2.1D605K and NCX1.4 is illustrated in Figure 9C. At low Ca^{2+}_i concentrations (3 μM), Fss values for NCX1.4 and NCX2.1D605K are very similar, whereas NCX2.1 displays a higher value. Although the differences are not statistically significant ($p=0.06$), the trend demonstrates that Na^+-dependent inactivation is not as prominent in NCX2.1. However, as Ca^{2+}_i concentrations increase to 30 μM Ca^{2+}, Fss values for NCX2.1 decrease whereas they increase significantly for both NCX1.4 and NCX2.1D605K, corresponding to alleviation of I_1. Thus, the presence of charged residues in proximity to the acidic

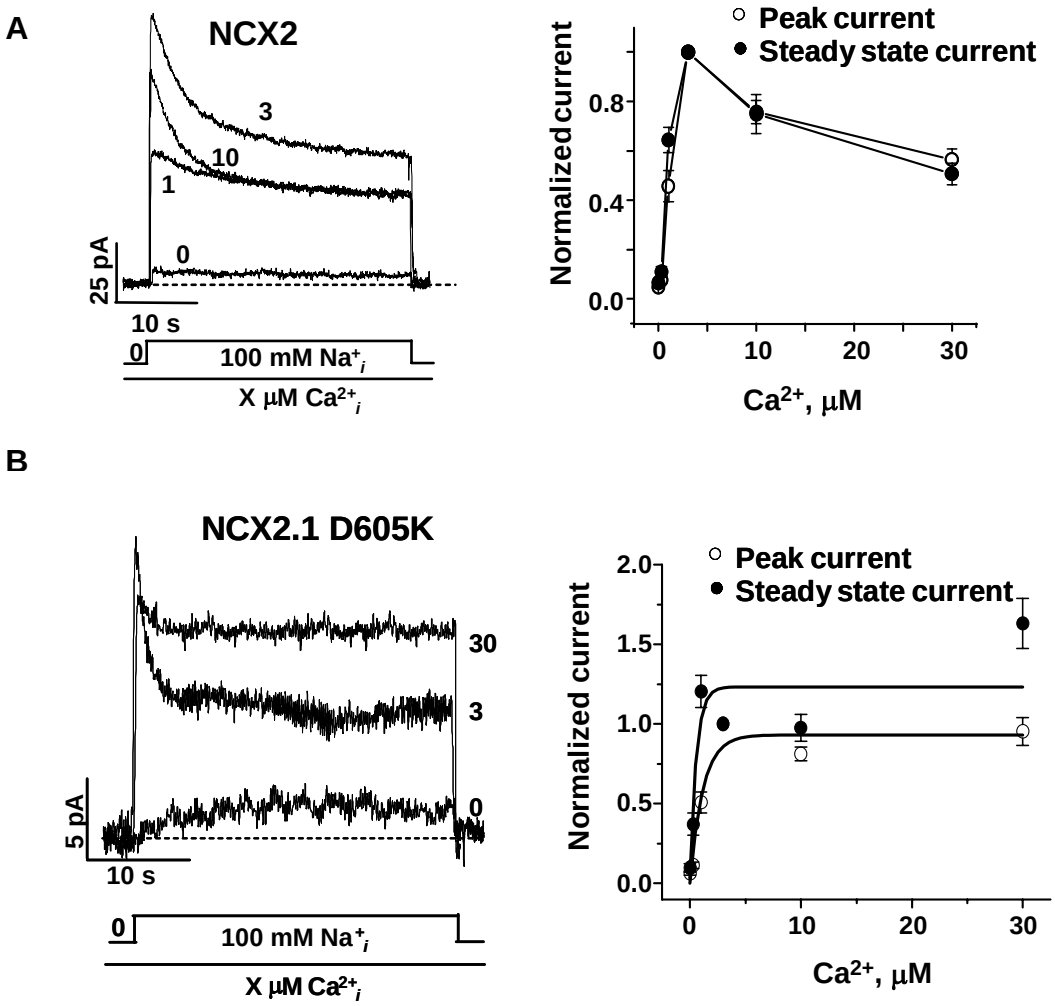


Figure 9. $Ca^{2+}{}_i$-dependence of NCX2-mediated outward currents. Overlapping representative current transients at various μM [$Ca^{2+}{}_i$] for A. NCX2.1 and B. the NCX2 D605K mutant, mimicking exon A residues shown to be responsible for alleviation of I_1 in NCX1.4. Pooled data for normalized peak and steady state currents are at the right, demonstrating activation of outward currents by Ca^{2+}. C. Fractional steady state comparison between NCX2.1, its D605K mutant and NCX1.4, with respect to low (3μM) and high (30 μM) intracellular Ca^{2+} (n ≥5). Statistical significance determined by Student t test, $p<0.05$ indicated by an asterisk; number sign shows differences which are not statistically significant (P=0.06) but demonstrate a trend.

segment in the region corresponding to the mutually exclusive exon can influence regulation of the Na^+-dependent inactivation in response to regulatory Ca^{2+} in both NCX1 and NCX2.1 isoforms.

4.3 The role of the region corresponding to the mutually exclusive exon on Na^+-dependent inactivation in NCX2.1

As our initial results demonstrate, replacement of the mutually exclusive exon region in NCX1 with its counterpart from NCX2.1 (chimaera NCX1-2A) appears to have little influence on the basic function of the exchanger and its ionic regulation. To explore further, we performed the reverse experiment, substituting the analogous region in NCX2.1 with either the A or B exon from NCX1, creating the chimaeras NCX2-1A (containing exon A from NCX1.4) and NCX2-1B (containing exon B from NCX1.3). As shown by representative traces in Figures 10A and 10B, it is clearly evident that for both chimaeras, Na^+-dependent inactivation is limited, at all $Ca^{2+}{}_i$ concentrations assayed. Peak currents do not degrade significantly and elevated steady state levels are maintained in the presence of elevated intracellular Na^+. Although wild-type NCX2.1 exhibits only moderate I_1, especially at higher $Ca^{2+}{}_i$ concentrations (Figure 9A), it is obvious that both NCX2-1A and NCX2-1B chimaeras exhibit less. This is clearly depicted in Figure 10C, with comparison of fractional steady states for the three exchangers. The difference is most noticeable for NCX2-1B, where F_{ss} values of 1 at low $Ca^{2+}{}_i$ concentrations represent no inactivation. Furthermore, both chimaeras are less responsive to elevations of regulatory $Ca^{2+}{}_i$ levels, as can be determined by minimal changes in F_{ss} values as $Ca^{2+}{}_i$

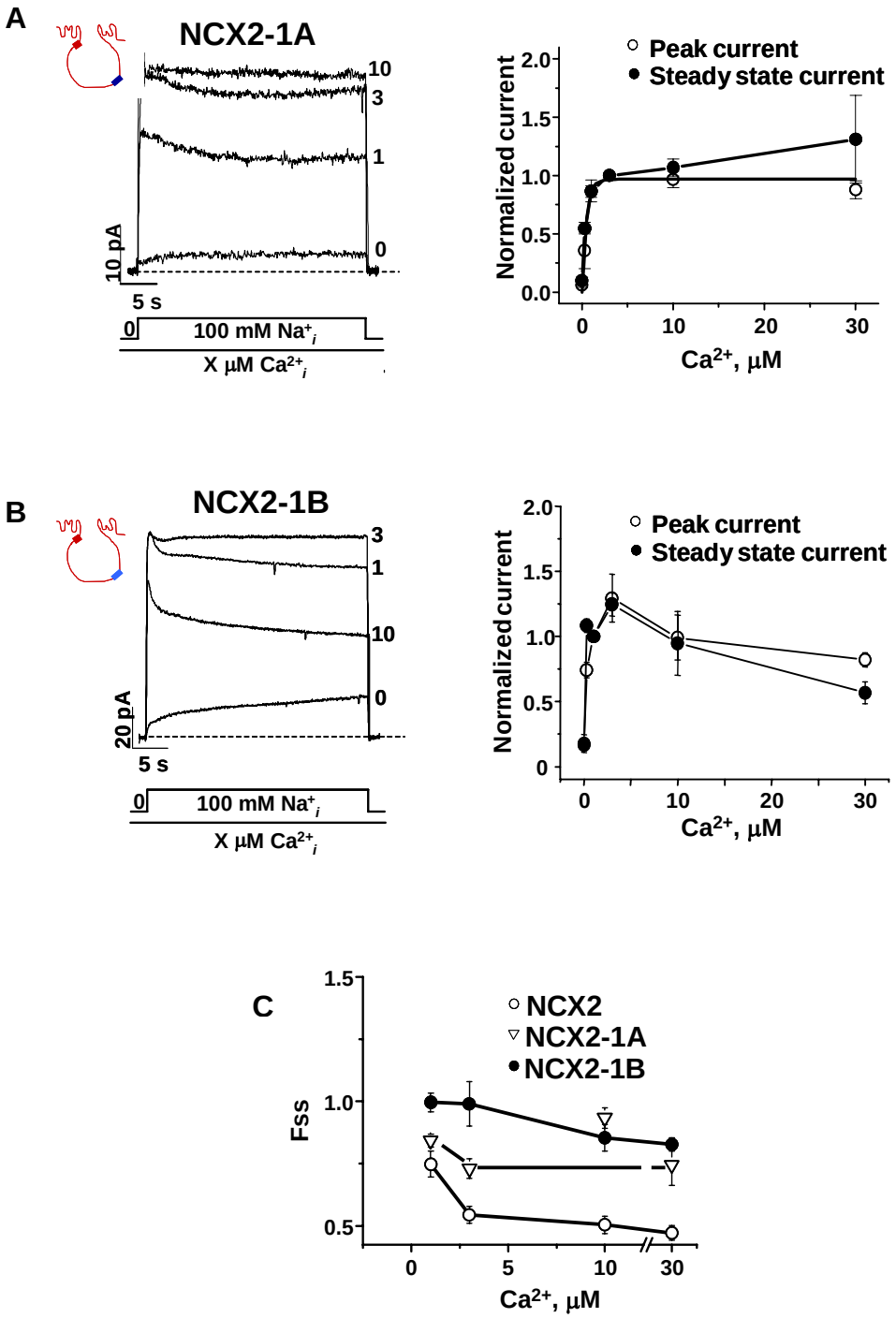


Figure 10. Ca^{2+}_i-dependence of NCX2.1 chimaera-mediated outward currents. Overlapping representative current transients at 0, 1, 3 and 10 µM Ca^{2+}_i for NCX2.1 chimaeric constructs with either A. exon A or B. exon B substitution from NCX1. Pooled data for normalized peak and steady state currents at increasing Ca^{2+} concentrations (n ≥5) are at the right. C. Ca^{2+} dependence of fractional steady state current (Fss) for NCX2.1 and its exon chimaeras. A shift in Na^+-dependent inactivation for exon A and B chimaeras is observed, with decreased inactivation and responsiveness to elevations of regulatory Ca^{2+}_i levels as compared to native NCX2.1 (n≥5).

concentrations increase, in contrast to NCX2.1, where Fss values decrease by 40 %, from 0.75 ± 0.05 at 1 μM Ca^{2+}_i to 0.47 ± 0.03 at 30 μM Ca^{2+}_i.

To test if the reduction in Na^+-dependent inactivation observed for NCX2.1 chimaeras is due to their inability to enter into the Na^+-dependent inactive state, outward exchange currents were measured in the presence of the inhibitor SEA0400. This pharmacological agent preferentially blocks the outward mode of exchange mediated by NCX in the presence of elevated Na^+_i levels by promoting and stabilizing the inactive state of the exchanger (119). If the inactive state is unable to form, the presence of the inhibitor should not influence the outward exchange current profile. However, if the inactive state is possible but not stable, the inhibitor may assist is maintaining the structure required to keep the exchanger in its inactive form.

Representative traces of outward exchange currents mediated by NCX2.1 and its chimaeras in the presence of 0.1 μM SEA0400 applied to the cytoplasmic side of the patch are depicted in Figures 11A-11C. The SEA0400 concentration used for all experiments has been shown to achieve maximal inhibitory effect without becoming toxic to the oocytes (119). Outward currents were measured on the second or third pulse following inhibitor application, when the maximal inhibitory effect is observed. Although peak currents in the presence of SEA0400 were only inhibited by approximately 20-40 %, steady state currents decreased by 60 % for NCX2.1 and 78 % for both NCX2 chimaeras (Figure 11D, bar graph). This suggests that these chimaeras maintain their ability to enter the Na^+-dependent inactive state, which can only be observed in the presence of the inhibitor SEA0400. These chimaeras may therefore be lacking appropriately interacting residues necessary for forming and maintaining the secondary

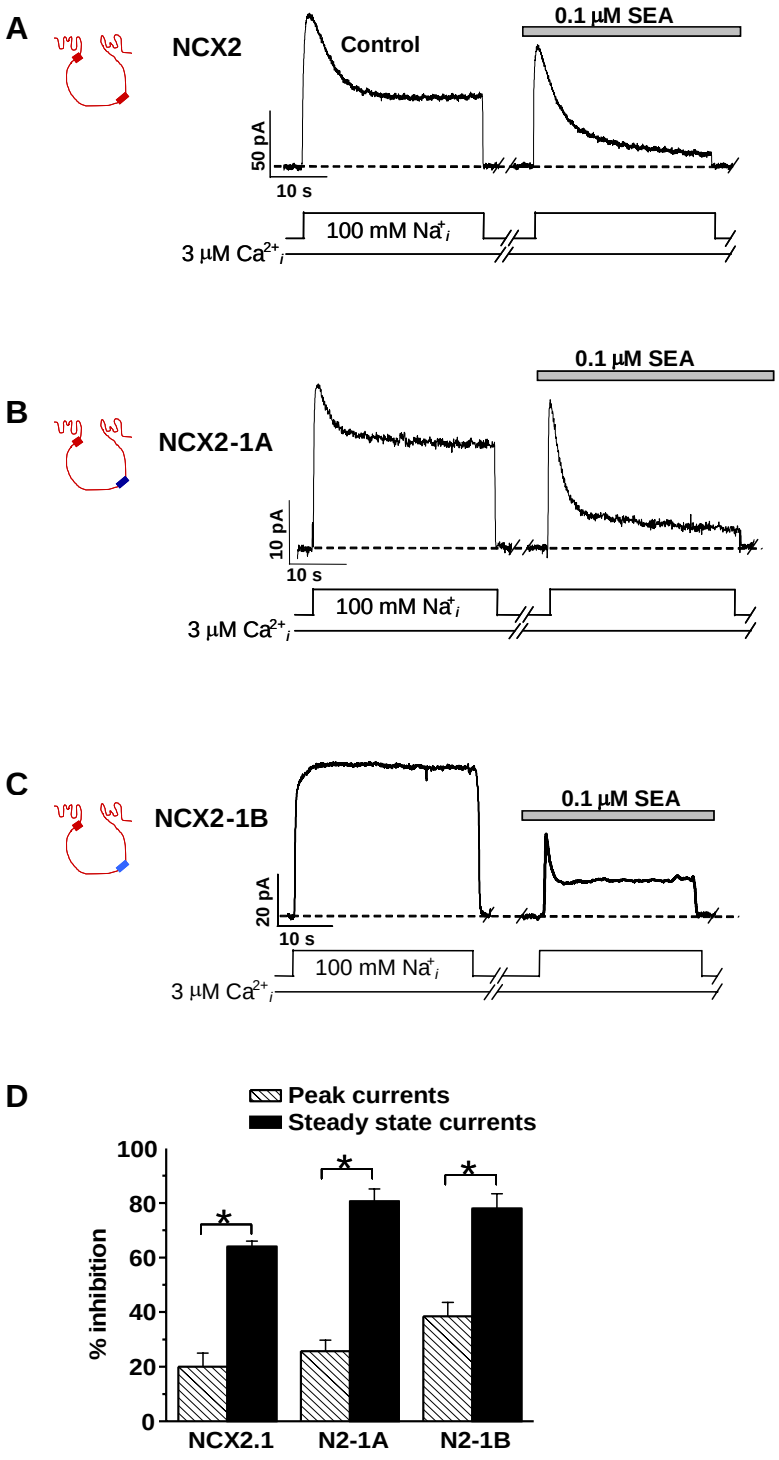


Figure 11. Inhibition of outward exchange currents in the presence of SEA0400. Representative traces of outward current mediated by A. NCX2.1, B. NCX2-1A and C. NCX2-1B chimaeras before and 2-3 pulses following application of 0.1 µM SEA0400. D. Pooled data for SEA0400-mediated inhibition of peak and steady state currents for above-mentioned exchangers (n≥4). Statistical significance determined by Student t test, $p<0.05$ indicated by an asterisk.

structure required for stability of the inactive state.

The phenotypes exhibited by chimaeras NCX2-1A and NCX2-1B suggest that the region analogous to the mutually exclusive exon in NCX2.1 plays a greater role in ionic regulation of outward exchange currents, particularly in Na^+-dependent inactivation, in comparison to the mutually exclusive exons in the NCX1 isoform. Alternatively, it is also plausible that the exons A and B in NCX1 require interactions with other key residues in their own native sequence to mediate Na^+-dependent inactivation. To test the hypothesis that a link between the mutually exclusive exon and other regulatory regions of the exchanger may exist, double chimaeras were constructed. As the extent of Na^+-dependent inactivation was significantly modified in the NCX2.1 exon chimaeras, interactions with the XIP region, essential for Na^+-dependent inactivation (56; 142; 144), could potentially be affected. I therefore chose to create double chimaeras substituting the region analogous to the mutually exclusive exon, in combination with the XIP region, between the two NCX isoforms, NCX1 and NCX2.1

4.4 Interaction between the mutually exclusive exon and the XIP region from NCX1

Key aromatic and positively charged residues in the XIP region of NCX are highly conserved amongst the two isoforms used in this study. Comparison between NCX1 and NCX2.1 amino acid sequences highlight only five amino acids at the C-terminal end of the XIP region which are non-homologous (Figure 7B). The first residue in the XIP region of NCX1 is R219, and with its positively charged side chain, it is comparable to the lysine found at the corresponding position in NCX2.1. In the non-

conserved section of the C-terminal end of the XIP region, the first amino acid is maintained as an uncharged polar residue, with an alanine in NCX1 and a threonine in NCX2.1. However, the following residues differ significantly between NCX1 and NCX2.1. Whereas NCX1 has two positively charged residues in this region, NCX2.1 has a negatively charged aspartate, a proline, whose conformational constraint imposed by its cyclic nature may cause a change in the secondary structure of the entire XIP region, a positively charged arginine and a serine, with its polar hydroxyl side chain and potential phosphorylation site. Hence, the differences in charge and structure imposed by these residues distinguishing between NCX1 and NCX2.1 XIP regions may influence not only the secondary structure of the region, but also possible interactions with other residues in the cytoplasmic loop. This is evidenced by their respective regulatory profiles, as generally, NCX1 splice variants have a strong Na^+-dependent inactivation, whereas NCX2.1 displays only moderate I_1.

To determine the importance of the non-conserved residues in the XIP region on ionic regulation, single chimaeric exchangers were constructed, substituting the entire XIP region from NCX1 into NCX2.1 and vice versa into both NCX1.4 and NCX1.3. Furthermore, to establish if the mutually exclusive exon in NCX1 and its corresponding region in NCX2.1 influences the regulatory profile exhibited by the XIP region from the same isoform, we created double chimaeras, substituting both regions from one isoform into the other. We then measured outward exchange currents mediated by these constructs to determine if substitution of the XIP region, alone or in combination with the region corresponding to the mutually exclusive exon, modifies ionic regulation.

As shown in Figure 12A, substituting the XIP region in NCX2.1 with its counterpart from NCX1 (chimaera N2-XIP1) has little impact on ionic regulation of outward currents when compared to the ionic profile for native NCX2.1 (Figure 9A). Ca^{2+}-dependence curves of normalized peak and steady state currents are very similar. The extent of Na^{+}-dependent inactivation, as determined by the Fss values, is greater as Ca^{2+}_{i} concentrations increase, but remain at moderate levels for both exchangers (Figure 13A, NCX2.1 in white bars, NCX2-XIP1 in grey bars). Taken together, these data demonstrate that substitution of the XIP region in NCX2.1 with its homologue from NCX1 does not cause significant changes in NCX2.1 ionic regulatory profile.

The presence of both the mutually exclusive exon A and the XIP region from NCX1 in an NCX2.1 background causes changes in ionic regulation of outward exchange currents as compared to wild type NCX2.1 and its single chimaeric constructs, NCX2-1A and NCX2-XIP1. Currents mediated by the NCX2-1A-XIP1 chimaera exhibit moderate Na^{+}-dependent inactivation at low regulatory Ca^{2+} levels (1 and 3μM), but this inactivation is suppressed at 10 μM Ca^{2+} (Figure 12B and Figure 13A, NCX2-1A-XIP1 in striped bars). Thus, Na^{+}-dependent inactivation is moderate, such as observed in native NCX2.1, and is alleviated at higher Ca^{2+}_{i} concentrations, as observed for NCX1.4. This chimaeric construct therefore displays a regulatory phenotype with properties from both the parent and the donor exchangers. In comparison with the chimaeric construct NCX2-1A, where Na^{+}-dependent inactivation is limited over the range of Ca^{2+} concentrations assayed (Figure 13A, NCX2-1A in black bars), it would appear that the presence of the XIP region from NCX1.4 is also required for Na^{+}-dependent inactivation to occur. Potentially, an interaction between residues in the mutually exclusive exon A and the XIP

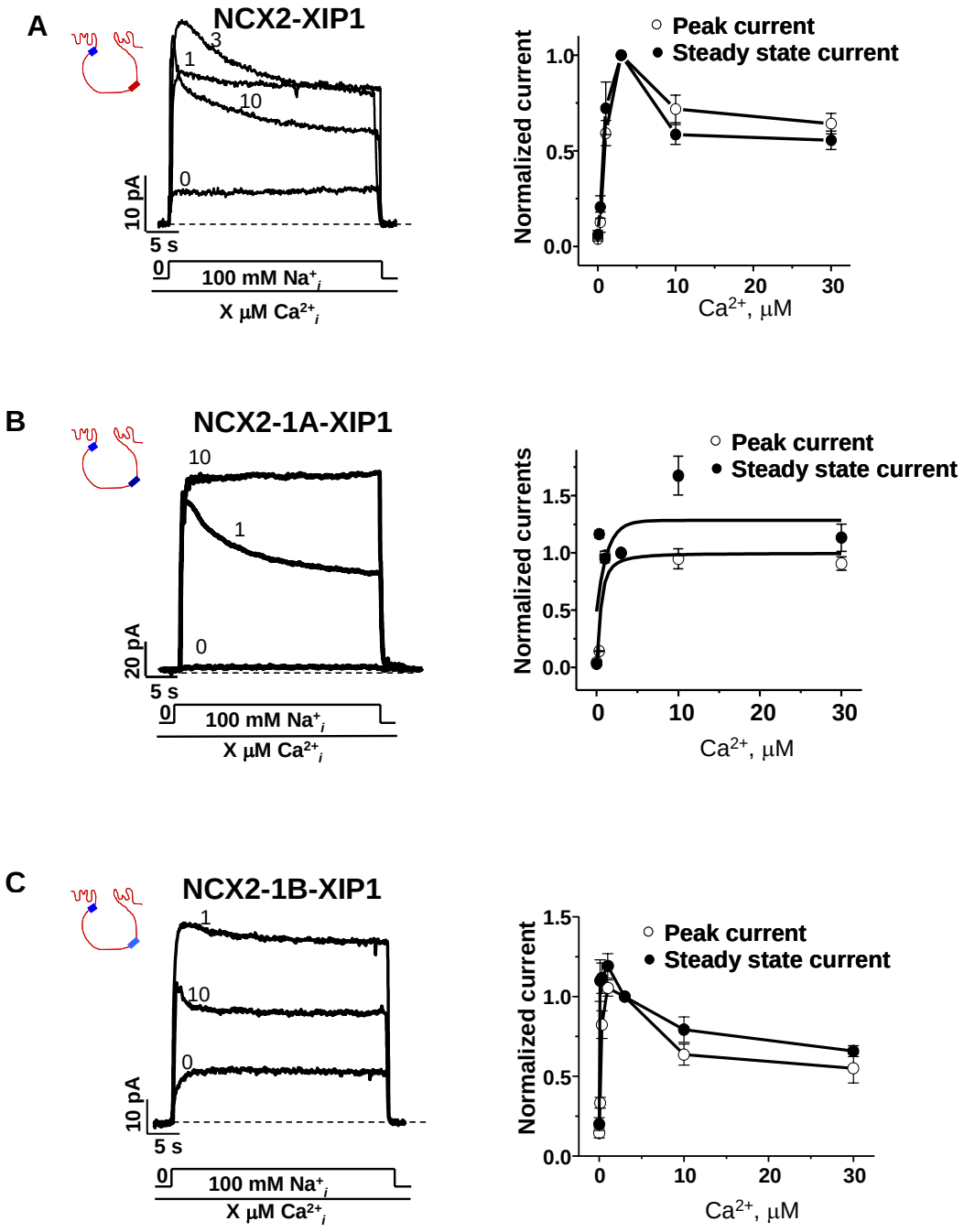


Figure 12. Ca^{2+}_i-dependence of NCX2 double chimaeras for outward exchange currents. Overlapping representative current transients at 0, 1, 3 and 10 µM Ca^{2+}_i for A. NCX2.1-XIP1, B. NCX2-1A-XIP1 and C. NCX2-1B-XIP1 chimaeric constructs. Pooled data for normalized peak and steady state currents (n ≥5) are depicted at the right.

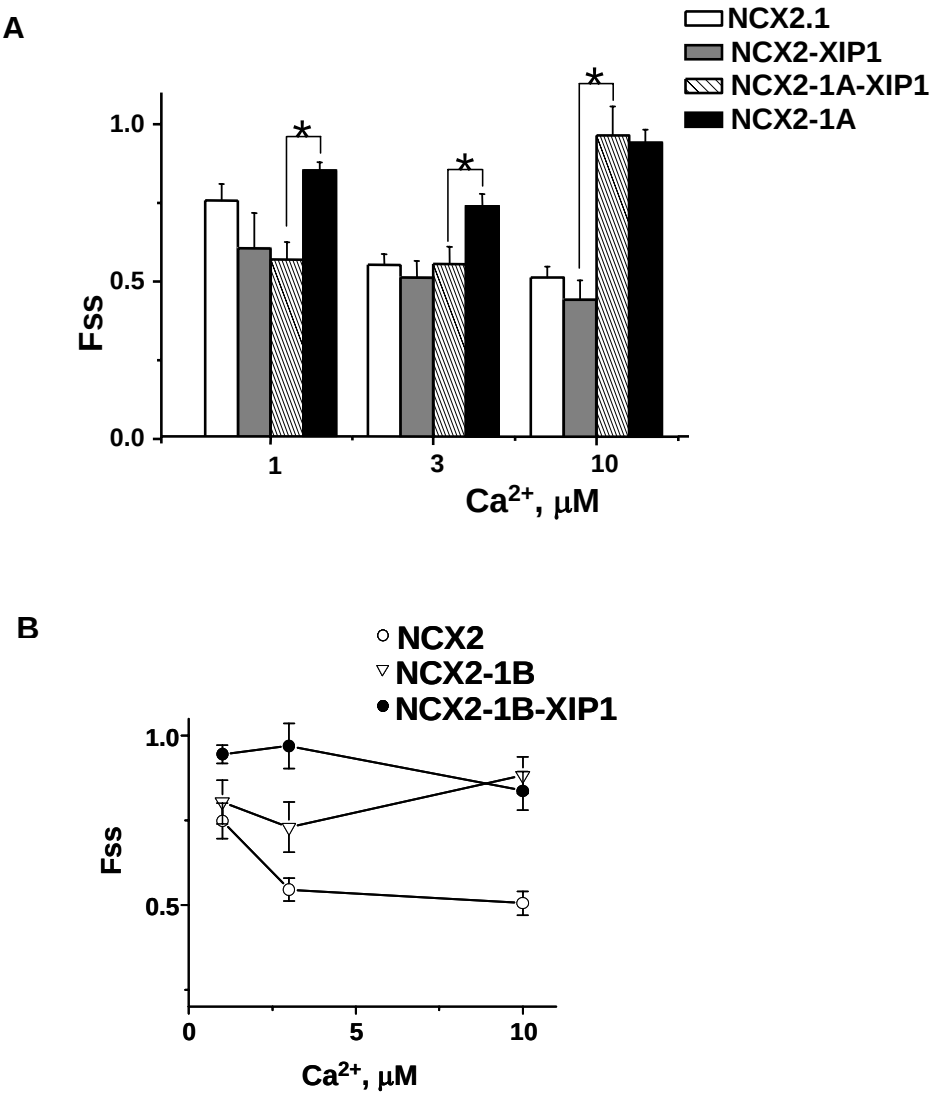


Figure 13. Ca^{2+}_i-dependence of Fss for NCX2 double chimaeras. A. Ca^{2+} dependence of the fractional steady state current (Fss) for NCX2.1 and its exon/XIP chimaeras at 1, 3 and 10 μM Ca^{2+}_i (n≥4). B. Ca^{2+} dependence of the fractional steady state current (Fss) for NCX2.1 and its exon B/XIP chimaeras at 1, 3 and 10 μM Ca^{2+}_i (n≥4). Statistical significance determined by Student t test; $p<0.05$ indicated by an asterisk.

region is required for the Na^+-dependent inactive conformation to occur or to become stable.

Substitution of the region corresponding to the mutually exclusive exon in NCX2.1 with exon B from NCX1.3 does not follow the same trend as what has been demonstrated with exon A from NCX1.4. Minimal Na^+-dependent inactivation is observed with the NCX2-1B chimaera (Figure 10B), and substitution of both the exon B and XIP region from NCX1.3 give a similar response, where Na^+-dependent inactivation is not as strong as what is observed for either NCX2.1 or NCX1.3 (Figures 12C and 13B). Surprisingly, Fss values are higher for the NCX2-1B-XIP1 chimaera than what is observed for NCX2-1B (Figure 13B). Thus, the mutually exclusive exons A and B of NCX1 do not necessarily interact with the XIP region in a similar fashion, suggesting that they may also associate with other regions of the protein to mediate a specific regulatory effect.

4.5 Characterization of the XIP region from NCX2.1

Differences between amino acid sequence of the XIP regions from NCX1 and NCX2.1 are few, yet their impact on Na^+-dependent inactivation is evident, as I_1 is greater in outward exchange currents mediated by the NCX1 splice variants in comparison to NCX2.1. To gain insight into the possible mechanism influencing this regulatory phenotype, chimaeric constructs substituting the XIP region in both NCX1.3 and NCX1.4 with the corresponding region from NCX2.1 were constructed. Figure 14 depicts representative traces of outward exchange currents at increasing $Ca^{2+}{}_i$ concentrations for native NCX1.4 (Figure 14A) and its NCX1.4-XIP2 chimaera

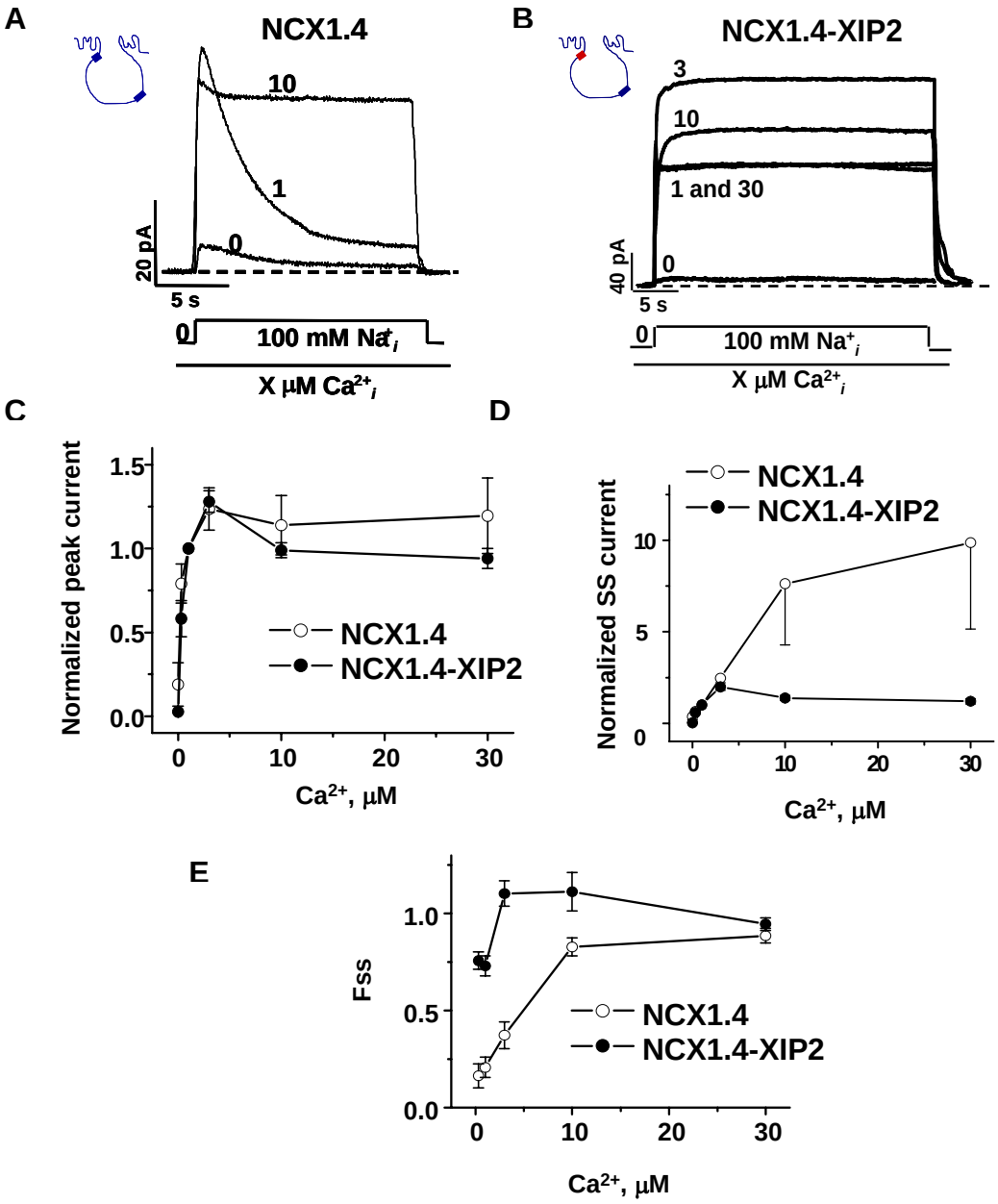


Figure 14. $Ca^{2+}{}_i$-dependence of NCX1.4 and its XIP2 chimaera for outward exchange currents and Fss. Overlapping representative current transients at 0, 1, 3 and 10 μM $Ca^{2+}{}_i$ for A. wild-type NCX1.4 and B. NCX1.4-XIP2 chimaeric construct. C. Pooled data for normalized peak for NCX1.4 and its XIP2 chimaera. D. Pooled data for normalized steady state currents for NCX1.4 and its XIP2 chimaera (n ≥5). E. Ca^{2+} dependence of the fractional steady state current (Fss) comparing NCX1.4 and its XIP2 chimaera at 0, 1, 3, 10 and 30 μM $Ca^{2+}{}_i$ (n≥4). Statistical significance determined by Student t test.

(Figure 14B). Loss of Na^+-dependent inactivation is observed in the NCX1.4-XIP2 chimaera, independently of intracellular Ca^{2+} concentration assayed. Comparison of normalized peak (Figure 14C) and steady state curves (Figure 14D) between the native and chimaeric construct demonstrates that peak currents are very similar, but steady state currents differ significantly. Steady state currents mediated by native NCX1.4 increase considerably as Ca^{2+} concentrations increase, whereas they remain at a low level for NCX1.4-XIP2 mediated currents. The Ca^{2+} dependence of Fss representing the extent of Na^+-dependent inactivation curve for the NCX1.4-XIP2 chimaera shows that above 1 μM Ca^{2+}_i, the extent of inactivation is negligible and does not change significantly as the Ca^{2+} concentration increases to 30 μM, in contrast to the profile for NCX1.4 mediated currents, where I_1 is strong at low Ca^{2+} concentrations and inhibited at higher Ca^{2+} concentrations (Figure 14E). Therefore, substitution of the XIP region in NCX1.4 with its corresponding region from NCX2.1 causes a significant decrease in Na^+-dependent inactivation. This suggests that the five non-conserved residues at the C-terminal end of the XIP region of NCX1 are required for formation or stability of the Na^+-dependent inactive state.

The regulatory profiles for NCX1.3 and its chimaeric construct, exchanging its XIP region with the analogous region from NCX2.1, are illustrated in Figures 15A-15D. Comparison of the representative traces and Ca^{2+} dependence curves for Fss (Figure 15E) suggests that although Na^+-dependent inactivation is not as strong for the NCX1.3-XIP2 chimaera as it is for the native NCX1.3, different Ca^{2+} concentrations do not alter this phenotype significantly. Normalized peak currents profiles are very similar, whereas steady state currents are more stable for NCX1.3 with respect to Ca^{2+}_i concentrations.

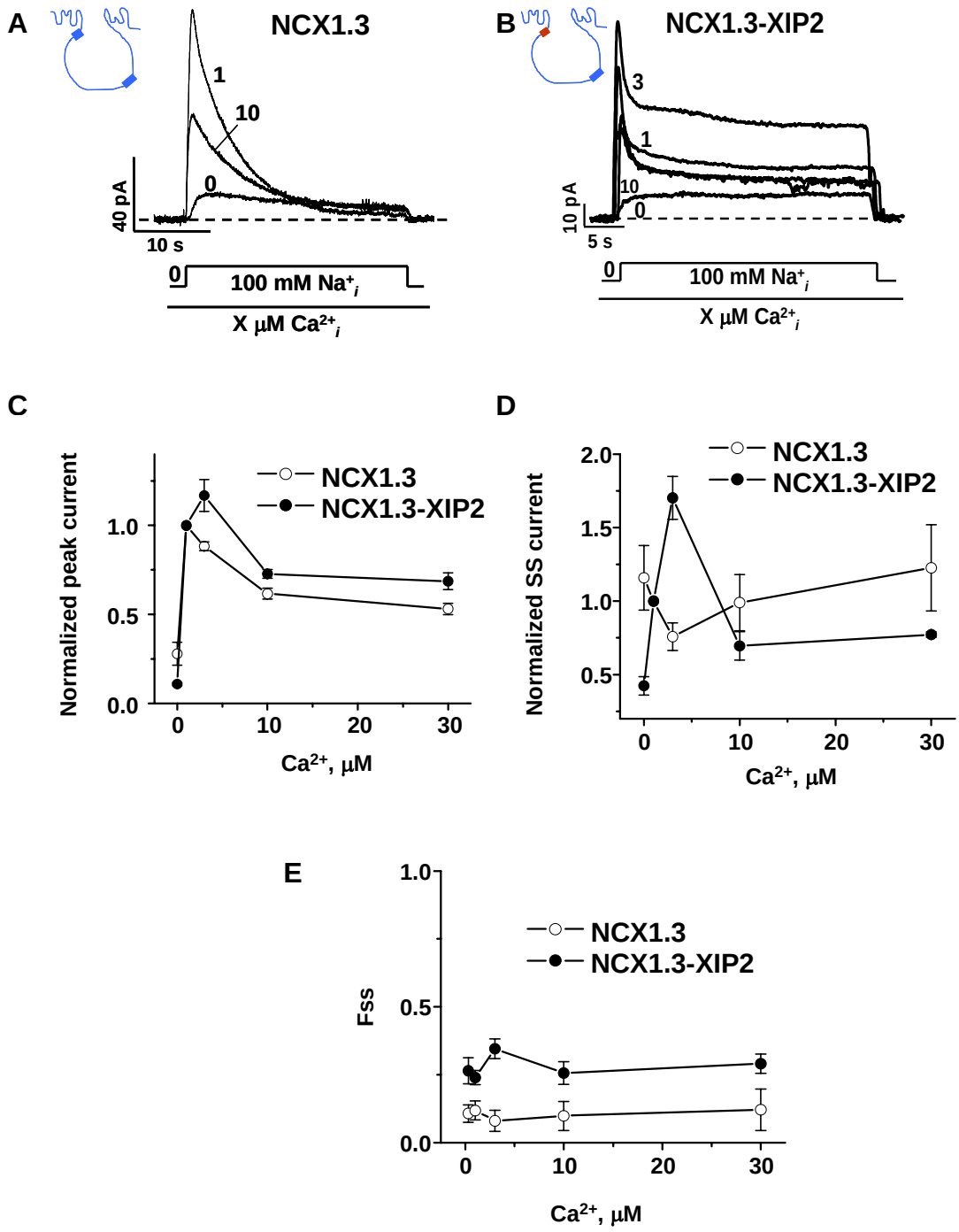


Figure 15. Ca^{2+}_i-dependence of NCX1.3 and its XIP2 chimaera for outward exchange currents and Fss. Overlapping representative current transients at 0, 1, 3 and 10 µM Ca^{2+}_i for A. wild-type NCX1.3 and B. NCX1.3-XIP2 chimaeric construct. C. Pooled data for normalized peak current, comparing NCX1.3 and its XIP2 chimaera. D. Pooled data for normalized steady state currents, comparing NCX1.3 and its XIP2 chimaera (n ≥5). E. Ca^{2+} dependence of the fractional steady state current (F_{ss}) comparing NCX1.3 and its XIP2 chimaera at 0, 1, 3, 10 and 30 µM Ca^{2+}_i (n≥4). Statistical significance determined by Student t test.

For the NCX1.3-XIP2 chimaera, peak and steady state currents are highest at 3 μM Ca^{2+} and stabilize between 10 and 30 μM Ca^{2+}. Nonetheless, the Na^{+}-dependent inactive state can be formed and maintained independently of the intracellular Ca^{2+} concentration.

The presence of the mutually exclusive exon in combination with the XIP region from the same exchanger may influence the exchanger's specific ionic regulatory profile, as previously described for the NCX2-1A-XIP1 chimaera (Figure 13A). To determine if this is also the case for the corresponding regulatory regions from NCX2.1, the NCX1-2A-XIP2 chimaera was constructed, where the region corresponding to the mutually exclusive exon and the XIP region from NCX2.1 were used to substitute the corresponding regions in the NCX1 parent exchanger. As shown in Figure 8C, substituting only the region corresponding to the mutually exclusive exon into NCX1 had no significant impact on the ionic regulatory profile. The N1-2A chimaeric construct had a very similar profile to NCX1.3, with strong Na^{+}-dependent inactivation which remains evident at higher Ca^{2+}_{i} concentrations.

As shown in Figure 16, the presence of both regions corresponding to the mutually exclusive exon and the XIP region from NCX2.1 into an NCX1 background does modify ionic regulation of outward exchange currents as compared to the N1-2A chimaera. Although normalized peak and steady state current curves appear similar for NCX1-2A and NCX1-2A-XIP2 (Figures 16C and 16D), the difference is striking upon observation of the representative traces of outward exchange currents and the Ca^{2+}-dependence curve for the fractional steady state currents. Whereas NCX1-2A chimaera has strong Na^{+}-dependent inactivation at all Ca^{2+} concentrations assayed, the presence of the XIP2 region in this context causes alleviation of I_1 at higher Ca^{2+} levels.

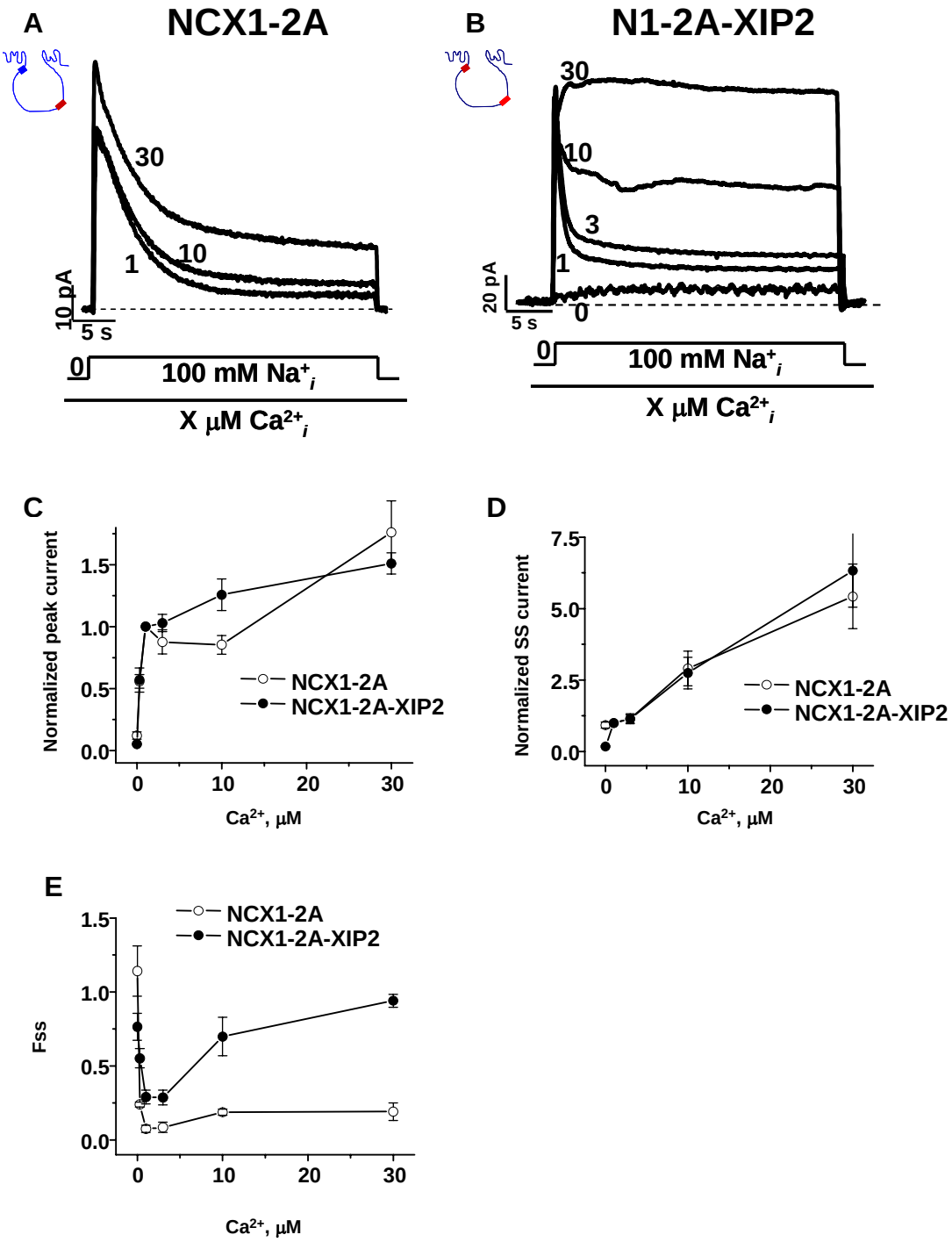


Figure 16. Ca^{2+}_i-dependence of NCX1-2A and N1-2A-XIP2 chimaeras for outward exchange currents and Fss. Overlapping representative current transients at 0, 1, 3, 10 and 30 μM Ca^{2+}_i for A. NCX1-2A and B. NCX1-2A-XIP2 chimaeric constructs. C. Pooled data for normalized peak, comparing NCX1-2A and its XIP2 chimaera. D. Pooled data for normalized steady state currents, comparing NCX1-2A and its XIP2 chimaera (n ≥5). E. Ca^{2+} dependence of the fractional steady state current (Fss) comparing NCX1-2A and its XIP2 chimaera at 0, 1, 3, 10 and 30 μM Ca^{2+}_i (n≥4). Statistical significance determined by Student t test.

Comparison of the extent of Na^+-dependent inactivation with respect to regulatory Ca^{2+} concentration (Figure 16E) clearly shows that the presence of both regions allows for a Ca^{2+}-dependent regulation of I_1, where Na^+-dependent inactivation is alleviated as $Ca^{2+}{}_i$ concentrations increase. As this phenotype is not typical of NCX2.1, which displays only moderate I_1, even at high Ca^{2+}, it is possible that another region in the NCX1 exchanger, in association with the XIP2 region, is required to mediate this effect.

4.6 Recovery from Na^+-dependent inactivation

It is evident that differences in amino acid sequence of the XIP regions of NCX1 and NCX2.1 impart an effect predominantly on Na^+-dependent inactivation, depending on which mutually exclusive exon is present. For NCX1.3, which normally exhibits the highest level of inactivation, fractional steady state values double when the XIP region is substituted with the XIP region from NCX2.1, demonstrating a weakened Na^+-dependent inactive state. For NCX1.4, the effect is even more noticeable, as I_1 becomes negligible in the NCX1.4-XIP2 chimaera. To test the stability of the Na^+-dependent inactive state of the NCX1-XIP2 chimaeric constructs, paired-pulse experiments were performed. The rate of recovery from inactivation was calculated using the ratio of initial peak current level following application of 100 mM $Na^+{}_i$ with the peak current level achieved on the second pulse of 100 mM $Na^+{}_i$. The second pulse was activated at timed intervals ranging from 4 ms to 32 s following the first pulse. The magnitude of the second peak reflects the extent of recovery from $Na^+{}_i$-induced inactivation of the entire exchanger population (65). Paired-pulse experiments were also used to evaluate recovery rate from inactivation for

NCX1.3 mutants of the non-conserved residues at the C-terminal portion of the XIP region, substituting for the corresponding amino acids in NCX2.1.

Figure 17 illustrates recovery from inactivation of outward exchange currents mediated by wild type NCX1.3 and NCX2.1 in comparison to the NCX1.3-XIP2 chimaeric construct and the point mutation at position 235 in the XIP region, substituting a lysine for a proline. As shown for NCX1.3, the Na^+-dependent inactive state appears to be quite stable, as peak currents obtained at short intervals following formation of the inactive state only increase slightly as compared to the steady state of current at pulse 1. For NCX2.1, as the extent of I_1 is approximately 50 % at 3 μM Ca^{2+}, the inactive state is possibly not as stable. This is evidenced by the high level of peak current achieved on the second pulse, 6.4 s following the initial pulse. Thus, the XIP region in NCX2.1 appears to confer a less stable conformation during Na^+-dependent inactivation. This phenotype is more evident when the XIP2 region from NCX2.1 is found in an NCX1.3 background. Recovery from inactivation for the NCX1.3- XIP2 chimaeric construct is significantly quicker. Even at 1.6 s, peak currents at pulse 2 are almost equivalent to peak currents on pulse 1. At 6.4 s, total recovery from inactivation is achieved.

To determine which residue may be involved in the secondary structure needed for stability of the inactive state, we tested the point mutants of all five non-conserved residues at the C-terminal end of the XIP region, replacing NCX1.3 residues with their analogue from the NCX2.1 XIP sequence. The representative trace of outward exchange current at 3 μM Ca^{2+} for NCX1.3 K235P depicts the mutant with the greatest effect on the rate of recovery, with a profile very similar to NCX2.1 (Figure 17). Analysis of recovery rates (β recovery) for all point mutants are represented in the bar graph

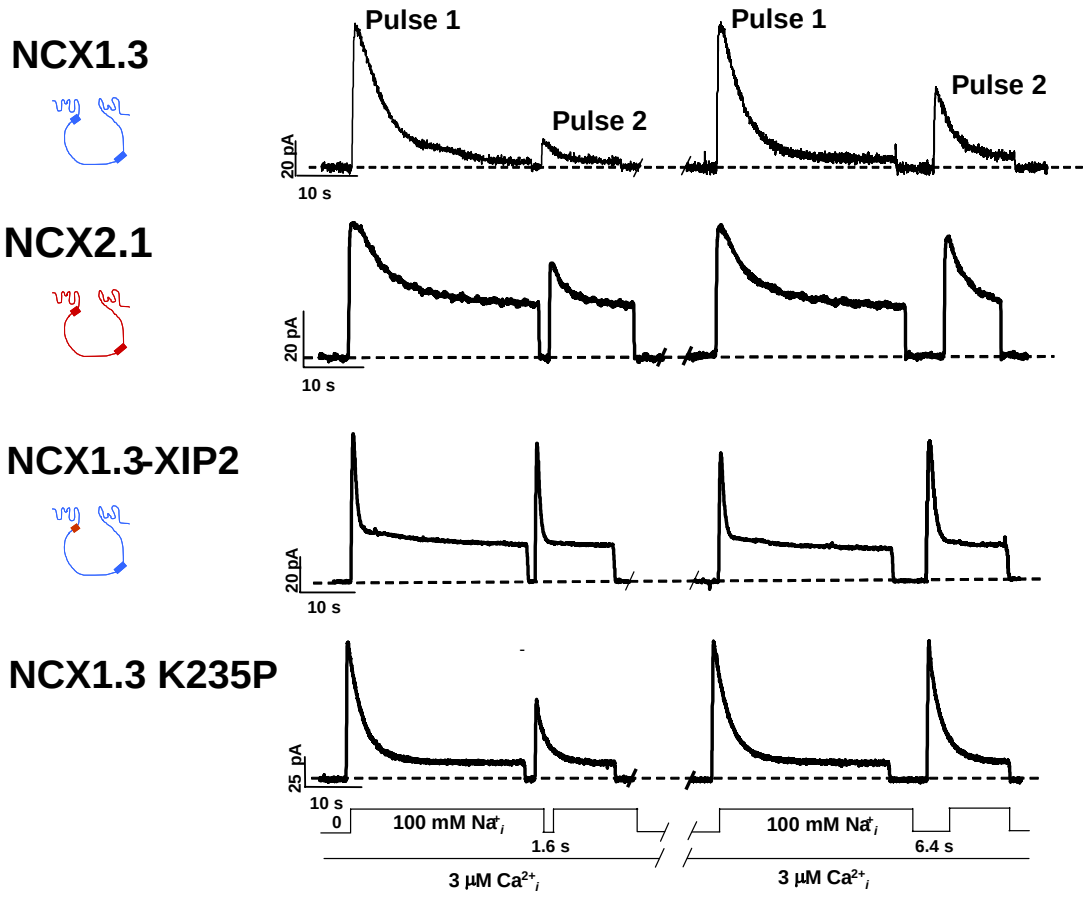


Figure 17. Recovery from Na^+-dependent inactivation. Representative traces demonstrating rate of recovery from inactivation of outward exchange currents mediated by NCX1.3, its chimaera with the XIP region substitution from NCX2.1, the NCX1.3-K235P mutant and wild type NCX2.1. Recovery from inactivation is observed at pulse 2, measured at an interval of 1.6 and 6.4 seconds following pulse 1 ($n \geq 5$).

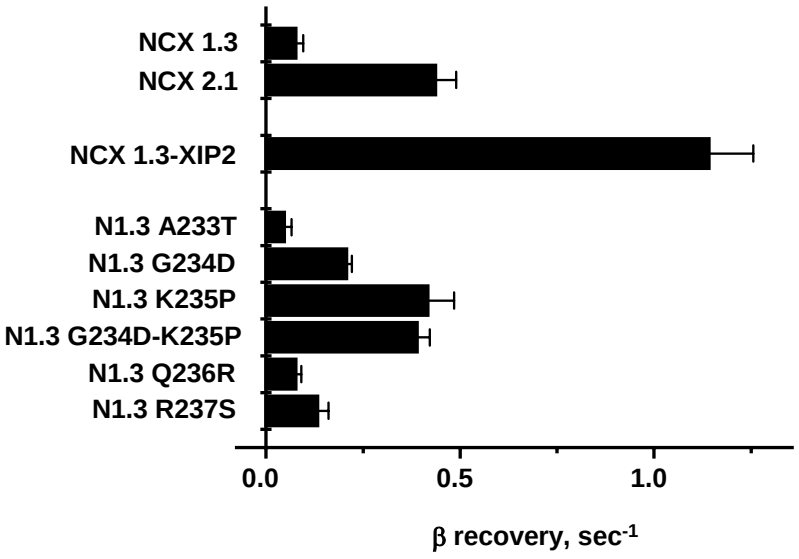


Figure 18. Comparison of recovery rates from inactivation for NCX1.3 chimaeric and point mutation constructs. Rate of recovery for NCX1.3-XIP2, and double or single amino acid mutants of the non-conserved residues in the XIP2 region (n≥4).

Exchanger	Fss	n	β recovery	n
NCX1.4	0.208 ± 0.05	4	0.141 ± 0.02	4
NCX1.3	0.119 ± 0.03	4	0.077 ± 0.019	4
NCX2.1	0.748 ± 0.052	4	0.437 ± 0.053	4
NCX1.3-XIP2	0.255 ± 0.01	42	1.141 ± 0.114	6
NCX1.3 A233T	0.074 ± 0.012	14	0.047 ± 0.019	4
NCX1.3 G234D	0.126 ±.005	53	0.208 ±0.013	9
NCX1.3 K235P	0.209 ± 0.009	66	0.417 ± 0.068	9
NCX1.3 G234D-K235P	0.268 ± 0.012	41	0.390 ± 0.03	5
NCX1.3 Q236R	0.075 ± 0.01	21	0.077 ± 0.014	5
NCX1.3 R237S	0.142 ± 0.01	39	0.133 ± 0.028	5
N1-2A	0.075 ± 0.024	5	0.064 ± 0.006	5
N1-2A-XIP2	0.29 ± 0.046	5	1.37 ± 0.175	5

Table I. Values for fractional steady state (Fss) and rate of recovery for NCX isoforms, NCX1 chimaeric and point mutation constructs. Data were calculated for outward exchange currents at 3 μM Ca^{2+}_i (n≥4).

in Figure 18, with values for Fss and rate of recovery in Table I. The rate of recovery is approximately three-fold greater for NCX2.1 as compared to NCX1.3, and is almost equivalent to the value obtained for the point mutation NCX1.3-K235P and the double mutant NCX1.3 G234D- K235P. However, the rate of recovery is at its highest for the NCX1.3-XIP2 and the NCX1-2A-XIP2 chimaeras, with values reaching 1.2 ± 0.1 sec^{-1} and 1.4 ± 0.2 sec^{-1}, respectively. No single point mutation or double mutation of the charged residues is sufficient to reproduce this effect, suggesting that the combination of all five residues confers a specific conformation rendering the inactive state unstable. This effect appears to be dependent on the mutually exclusive exon, as NCX1.4-XIP2's inactive state is unstable to the point that it appears to have no detectable I_1. With NCX1.3-XIP2, Fss values are higher and recovery rates from inactivation are quicker than those observed for wild-type NCX1.3, supporting the proposition that a structural modification provoked by the residues in the XIP2 region may prevent the formation of a strong Na^+-dependent inactive state.

5. DISCUSSION

The Na^+-Ca^{2+} exchanger plays an important role in Ca^{2+} homeostasis in several tissues of the body and in a variety of organisms. Located in the plasma membrane of most cells, it has the ability to countertransport Na^+ and Ca^{2+}. Depending on the membrane potential and the electrochemical gradient across the membrane, the exchanger functions either in the inward mode, causing Ca^{2+} efflux, or in the outward mode, leading to Ca^{2+} influx. This versatility in mode of exchange has its advantages and disadvantages. On the positive side, it allows for rapid movement of Ca^{2+} in response to ionic fluctuations in the intracellular space, such as in cardiac muscle, where the exchanger responds to Ca^{2+} flux on a beat to beat basis and is essential for relaxation to occur prior to the next contraction (14; 174). However, when cellular ionic homeostasis is compromised and intracellular Na^+ levels rise above normal, the exchanger responds by promoting Na^+ efflux, thereby causing Ca^{2+} entry into the cell. As Ca^{2+} is an important signalling molecule involved in a multitude of mechanisms including apoptotic and necrotic cell death pathways, it would be preferable that the exchanger remain inactive in this instance. This is unfortunately not the case, hence the interest in gaining insight into NCX regulation and inhibition, leading to the development of pharmacological agents targeting this mode of action to prevent cellular demise.

Interestingly, nature has endowed mammals with not only one exchanger, but with three isoforms which are expressed independently, as each is encoded on separate genes and on different chromosomes. Additional diversity is achieved by alternative splicing of transcripts in two of these isoforms, NCX1 and NCX3. The body therefore has

the possibility of expressing over 20 different exchangers. Of the exchangers which have been cloned and characterized, all appear to have essentially the same function, but each exhibits unique regulatory profiles and is expressed in specific tissues. Furthermore, mRNA and protein expression are dependent on the developmental stage of the organism, and may also be influenced by the cellular environment in health and under duress. Thus, it is highly probable that differential expression of NCX isoforms and splice variants throughout the body reflects the Ca^{2+} homeostatic requirements specific to the tissue in which it is expressed and at a time when it is required, adding to the versatility of this protein. Subtle differences in regulation of these exchangers may be important physiologically and may influence the response to intracellular ionic fluctuations necessary for cells to remain functional and healthy.

Among the three mammalian isoforms identified to date, NCX1 is the most extensively expressed and has been the most thoroughly studied. NCX1.1 is ubiquitously expressed, whereas the additional splice variants are restricted to a few tissues. Splicing patterns are noticeable, with exon A-expressing variants found only in excitable tissues such as heart, brain and skeletal muscle. These exchangers have a particular ionic regulatory phenotype, where high intracellular Na^{+} levels cause inactivation of outward currents, preventing excessive Ca^{2+} entry. This is an important feature, as timely regulation of rapid Ca^{2+} transient fluxes are essential in muscular and neuronal tissues. Furthermore, high intracellular Ca^{2+} concentrations can alleviate the Na^{+}-dependent inactivation, possibly by modifying the secondary structure of the Ca^{2+}-binding domains and destabilizing the inactive state. Therefore, depending on intracellular Na^{+} and Ca^{2+}

levels, the exchanger's secondary structure may change and thus modulate exchange activity.

The ionic regulation of the exchanger is dependent on specific domains located within the cytoplasmic loop. The alternative splice region, located in the Ca^{2+}-binding domain 2, is one of the regions which may influence ionic regulation. Because of alternative splicing, only certain exons are included in the amino acid sequence of the mature exchanger. Interactions between residues within these exons and other regions in the cytoplasmic loop may be required for the secondary structure of the protein, allowing for activation or inactivation of exchange activity as it pertains to the cellular ionic environment. The exclusion of these same exons in other splice variants may also have an impact on the secondary structure of the exchanger, as has been observed in the differential regulatory responses exhibited on the outward exchange currents mediated by various splice variants. The alternative splice region therefore plays an important role in ionic regulation of the exchanger, and exploring its structure is essential in understanding the subtle differences in NCX variant functions.

This study focuses on the area corresponding to the mutually exclusive exon in the alternative splice region of the Na^{+}-Ca^{2+} exchangers, NCX1 and NCX2, specifically examining the influence of the exon on ionic regulation of outward exchange currents. As the mutually exclusive exon is located within the Ca^{2+}-binding domain, it is feasible that it is involved in the secondary structure of this region essential to binding of regulatory Ca^{2+}. The 3-dimensional structure of the Ca^{2+}-binding domains proposed by NMR and crystallography studies, along with mutational analysis of key residues in this region, illustrate a possible role for residues within the mutually exclusive exon in stability of the

domain in the absence of Ca^{2+} and binding of regulatory Ca^{2+}, thus mediating exchange activity (17; 35; 59; 99; 164). Alternatively, the exon region may also influence Na^{+}-dependent regulation, as previously studied mutants in the Ca^{2+}-binding sites, which exhibit low affinity for regulatory Ca^{2+} binding, also display modifications in Na^{+}-dependent inactivation (142; 175). Previous studies by our laboratory, exploring differences in ionic regulatory properties between *Drosophila*'s alternative splice variants, CALX1.1 and CALX1.2, have demonstrated that a five amino acid sequence difference in the alternative splice region can cause significant differences in both Na^{+} and Ca^{2+}-dependent regulatory profiles (169). Thus, there is evidence that the alternative splice region in NCX1 is required for Ca^{2+}-dependent regulation, and also influences Na^{+}-dependent inactivation. The actual mechanism by which this occurs has yet to be determined and will be the main objective of this study.

The method proposed for this structure-function study is measurement of chimaeric NCX-mediated currents in *Xenopus* oocytes using the giant, excised-patch clamp technique. Although this system is highly artificial and does not reflect actual physiological cellular conditions in mammals, it nonetheless has several advantages. Firstly, overexpression of NCX in oocytes is a relatively simple procedure, where cRNA is injected into the egg. The oocyte's internal machinery then proceeds to synthesize the protein and integrate it into the membrane (29). This procedure has limited toxic effects on the oocyte and therefore does not hinder their maintenance in culture. Secondly, as other ionic channels or transporters are either not naturally expressed in oocytes or are inhibited in the experimental bath solutions, this technique allows for measurement of currents mediated solely by the overexpressed exchanger (39; 60). Thirdly, analysis of

isoform specific ionic regulation is possible, as our system allows for control of ionic concentrations in the bath solutions on either side of the membrane. Hence, examination of forward and outward mode of exchange is possible (60). Lastly, comparison of currents produced by different isoforms normally expressed in different tissues is more easily achieved in a system where conditions are similar and constant. Thus, although the cellular environment is important, it will have the same impact on all overexpressed exchangers in this common membrane environment.

To determine the importance of the first exon in the alternative splice region in mediating ionic regulation of the exchanger, single chimaeras were constructed, exchanging the mutually exclusive exons from NCX1 with the corresponding region from NCX2.1. For clarity and simplicity, the corresponding region in NCX2.1 was arbitrarily labelled exon 2A. Although the name suggests that this exon is mutually exclusive, the author fully realizes that this is not the case, as no findings to date demonstrate that NCX2.1 is alternatively spliced. The rationale for creating chimaeras rather than deleting the region of interest is that substitution of the same number of residues, with a natural conservation of several amino acids, should cause less disruption and maintain the general secondary structure of the protein. This is important, as relative alignment between regulatory regions in different locations of the protein may still be preserved, allowing for interactions to occur. Also, comparing amino acid sequences between NCX1 and NCX2 in a restricted region facilitates the identification of key residues conferring a specific regulatory phenotype. Previous studies using chimaeric constructs substituting the Ca^{2+}-binding domain from NCX1.1 into the *Drosophila* CALX yielded functional proteins, as long as both transmembrane domains were from the same parent exchanger

(37). Furthermore, these CALX chimaeric constructs exhibited Ca^{2+}-dependent regulatory properties transferred from the donor exchanger, NCX1.1, demonstrating that the regulatory domains can retain function despite being in a different parent exchanger. Thus, the proposed model of investigation is feasible, as it is supported by previous experience acquired by our laboratory.

5.1 Similarities between NCX2.1 and NCX1.3 regulatory profiles conferred by residues in the region corresponding to the mutually exclusive exon

To determine the mechanism by which the mutually exclusive exon mediates Na^+ and Ca^{2+}-dependent regulation, chimaeric exchange of the mutually exclusive exon in NCX1, replacing it with the corresponding region from NCX2.1 (chimaera N1-2A), was performed and outward currents mediated by this chimaera were analyzed. This substitution confers a regulatory profile similar to what is observed with NCX1.3 mediated outward exchange currents as it pertains to Ca^{2+}'s ability to modulate Na^+-dependent inactivation. These findings are somewhat expected, given the regulatory profiles of these two exchangers. NCX1.3 exhibits very strong Na^+-dependent inactivation (I_1) of outward currents which is not influenced by high regulatory $Ca^{2+}{}_i$ concentrations. Similarly, high $Ca^{2+}{}_i$ levels do not lessen Na^+-dependent inactivation of outward currents mediated by NCX2.1, but rather maintain it. In contrast to NCX1.3, Na^+-dependent inactivation is only moderate for NCX2.1, and becomes apparent only at higher $Ca^{2+}{}_i$. This is possibly due to a reduced affinity for regulatory Ca^{2+} by NCX2.1 and suggests that for this isoform, regulatory Ca^{2+} is required to stabilize the Na^+-dependent inactive state (171). Nonetheless, high Ca^{2+} does not alleviate I_1 for either NCX1.3 or

NCX2.1, and the N1-2A chimaera demonstrates that the region corresponding to the mutually exclusive exon in NCX2.1 has a very similar function as exon B in NCX1.3 in mediating this phenotype.

Comparison of the amino acid sequence of the region corresponding to the mutually exclusive exon of NCX1.3 and NCX2.1 may explain the similarity in the observed regulatory profiles. The exon region in NCX1 has been studied extensively by mutagenesis analysis, and key residues involved in Ca^{2+}'s ability to destabilize the Na^{+}-dependent inactive state have been identified (35). The negatively charged aspartate residue at position 578 and the positively charged lysine at position 585 in exon A of NCX1.4 are required for alleviation of I_1 at high $Ca^{2+}{}_i$, as shown by mutations of these residues and supported by the 3-dimensional structural model proposed by Hilge (59). It would appear that D578 coordinates Ca^{2+} ions in both binding sites of CBD2 whereas K585 forms a salt bridge with the adjacent D552, located in the second Ca^{2+} binding site of CBD2, thus stabilizing the surrounding negatively charged residues, such as D578, E579 and E580, and preventing the unfolding of CBD2 in the absence of bound Ca^{2+} (see Figure 4). In exon B-expressing exchangers, the presence of a positively charged residue at position 578 and an uncharged residue at position 585 causes instability in this Ca^{2+} binding domain, and high $Ca^{2+}{}_i$ concentrations do not bring about a conformational change disrupting the Na^{+}-dependent inactive state. This has been demonstrated by the NCX1 K585E mutant, which led to electrostatic repulsion and unfolding of CBD2, suggesting a key role for this residue in the structural stability of this region (59). The unfolding of CBD2 results in a rearrangement of the Ca^{2+} binding sites that could alter

the interaction with other regulatory regions of the exchanger and prevent overcoming Na^+-dependent inactivation, as observed with NCX1.3.

Findings from this study demonstrate that the charged residues within the mutually exclusive exon may have the same function in an NCX2.1 context, where the acidic cluster forming the Ca^{2+} binding site is equally conserved but specific residues surrounding the cluster are not. The presence of a negatively charged aspartate residue at position 605 in NCX2.1, comparable to the cysteine at the corresponding position in NCX1.3 and in contrast to K585 in NCX1.4, may destabilize the Ca^{2+}-binding domain 2. Site directed mutagenesis, substituting the aspartate for a positively charged lysine at position 605 in NCX2.1, thus replicating K585 in the NCX1.4 amino acid sequence, causes the mutant exchanger to mediate outward currents with strong Na^+-dependent inactivation at low Ca^{2+} and its alleviation as Ca^{2+} concentrations increase. This mimics the NCX1.4 phenotype and contrasts with what is observed for currents mediated by native NCX2.1. Although I_1 is not completely overcome at 30 μM Ca^{2+} in the NCX2.1 D605K mutant as it is with NCX1.4, it is possible that a higher Ca^{2+} concentration may be required for this to occur, as native NCX2.1 has a lower regulatory Ca^{2+} affinity than NCX1.4 (171). Exchange currents were, however, not measured at a $Ca^{2+}{}_i$ concentration higher than 30 μM, as this would create competition for the transport site and complicate analysis of our observed results. Nonetheless, the absence of two charged residues at specific positions (578 and 585 in exon B of NCX1) confers the same regulatory phenotype in both an NCX1.3 and NCX2.1 context. This suggests that the region corresponding to the mutually exclusive exon in NCX2.1 plays a similar role as exon B in NCX1.3 in destabilizing the secondary structure of CBD2, resulting in a rearrangement of

its Ca^{2+} binding sites and possibly stabilizing an interaction with the XIP region, as Na^{+}-dependent inactivation is maintained in outward currents mediated by these exchangers. Therefore, the region corresponding to the mutually exclusive exon may mediate Na^{+}-dependent regulation indirectly by influencing Ca^{2+} binding to CBD2.

5.2 Role of the region corresponding to the mutually exclusive exon in NCX2.1 in maintaining Na^{+}-dependent inactivation

Our findings demonstrate that the region corresponding to the mutually exclusive exon in NCX1 and NCX2.1 play an important role in modulating Na^{+}-dependent inactivation in a Ca^{2+}-dependent manner. This region in NCX2.1 also appears to have a greater role in Na^{+}-dependent regulation, independently of Ca^{2+}_{i}. Substitution with either exon A or exon B from NCX1 into an NCX2.1 background causes a distinct phenotypic alteration. In both cases, Na^{+}-dependent inactivation is limited as compared to native NCX2.1, and is minimally influenced by intracellular Ca^{2+} levels. Outward currents peak rapidly, but do not degrade significantly in the presence of elevated Na^{+}_{i}. Formation of the inactive state may be dependent on specific residues located in the region corresponding to the mutually exclusive exon in NCX2.1, which may not be conserved in exons A or B of NCX1. This suggests that the XIP region in NCX2.1 alone is not sufficient to form or maintain the inactive state. Another possibility is that the region corresponding to the mutually exclusive exon may be part of the XIP binding site, and would therefore be required for interaction with the XIP region to achieve the inactive state.

The NCX2.1 chimaeric exchangers maintain their ability to form the inactive state, but require external assistance to do so. This has been observed in the presence of the pharmacological inhibitor SEA0400, which is known to stabilize the Na^+-dependent inactive state. Outward exchange currents measured before and after application of SEA0400 demonstrate that the chimaeric exchangers N2-1A and N2-1B are able to achieve the conformational change required for formation of the inactive state, but only in the presence of the inhibitor. Therefore, it would appear that residues located within the region corresponding to the mutually exclusive exon in native NCX2.1 are not essential, but rather facilitate the formation or the stabilisation of the Na^+-dependent inactive state. This may be achieved by involvement in the secondary structure of the protein or structural interactions with other regions of the exchanger.

5.3 Interaction between the XIP region and the region corresponding to the mutually exclusive exon in NCX1 required for Na^+-dependent inactivation

The 3-dimensional structural model of NCX1 proposed by Hilge et al (2006) suggests that CBD2 is in close proximity to a third domain called the catenin-like domain (CLD, see Figure 3). This region, comprised of most of the regulatory loop, excluding the Ca^{2+}-binding domains, corresponds to residues 217-370 and 651-705. The CLD therefore contains the XIP region, suggested to be responsible for Na^+-dependent inactivation (59). The proximity between the alternative splice region within CBD2 and the XIP region is therefore possible, and residues in the mutually exclusive exon may be involved in XIP binding, either by a direct association with the XIP region or by conferring a specific conformation required for the XIP region to bind to its binding site and form the inactive

state. Alternatively, residues located in other regions of the exhanger may assist in formation of the inactive state, and may be required for stabilisation of the conformation leading to inactivation. To determine if this is the case with NCX1, double chimaeric exchangers were constructed, where both the XIP region in combination with the mutually exclusive region from NCX1 are expressed in an NCX2.1 parent exchanger.

Results obtained with the double chimaeras in NCX2.1 suggest that indeed, conformational stability is enhanced in the presence of both the mutually exclusive exon and the XIP region from NCX1 in the same exchanger. However, this is dependent on the substituting exon: in the presence of exon A and the XIP region from NCX1 in an NCX2.1 background, Na^+-dependent inactivation is re-established to similar levels as native NCX2.1, suggesting that both regions are required for formation and stability of the Na^+-dependent inactive form. However, the combination of exon B and the XIP region from NCX1 is not sufficient to achieve the Na^+-dependent inactive state, irrespective of the intracellular Ca^{2+} concentration. Therefore, this implies a new role for the mutually exclusive exon in NCX1, as well as a distinction between exon A and exon B. It appears that residues in exon A, in association with the XIP region in NCX1, are sufficient to achieve a specific conformation of the exchanger allowing for the Na^+-dependent inactive state to occur, but exchangers expressing exon B require more than the XIP region to achieve this conformation. The mutually exclusive exon therefore plays an important role in stabilizing the Na^+-dependent inactive state and works in concert with not only the XIP region but other parts of the exchanger to mediate this phenotype.

The actual localization of the XIP binding site within the exchanger has yet to be determined, but, it has been proposed to be located between residues 562 and 679 in

NCX1 (135; 144). This region covers the alternative splice region, in combination with a short sequence downstream of exon F, which has no counterpart in CBD1. This unique sequence, from residues 610-625, is comprised of a highly acidic cluster which may be involved in electrostatic interactions with the basic residues in the XIP region. Alternatively, the mutually exclusive exon may have some impact on the structural conformation required for access to this site and thus influence Na^+-dependent regulation indirectly.

5.4 The XIP region and Na^+-dependent inactivation in NCX2.1

Ionic regulatory profiles of outward exchange currents mediated by NCX2.1 illustrate that Na^+-dependent inactivation is only moderate as compared to what is observed in NCX1. Peak currents measured by giant excised patch-clamp technique in oocytes overexpressing the exchanger degrade to steady state currents by approximately 50 %, demonstrating that only half of the exchangers are active during steady state currents (171). Although the amino acid sequence comparison between the XIP region from NCX1 and NCX2.1 has high homology, the five non-conserved residues at the C-terminal end of this region may confer a specific conformation in the structure of the XIP region and destabilize the Na^+-dependent inactive state.

Secondary to our observations with the XIP chimaeric constructs in NCX2.1, with substitution of the XIP region with its equivalent from NCX1 (chimaera NCX2-XIP1), it appears that the non-conserved residues within the XIP region have little influence on NCX2.1 ionic regulatory profile. However, the reverse substitution, where the XIP region from NCX1 is exchanged for the equivalent sequence from NCX2.1 (chimaera NCX1.4-

XIP2, NCX1.3-XIP2), a definite trend toward instability of the Na^+-dependent inactive state is observed. The chimaeric construct NCX1.4-XIP2 demonstrates significant loss of Na^+-dependent inactivation. In comparison, NCX1.3-XIP2 chimaera displays moderate I_1, as compared to native NCX1.3. However, rapid recovery rate from inactivation for this chimaeric exchanger supports the idea that the Na^+-dependent inactive state is less stable.

Five residues in the C-terminal end of the XIP region are not conserved between NCX1 and NCX2, therefore it is highly probable that those residues are involved in the secondary structure of the XIP region and influence binding of the XIP region to its binding site located elsewhere in the cytoplasmic loop. As no single amino acid mutant was able to reproduce the effect mediated by the NCX1.3-XIP2 chimaeric construct, it is highly probable that the combination of all five residues causes a specific conformation needed to prevent binding of the XIP region and inactivation. Previously studied truncated mutations of the XIP region from NCX1 have demonstrated that very few residues can be removed from either end without influencing inhibition, and that the total length may be required for the proper structure of this region for inhibitory action (56). Also, basic or aromatic residue substitutions within the XIP region were shown to have the greatest effects on XIP potency and may also influence its conformation. Lastly, a potential cAMP-dependent kinase or protein kinase C phosphorylation site has been proposed in the NCX2.1 XIP region and not in NCX1. The additional negative charge brought about by phosphorylation may assist in attracting the XIP region, which is highly basic, thus facilitating an interaction between the XIP region and its binding site (162).

The 3-dimensional structural model proposed by Hilge et al suggests that cassette exons C to F are located directly opposite the CBD1 Ca^{2+} binding sites, enabling splice

variants to modulate Ca^{2+} binding directly and affect NCX activity (59). NCX2.1 does not express exons D, E and F. Possibly, the last three exons in the alternative splice region may by involved in binding of Ca^{2+} at CBD1, and this could explain why NCX2.1 has a reduced affinity for regulatory Ca^{2+}. Furthermore, these exons may be required for formation or stabilisation of the Na^{+}-dependent inactive state. This may be the explanation to why NCX2.1 mediated outward currents exhibit only moderate Na^{+}-dependent inactivation, as exons D, E and F are not expressed in NCX2.1. All NCX1 splice variants express exon D (198), and therefore this region may be involved in Na^{+}-dependent regulation in this isoform.

5.5 NCX2.1 regulatory profile confers neuroprotective properties

NCX2.1 is the predominant isoform expressed in the adult brain (49; 213) and appears to be involved in restoring baseline Ca^{2+} levels in presynaptic terminals after electrical stimulation (207), allowing for proper control of the neurotransmission in hippocampal neurons (20). This is supported by findings in NCX2.1 knockout mice, which exhibit delayed clearance of elevated Ca^{2+} following depolarization, thus increasing long term potentiation as evidenced by enhanced memory and spatial learning (98). Furthermore, NCX2.1 mRNA and protein levels do not change significantly following transient focal cerebral ischemia in rats (122), suggesting a neuroprotective role equally observed with NCX2.1 overexpression during excitotoxicity (11). This may partially be linked to NCX2.1's high expression in glial cells, where NCX function in its outward mode may be neuroprotective. Ca^{2+} entry into the glial cells rather than into the neurons may protect the latter from Ca^{2+} overload for some time (243). It has also been

proposed that NCX2 be neuroprotective during excitotoxicity due to its resistance to calpain cleavage (11). Although still controversial, much evidence suggests that NCX2 function in neuropathological conditions is beneficial.

There may be a link between NCX2.1's regulatory profile and its neuroprotective properties. Although Na^+-dependent inactivation is moderate for NCX2.1, this phenotype is maintained at high Ca^{2+} concentrations. This limits Ca^{2+} influx, even when high Na^+_i concentrations prevail, as during ischemia-reperfusion injury. In comparison, neuronal cells expressing NCX1.4 are not protected from Ca^{2+} overload under these ionic cellular conditions, as Na^+-dependent inactivation is not achieved at high Ca^{2+} concentrations. Therefore, these cells are vulnerable to high Na^+_i and Ca^{2+}_i levels, as the Ca^{2+} influx mode prevails and is not restricted by inactivation of the exchanger. As our studies demonstrate, the region corresponding to the mutually exclusive exon is responsible for this phenotype, and specific residues have been identified as key in mediating structural changes required for the inactive state to be maintained. Overexpression of the mutant form of NCX2 (D605K) which demonstrates alleviation of inactivation at high Ca^{2+}_i levels, could be studied under ischemic conditions to determine if NCX2's regulatory profile is indeed responsible for its neuroprotective effects.

6. FUTURE STUDIES

Since the cloning of the first Na^+-Ca^{2+} exchanger in 1990, much has been discovered with respect to NCX structure, function and regulation and the impact on Ca^{2+} transport under both physiological and pathological conditions. Future studies could be undertaken to clarify the importance of phosphorylation of specific sites within the exchanger and the mechanism by which phosphorylation modifies the protein's structure and function. Two potential phosphorylation sites in the non-conserved residues of the XIP region of NCX2 may play a role in destabilizing the inactive state and allow for rapid recovery of the exchanger. Determining if these residues are phosphorylated and by which kinase would be of interest, as different kinases may be activated under different disease conditions and in different tissues and may therefore be critical determinants of activation of NCX exchange activity.

The other NCX isoform which is alternatively spliced but poorly characterized is NCX3. Preliminary data suggests that this isoform has a unique regulatory profile, with regulatory Ca^{2+}-induced activation and inactivation (140). NCX3 is essential for Ca^{2+} homeostasis in neuromuscular transmission and skeletal muscle function (235) and is believed to be neuroprotective (155; 183). As NCX3 exhibits different affinities to inhibitors (87; 88; 95) and is resistant to ATP depletion (126), examination of its structure-function relationship would be beneficial in gaining insight into regulation of NCX exchange activity. A similar study of outward exchange currents mediated by chimaeric NCX3 exchangers may help elucidate the role of the mutually exclusive exon and its interaction with other regulatory regions of the exchanger, such as the XIP region.

A three-dimensional model of the entire cytoplasmic loop of NCX would be beneficial in determining the potential interaction between the XIP region and the region corresponding to the mutually exclusive exon. Furthermore, structural differences between exon A and exon B expressing exchangers could be examined with respect to both the Na^+-dependent inactive state and the regulatory Ca^{2+}-binding domains. The yet unidentified regulatory regions, the XIP binding site, and the role of the cassette exons could also be determined. These structural discoveries could assist us in gaining insight into the structure-function relationship of the many regulatory regions of the exchanger which are essential in regulating NCX exchange activity in response to intracellular ionic conditions. This could assist us in determining isoform-specific roles in physiology and in disease states and may also provide an explanation for the expression of a wide variety of NCX variants in the mammalian systems.

7. CONCLUSION

This study proposes a potential role for the region corresponding to the mutually exclusive exon in the alternative splice region of the Na^+-Ca^{2+} exchangers, NCX1 and NCX2. In the NCX1 isoform, key residues in the mutually exclusive exons A and B have previously been identified as critical determinants regulating Ca^{2+}'s ability to modulate Na^+-dependent inactivation. In NCX2.1, I have been able to demonstrate, by measuring outward exchange currents mediated by chimaeric constructs and single amino acid substitutions, that the region corresponding to the mutually exclusive exon also plays this role, and key residues are required for destabilizing CBD2 secondary structure, allowing the Na^+-dependent inactive state to be maintained despite increases in intracellular Ca^{2+} levels. The ensuing effects of reduced Ca^{2+} entry may be linked to the neuroprotective effects imparted by NCX2.1 during ischemic injury.

A new role has been identified for the region corresponding to the mutually exclusive exon, involving stabilization of the Na^+-dependent inactive state independently of Ca^{2+}-binding. This requires interaction with different regions of the exchanger, such as the XIP region, which is required for Na^+-dependent inactivation to occur. The mutually exclusive exons impart a structural conformation facilitating the formation or stabilization of the Na^+-dependent inactive state. Moreover, depending on which mutually exclusive exon is expressed, this structural stability is dependent not only on interaction between the mutually exclusive exon and the XIP region, but also on yet to be identified residues elsewhere in the exchanger. The alternative splice region is key in mediating both Na^+ and Ca^{2+}-dependent regulation of NCX isoforms, NCX1 and NCX2.

8. REFERENCES

1. **Amran MS, Homma N and Hashimoto K**. Pharmacology of KB-R7943: a $Na^{+}Ca^{2+}$ exchange inhibitor. *Cardiovasc Drug Rev* 21: 255-276, 2003.

2. **Ander BP, Hurtado C, Raposo CS, Maddaford TG, Deniset JF, Hryshko LV, Pierce GN and Lukas A**. Differential sensitivities of the NCX1.1 and NCX1.3 isoforms of the $Na(^{+})$-$Ca(^{2+})$ exchanger to alpha-linolenic acid. *Cardiovasc Res* 73: 395-403, 2007.

3. **Anderson SE, Cala PM, Steenbergen C, London RE and Murphy E**. Effects of hypoxia and acidification on myocardial Na and Ca. Role of Na-H and Na-Ca exchange. *Ann N Y Acad Sci* 639: 453-455, 1991.

4. **Annunziato L, Cataldi M, Pignataro G, Secondo A and Molinaro P**. Glutamate-independent calcium toxicity: introduction. *Stroke* 38: 661-664, 2007.

5. **Arakawa N, Sakaue M, Yokoyama I, Hashimoto H, Koyama Y, Baba A and Matsuda T**. KB-R7943 Inhibits Store-Operated Ca^{2+} Entry in Cultured Neurons and Astrocytes. *Biochem Biophys Res Commun* 279: 354-357, 2000.

6. **Araujo IM and Carvalho CM**. Role of nitric oxide and calpain activation in neuronal death and survival. *Curr Drug Targets CNS Neurol Disord* 4: 319-324, 2005.

7. **Armoundas AA, Hobai IA, Tomaselli GF, Winslow RL and O'Rourke B**. Role of sodium-calcium exchanger in modulating the action potential of ventricular myocytes from normal and failing hearts. *Circ Res* 93: 46-53, 2003.

8. **Arundine M and Tymianski M**. Molecular mechanisms of glutamate-dependent neurodegeneration in ischemia and traumatic brain injury. *Cell Mol Life Sci* 61: 657-668, 2004.

9. **Arundine M and Tymianski M**. Molecular mechanisms of calcium-dependent neurodegeneration in excitotoxicity. *Cell Calcium* 34: 325-337, 2003.

10. **Baker PF, Blaustein MP, Hodgkin AL and Steinhardt RA**. The influence of calcium on sodium efflux in squid axons. *J Physiol (Lond)* 200: 431-458, 1969.

11. **Bano D, Young KW, Guerin CJ, Lefeuvre R, Rothwell NJ, Naldini L, Rizzuto R, Carafoli E and Nicotera P**. Cleavage of the plasma membrane Na^{+}/Ca^{2+} exchanger in excitotoxicity. *Cell* 120: 275-285, 2005.

12. **Bers DM**. Cardiac excitation-contraction coupling. *Nature* 415: 198-205, 2002.

13. **Bers DM**. Calcium cycling and signaling in cardiac myocytes. *Annu Rev Physiol* 70: 23-49, 2008.

14. **Bers DM**. Calcium fluxes involved in control of cardiac myocyte contraction. *Circ Res* 87: 275-281, 2000.

15. **Bers DM, Barry WH and Despa S**. Intracellular Na^+ regulation in cardiac myocytes. *Cardiovasc Res* 57: 897-912, 2003.

16. **Bers DM, Despa S and Bossuyt J**. Regulation of Ca2+ and Na+ in normal and failing cardiac myocytes. *Ann N Y Acad Sci* 1080: 165-177, 2006.

17. **Besserer GM, Ottolia M, Nicoll DA, Chaptal V, Cascio D, Philipson KD and Abramson J**. The second Ca^{2+}-binding domain of the Na^+-Ca^{2+} exchanger is essential for regulation: crystal structures and mutational analysis. *Proc Natl Acad Sci U S A* 104: 18467-18472, 2007.

18. **Boscia F, Gala R, Pignataro G, de Bartolomeis A., Cicale M, Ambesi-Impiombato A, Di Renzo G. and Annunziato L**. Permanent focal brain ischemia induces isoform-dependent changes in the pattern of Na^+/Ca^{2+} exchanger gene expression in the ischemic core, periinfarct area, and intact brain regions. *J Cereb Blood Flow Metab* 26: 502-517, 2006.

19. **Bouchard R, Omelchenko A, Le HD, Choptiany P, Matsuda T, Baba A, Takahashi K, Nicoll DA, Philipson KD, Hnatowich M and Hryshko LV**. Effects of SEA0400 on mutant NCX1.1 Na^+-Ca^{2+} exchangers with altered ionic regulation. *Mol Pharmacol* 65: 802-810, 2004.

20. **Bouron A and Reuter H**. A role of intracellular Na+ in the regulation of synaptic transmission and turnover of the vesicular pool in cultured hippocampal cells. *Neuron* 17: 969-978, 1996.

21. **Breder J, Sabelhaus CF, Opitz T, Reymann KG and Schroder UH**. Inhibition of different pathways influencing Na^+ homeostasis protects organotypic hippocampal slice cultures from hypoxic/hypoglycemic injury. *Neuropharmacology* 39: 1779-1787, 2000.

22. **Bridge JH, Smolley JR and Spitzer KW**. The relationship between charge movements associated with I_{Ca} and I_{Na-Ca} in cardiac myocytes. *Science* 248: 376-378, 1990.

23. **Cai X and Lytton J**. The Cation/Ca^{2+} Exchanger Superfamily: Phylogenetic Analysis and Structural Implications. *Mol Biol Evol* 21: 1692-1703, 2004.

24. **Castaldo P, Cataldi M, Magi S, Lariccia V, Arcangeli S and Amoroso S**. Role of the mitochondrial sodium/calcium exchanger in neuronal physiology and in the pathogenesis of neurological diseases. *Prog Neurobiol* 87: 58-79, 2009.

25. **Chen F, Mottino G, Shin VY and Frank JS**. Subcellular distribution of ankyrin in developing rabbit heart-- relationship to the Na^+-Ca^{2+} exchanger. *J Mol Cell Cardiol* 29: 2621-2629, 1997.

26. **Cho CH, Kim SS, Jeong MJ, Lee CO and Shin HS**. The Na^+ -Ca^{2+} exchanger is essential for embryonic heart development in mice. *Mol Cells* 10: 712-722, 2000.

27. **Condrescu M, Gardner JP, Chernaya G, Aceto JF, Kroupis C and Reeves JP**. ATP-dependent regulation of sodium-calcium exchange in Chinese hamster ovary cells transfected with the bovine cardiac sodium- calcium exchanger. *J Biol Chem* 270: 9137-9146, 1995.

28. **Dan P, Lin E, Huang J, Biln P and Tibbits GF**. Three-Dimensional Distribution of Cardiac Na^+-Ca^{2+} Exchanger and Ryanodine Receptor during Development. *Biophys J* 93: 2504-2518, 2007.

29. **Dascal N**. The use of Xenopus oocytes for the study of ion channels. *CRC Crit Rev Biochem* 22: 317-387, 1987.

30. **Davis KA, Samson SE, Hammel KE, Kiss L, Fulop F and Grover AK**. Functional linkage of Na(+)-Ca(2+)-exchanger to sarco/endoplasmic reticulum Ca(2+) pump in coronary artery: comparison of smooth muscle and endothelial cells. *J Cell Mol Med* 2008.

31. **Despa S, Islam MA, Weber CR, Pogwizd SM and Bers DM**. Intracellular Na^+ concentration is elevated in heart failure but Na/K pump function is unchanged. *Circulation* 105: 2543-2548, 2002.

32. **Dipla K, Mattiello JA, Margulies KB, Jeevanandam V and Houser SR**. The sarcoplasmic reticulum and the Na^+/Ca^{2+} exchanger both contribute to the Ca^{2+} transient of failing human ventricular myocytes. *Circ Res* 84: 435-444, 1999.

33. **DiPolo R and Beauge L**. Phosphoarginine stimulation of Na^+-Ca^{2+} exchange in squid axons-a new pathway for metabolic regulation? *J Physiol (Lond)* 487: 57-66, 1995.

34. **Doering AE, Nicoll DA, Lu Y, Lu L, Weiss JN and Philipson KD**. Topology of a functionally important region of the cardiac Na^+/Ca^{2+} exchanger. *J Biol Chem* 273: 778-783, 1998.

35. **Dunn J, Elias CL, Le HD, Omelchenko A, Hryshko LV and Lytton J**. The molecular determinants of ionic regulatory differences between brain and kidney Na^+/Ca^{2+} exchanger (NCX1) isoforms. *J Biol Chem* 277: 33957-33962, 2002.

36. **Durkin JT, Ahrens DC, Pan YC and Reeves JP**. Purification and amino-terminal sequence of the bovine cardiac sodium- calcium exchanger: evidence for the presence of a signal sequence. *Arch Biochem Biophys* 290: 369-375, 1991.

37. **Dyck C, Maxwell K, Buchko J, Trac M, Omelchenko A, Hnatowich M and Hryshko LV**. Structure-function analysis of CALX1.1, a Na^+-Ca^{2+} exchanger from *Drosophila*. Mutagenesis of ionic regulatory sites. *J Biol Chem* 273: 12981-12987, 1998.

38. **Dyck C, Omelchenko A, Elias CL, Quednau BD, Philipson KD, Hnatowich M and Hryshko L**. Ionic regulatory properties of brain and kidney splice variants of the NCX1 Na^+-Ca^{2+} exchanger. *J Gen Physiol* 114: 701-711, 1999.

39. **Elias CL, Lukas A, Shurraw S, Scott J, Omelchenko A, Gross GJ, Hnatowich M and Hryshko LV**. Inhibition of Na^+/Ca^{2+} exchange by KB-R7943: transport mode selectivity and antiarrhythmic consequences. *Am J Physiol Heart Circ Physiol* 281: H1334-H1345, 2001.

40. **Enyedi A, Vorherr T, James P, McCormick DJ, Filoteo AG, Carafoli E and Penniston JT**. The calmodulin binding domain of the plasma membrane Ca^{2+} pump interacts both with calmodulin and with another part of the pump. *J Biol Chem* 264: 12313-12321, 1989.

41. **Fierro L, DiPolo R and Llano I**. Intracellular calcium clearance in Purkinje cell somata from rat cerebellar slices. *J Physiol* 510 (Pt 2): 499-512, 1998.

42. **Flesch M, Schwinger RH, Schiffer F, Frank K, Sudkamp M, Kuhn-Regnier F, Arnold G and Bohm M**. Evidence for functional relevance of an enhanced expression of the Na^+-Ca^{2+} exchanger in failing human myocardium. *Circulation* 94: 992-1002, 1996.

43. **Folmes CD, Sowah D, Clanachan AS and Lopaschuk GD**. High rates of residual fatty acid oxidation during mild ischemia decrease cardiac work and efficiency. *J Mol Cell Cardiol* 2009.

44. **Formisano L, Saggese M, Secondo A, Sirabella R, Vito P, Valsecchi V, Molinaro P, Di Renzo G and Annunziato L**. The two isoforms of the Na+/Ca2+ exchanger, NCX1 and NCX3, constitute novel additional targets for the prosurvival action of Akt/protein kinase B pathway. *Mol Pharmacol* 73: 727-737, 2008.

45. **Fowler MR, Naz JR, Graham MD, Bru-Mercier G, Harrison SM and Orchard CH**. Decreased Ca^{2+} extrusion via Na^{+}/Ca^{2+} exchange in epicardial left ventricular myocytes during compensated hypertrophy. *Am J Physiol Heart Circ Physiol* 288: H2431-H2438, 2005.

46. **Fraysse B, Rouaud T, Millour M, Fontaine-Perus J, Gardahaut MF and Levitsky DO**. Expression of the Na^{+}/Ca^{2+} exchanger in skeletal muscle. *Am J Physiol Cell Physiol* 280: C146-C154, 2001.

47. **Fujiyoshi Y, Mitsuoka K, de Groot BL, Philippsen A, Grubmuller H, Agre P and Engel A**. Structure and function of water channels. *Curr Opin Struct Biol* 12: 509-515, 2002.

48. **Furman I, Cook O, Kasir J, Low W and Rahamimoff H**. The putative amino-terminal signal peptide of the cloned rat brain Na^{+}-Ca^{2+} exchanger gene (RBE-1) is not mandatory for functional expression. *J Biol Chem* 270: 19120-19127, 1995.

49. **Gibney GT, Zhang JH, Douglas RM, Haddad GG and Xia Y**. Na^{+}/Ca^{2+} exchanger expression in the developing rat cortex. *Neuroscience* 112: 65-73, 2002.

50. **Gilbert JR and Meissner G**. Sodium-calcium ion exchange in skeletal muscle sarcolemmal vesicles. *J Membr Biol* 69: 77-84, 1982.

51. **Gomez AM, Valdivia HH, Cheng H, Lederer MR, Santana LF, Cannell MB, McCune SA, Altschuld RA and Lederer WJ**. Defective excitation-contraction coupling in experimental cardiac hypertrophy and heart failure. *Science* 276: 800-806, 1997.

52. **Hale CC, Bliler S, Quinn TP and Peletskaya EN**. Localization of an exchange inhibitory peptide (XIP) binding site on the cardiac sodium-calcium exchanger. *Biochem Biophys Res Commun* 236: 113-117, 1997.

53. **He LP, Soldatov NM, Cleemann L and Morad M**. Molecular determinants of cAMP regulation of recombinant Na^{+}-Ca^{2+} exchanger. *Biophys J* 78: 373A, 2000.

54. **He S, Ruknudin A, Bambrick LL, Lederer WJ and Schulze DH**. Isoform-specific regulation of the Na^{+}/Ca^{2+} exchanger in rat astrocytes and neurons by PKA. *J Neurosci* 18: 4833-4841, 1998.

55. **He Z, Feng S, Tong Q, Hilgemann DW and Philipson KD**. Interaction of PIP_2 with the XIP region of the cardiac Na/Ca exchanger. *Am J Physiol* 278: C661-C666, 2000.

56. **He Z, Petesch N, Voges K, Roben W and Philipson KD**. Identification of important amino acid residues of the Na^+-Ca^{2+} exchanger inhibitory peptide, XIP. *J Membr Biol* 156: 149-156, 1997.

57. **Henderson SA, Goldhaber JI, So JM, Han T, Motter C, Ngo A, Chantawansri C, Ritter MR, Friedlander M, Nicoll DA, Frank JS, Jordan MC, Roos KP, Ross RS and Philipson KD**. Functional adult myocardium in the absence of Na^+-Ca^{2+} exchange. Cardiac-specific knockout of NCX1. *Circ Res* 95: 604-611, 2004.

58. **Hilge M, Aelen J, Perrakis A and Vuister GW**. Structural basis for Ca^{2+} regulation in the Na^+/Ca^{2+} exchanger. *Ann N Y Acad Sci* 1099: 7-15, 2007.

59. **Hilge M, Aelen J and Vuister GW**. Ca^{2+} regulation in the Na^+/Ca^{2+} exchanger involves two markedly different Ca^{2+} sensors. *Mol Cell* 22: 15-25, 2006.

60. **Hilgemann DW**. Giant excised cardiac sarcolemmal membrane patches: sodium and sodium- calcium exchange currents. *Pflugers Arch* 415: 247-249, 1989.

61. **Hilgemann DW**. Regulation and deregulation of cardiac Na^+-Ca^{2+} exchange in giant excised sarcolemmal membrane patches. *Nature* 344: 242-245, 1990.

62. **Hilgemann DW and Ball R**. Regulation of cardiac Na^+,Ca^{2+} exchange and K_{ATP} potassium channels by PIP_2. *Science* 273: 956-959, 1996.

63. **Hilgemann DW, Collins A, Cash DP and Nagel GA**. Cardiac Na^+-Ca^{2+} exchange system in giant membrane patches. *Ann N Y Acad Sci* 639: 126-139, 1991.

64. **Hilgemann DW, Collins A and Matsuoka S**. Steady-state and dynamic properties of cardiac sodium-calcium exchange. Secondary modulation by cytoplasmic calcium and ATP. *J Gen Physiol* 100: 933-961, 1992.

65. **Hilgemann DW, Matsuoka S, Nagel GA and Collins A**. Steady-state and dynamic properties of cardiac sodium-calcium exchange. Sodium-dependent inactivation. *J Gen Physiol* 100: 905-932, 1992.

66. **Hilgemann DW and Noble D**. Excitation-contraction coupling and extracellular calcium transients in rabbit atrium: reconstruction of basic cellular mechanisms. *Proc R Soc Lond B Biol Sci* 230: 163-205, 1987.

67. **Hobai IA, Maack C and O'Rourke B**. Partial inhibition of sodium/calcium exchange restores cellular calcium handling in canine heart failure. *Circ Res* 95: 292-299, 2004.

68. **Hoffman JW, Jr., Gilbert TB, Poston RS and Silldorff EP**. Myocardial reperfusion injury: etiology, mechanisms, and therapies. *J Extra Corpor Technol* 36: 391-411, 2004.

69. **Hotta Y, Lu X, Yajima M, Ishikawa N, Ito K, Inoue Y and Sakaue T**. Protective effect of SN-6, a selective Na^+-Ca^{2+} exchange inhibitor, on ischemia-reperfusion-injured hearts. *Jpn J Pharmacol* 88, Suppl. 1: 257, 2002.

70. **Hou ST and MacManus JP**. Molecular mechanisms of cerebral ischemia-induced neuronal death. *Int Rev Cytol* 221: 93-148, 2002.

71. **Hoyt KR, Stout AK, Cardman JM and Reynolds IJ**. The role of intracellular Na^+ and mitochondria in buffering of kainate- induced intracellular free Ca^{2+} changes in rat forebrain neurones. *J Physiol (Lond)* 509: 103-116, 1998.

72. **Hryshko LV**. Membrane pumps and exchangers. In: Cardiac Electrophysiology: From Cell to Bedside, edited by Zipes DP and Jalife J. W.B. Saunders Company, 2004, p. 42-50.

73. **Hryshko LV**. The cardiac Na^+-Ca^{2+} exchanger. In: Handbook of Physiology. Section 2: The Cardiovascular System. V. 1: The Heart, edited by Page.E., Fozzard HA and Solaro RJ. Oxford: Oxford University Press, 2002, p. 388-419.

74. **Hryshko LV, Matsuoka S, Nicoll DA, Weiss JN, Schwarz EM, Benzer S and Philipson KD**. Anomalous regulation of the *Drosophila* Na^+-Ca^{2+} exchanger by Ca^{2+}. *J Gen Physiol* 108: 67-74, 1996.

75. **Hryshko LV, Nicoll DA, Weiss JN and Philipson KD**. Biosynthesis and initial processing of the cardiac sarcolemmal Na^+- Ca^{2+} exchanger. *Biochim Biophys Acta* 1151: 35-42, 1993.

76. **Hurtado C, Ander BP, Maddaford TG, Lukas A, Hryshko LV and Pierce GN**. Adenovirally delivered shRNA strongly inhibits Na^+-Ca^{2+} exchanger expression but does not prevent contraction of neonatal cardiomyocytes. *J Mol Cell Cardiol* 38: 647-654, 2005.

77. **Hurtado C, Prociuk M, Maddaford TG, Dibrov E, Mesaeli N, Hryshko LV and Pierce GN**. CELLS EXPRESSING UNIQUE SODIUM-CALCIUM EXCHANGE (NCX1) SPLICE VARIANTS EXHIBIT DIFFERENT SUSCEPTIBILITIES TO CA2+ OVERLOAD. *Am J Physiol Heart Circ Physiol* e-pub: 2006.

78. **Isosaki M, Minami N and Nakashima T**. Pharmacological evidence for regulation of Na^+-Ca^{++} exchange by Ca^{++}/calmodulin-dependent protein kinase in isolated bovine adrenal medullary cells. *J Pharmacol Exp Ther* 270: 104-110, 1994.

79. **Iwamoto T**. Na^+/Ca^{2+} exchange as a drug target--insights from molecular pharmacology and genetic engineering. *Ann N Y Acad Sci* 1099: 516-528, 2007.

80. **Iwamoto T**. Vascular Na^+/Ca^{2+} exchanger: implications for the pathogenesis and therapy of salt-dependent hypertension. *Am J Physiol Regul Integr Comp Physiol* 290: R536-R545, 2006.

81. **Iwamoto T, Inoue Y, Ito K, Sakaue T, Kita S and Katsuragi T**. The exchanger inhibitory peptide region-dependent inhibition of Na^+/Ca^{2+} exchange by SN-6 [2-[4-(4-nitrobenzyloxy)benzyl]thiazolidine-4-carboxylic acid ethyl ester], a novel benzyloxyphenyl derivative. *Mol Pharmacol* 66: 45-55, 2004.

82. **Iwamoto T and Kita S**. Topics on the Na^+/Ca^{2+} exchanger: role of vascular NCX1 in salt-dependent hypertension. *J Pharmacol Sci* 102: 32-36, 2006.

83. **Iwamoto T and Kita S**. YM-244769, a novel Na^+/Ca^{2+} exchange inhibitor that preferentially inhibits NCX3, efficiently protects against hypoxia/reoxygenation-induced SH-SY5Y neuronal cell damage. *Mol Pharmacol* 70: 2075-2083, 2006.

84. **Iwamoto T, Kita S and Katsuragi T**. Endothelin-1 Aggravates Hypoxia/Reoxygenationinduced Injury in Renal Epithelial Cells through the Activation of a Na^+/Ca^{2+} Exchanger. *J Cardiovasc Pharmacol* 44 Suppl 1: S462-S466, 2004.

85. **Iwamoto T, Kita S and Katsuragi T**. Salt-sensitive hypertension, Na^+/Ca^{2+} exchanger, and vascular smooth muscle. *Trends Cardiovasc Med* 15: 273-277, 2005.

86. **Iwamoto T, Kita S and Shigekawa M**. [Functional analysis of Na^+/Ca^{2+} exchanger using novel drugs and genetically engineered mice]. *Nippon Yakurigaku Zasshi* 120: 91-93, 2002.

87. **Iwamoto T, Kita S, Uehara A, Imanaga I, Matsuda T, Baba A and Katsuragi T**. Molecular determinants of Na^+/Ca^{2+} exchange (NCX1) inhibition by SEA0400. *J Biol Chem* 279: 7544-7553, 2004.

88. **Iwamoto T, Kita S, Uehara A, Inoue Y, Taniguchi Y, Imanaga I and Shigekawa M**. Structural Domains Influencing Sensitivity to Isothiourea Derivative Inhibitor KB-R7943 in Cardiac $Na^{+/Ca2+\ Exchanger}$. *Mol Pharmacol* 59: 524-531, 2001.

89. **Iwamoto T, Kita S, Zhang J, Blaustein MP, Arai Y, Yoshida S, Wakimoto K, Komuro I and Katsuragi T**. Salt-sensitive hypertension is triggered by Ca^{2+} entry via Na^+/Ca^{2+} exchanger type-1 in vascular smooth muscle. *Nat Med* 10: 1193-1199, 2004.

90. **Iwamoto T, Nakamura TY, Pan Y, Uehara A, Imanaga I and Shigekawa M**. Unique topology of the internal repeats in the cardiac Na^+/Ca^{2+} exchanger. *FEBS Lett* 446: 264-268, 1999.

91. **Iwamoto T, Pan Y, Nakamura TY, Wakabayashi S and Shigekawa M**. Protein kinase C-dependent regulation of Na^+/Ca^{2+} exchanger isoforms NCX1 and NCX3 does not require their direct phosphorylation. *Biochemistry* 37: 17230-17238, 1998.

92. **Iwamoto T, Pan Y, Wakabayashi S, Imagawa T, Yamanaka HI and Shigekawa M**. Phosphorylation-dependent regulation of cardiac Na^+/Ca^{2+} exchanger via protein kinase C. *J Biol Chem* 271: 13609-13615, 1996.

93. **Iwamoto T and Shigekawa M**. Differential inhibition of Na^+/Ca^{2+} exchanger isoforms by divalent cations and isothiourea derivative. *Am J Physiol* 275: C423-C430, 1998.

94. **Iwamoto T, Uehara A, Imanaga I and Shigekawa M**. The Na^+/Ca^{2+} exchanger NCX1 has oppositely oriented reentrant loop domains that contain conserved aspartic acids whose mutation alters its apparent Ca^{2+} affinity. *J Biol Chem* 275: 38571-38580, 2000.

95. **Iwamoto T, Uehara A, Nakamura TY, Imanaga I and Shigekawa M**. Chimeric analysis of Na^+/Ca^{2+} exchangers NCX1 and NCX3 reveals structural domains important for differential sensitivity to external Ni^{2+} or Li^+. *J Biol Chem* 274: 23094-23102, 1999.

96. **Iwamoto T, Wakabayashi S and Shigekawa M**. Growth factor-induced phosphorylation and activation of aortic smooth muscle Na^+/Ca^{2+} exchanger. *J Biol Chem* 270: 8996-9001, 1995.

97. **Iwamoto T, Watano T and Shigekawa M**. A novel isothiourea derivative selectively inhibits the reverse mode of Na^+/Ca^{2+} exchange in cells expressing NCX1. *J Biol Chem* 271: 22391-22397, 1996.

98. **Jeon D, Yang YM, Jeong MJ, Philipson KD, Rhim H and Shin HS**. Enhanced learning and memory in mice lacking Na^+/Ca^{2+} exchanger 2. *Neuron* 38: 965-976, 2003.

99. **Johnson E, Bruschweiler-Li L, Showalter SA, Vuister GW, Zhang F and Brnschweiler R**. Structure and Dynamics of Ca^{2+}-Binding Domain 1 of the Na^+/Ca^{2+} Exchanger in the Presence and in the Absence of Ca^{2+}. *Journal of Molecular Biology* 377: 945-955, 2008.

100. **Juhaszova M, Church P, Blaustein MP and Stanley EF**. Location of calcium transporters at presynaptic terminals. *Eur J Neurosci* 12: 839-846, 2000.

101. **Karmazyn M**. The myocardial sodium-hydrogen exchanger (NHE) and its role in mediating ischemic and reperfusion injury. *Keio J Med* 47: 65-72, 1998.

102. **Karmazyn M, Gan XT, Humphreys RA, Yoshida H and Kusumoto K**. The myocardial Na^+-H^+ exchange. Structure, regulation, and its role in heart disease. *Circ Res* 85: 777-786, 1999.

103. **Katanosaka Y, Iwata Y, Kobayashi Y, Shibasaki F, Wakabayashi S and Shigekawa M**. Calcineurin inhibits Na^+/Ca^{2+} exchange in phenylephrine-treated hypertrophic cardiomyocytes. *J Biol Chem* 280: 5764-5772, 2005.

104. **Kiedrowski L**. Critical role of sodium in cytosolic [Ca2+] elevations in cultured hippocampal CA1 neurons during anoxic depolarization. *J Neurochem* 100: 915-923, 2007.

105. **Kiedrowski L, Czyz A, Baranauskas G, Li XF and Lytton J**. Differential contribution of plasmalemmal Na/Ca exchange isoforms to sodium-dependent calcium influx and NMDA excitotoxicity in depolarized neurons. *J Neurochem* 90: 117-128, 2004.

106. **Kintner DB, Wang Y and Sun D**. Role of membrane ion transport proteins in cerebral ischemic damage. *Front Biosci* 12: 762-770, 2007.

107. **Kita S, Katsuragi T and Iwamoto T**. Endothelin-1 Enhances the Activity of Na^+/Ca^{2+} Exchanger Type 1 in Renal Epithelial Cells. *J Cardiovasc Pharmacol* 44: S239-S243, 2004.

108. **Kofuji P, Hadley RW, Kieval RS, Lederer WJ and Schulze DH**. Expression of the Na-Ca exchanger in diverse tissues: a study using the cloned human cardiac Na-Ca exchanger. *Am J Physiol* 263: C1241-C1249, 1992.

109. **Kofuji P, Lederer WJ and Schulze DH**. Mutually exclusive and cassette exons underlie alternatively spliced isoforms of the Na/Ca exchanger. *J Biol Chem* 269: 5145-5149, 1994.

110. **Komuro I, Wenninger KE, Philipson KD and Izumo S**. Molecular cloning and characterization of the human cardiac Na^+/Ca^{2+} exchanger cDNA. *Proc Natl Acad Sci U S A* 89: 4769-4773, 1992.

111. **Koushik SV, Wang J, Rogers R, Moskophidis D, Lambert NA, Creazzo TL and Conway SJ**. Targeted inactivation of the sodium-calcium exchanger (Ncx1) results in the lack of a heartbeat and abnormal myofibrillar organization. *FASEB J* 15: 1209-1211, 2001.

112. **Kuramochi T, Kakefuda A, Yamada H, Tsukamoto I, Taguchi T and Sakamoto S**. Discovery of an N-(2-aminopyridin-4-ylmethyl)nicotinamide

derivative: a potent and orally bioavailable NCX inhibitor. *Bioorg Med Chem* 13: 4022-4036, 2005.

113. **Kuro T, Kobayashi Y, Takaoka M and Matsumura Y**. Protective effect of KB-R7943, a novel Na^+/Ca^{2+} exchange inhibitor, on ischemic acute renal failure in rats. *Jpn J Pharmacol* 81: 247-251, 1999.

114. **Kutryk MJ and Pierce GN**. Stimulation of sodium-calcium exchange by cholesterol incorporation into isolated cardiac sarcolemmal vesicles. *J Biol Chem* 263: 13167-13172, 1988.

115. **Ladilov Y, Haffner S, Balser-Schafer C, Maxeiner H and Piper HM**. Cardioprotective effects of KB-R7943: a novel inhibitor of the reverse mode of Na^+/Ca^{2+} exchanger. *Am J Physiol* 276: H1868-H1876, 1999.

116. **Lederer WJ, Berlin JR, Cohen NM, Hadley RW, Bers DM and Cannell MB**. Excitation-contraction coupling in heart cells. Roles of the sodium- calcium exchange, the calcium current, and the sarcoplasmic reticulum. *Ann N Y Acad Sci* 588: 190-206, 1990.

117. **Lederer WJ, He s, Luo S, duBell W, Kofuji P, Kieval R, Neubauer CF, Ruknudin A, Cheng H, Cannell MB, Rogers TB and Schulze DH**. The molecular biology of the Na^+-Ca^{2+} exchanger and its functional roles in heart, smooth muscle cells, neurons, glia, lymphocytes, and nonexcitable cells. *Ann N Y Acad Sci* 779: 7-17, 1996.

118. **Lee C, Dhalla NS and Hryshko LV**. Therapeutic potential of novel Na^+-Ca^{2+} exchange inhibitors in attenuating ischemia-reperfusion injury. *Can J Cardiol* 21: 509-516, 2005.

119. **Lee C and Hryshko LV**. SEA0400: a novel sodium-calcium exchange inhibitor with cardioprotective properties. *Cardiovasc Drug Rev* 22: 334-347, 2004.

120. **Lee SL, Yu AS and Lytton J**. Tissue-specific expression of Na^+-Ca^{2+} exchanger isoforms. *J Biol Chem* 269: 14849-14852, 1994.

121. **Levitsky DO, Nicoll DA and Philipson KD**. Identification of the high affinity Ca^{2+}-binding domain of the cardiac Na^+-Ca^{2+} exchanger. *J Biol Chem* 269: 22847-22852, 1994.

122. **Li LL, Sun LN, Zhou HY, Li ZB and Wang XL**. Selective alteration of expression of Na^+/Ca^{2+} exchanger isoforms after transient focal cerebral ischemia in rats. *Neurosci Lett* 404: 249-253, 2006.

123. **Li Z, Matsuoka S, Hryshko LV, Nicoll DA, Bersohn MM, Burke EP, Lifton RP and Philipson KD**. Cloning of the NCX2 isoform of the plasma membrane Na^+-Ca^{2+} exchanger. *J Biol Chem* 269: 17434-17439, 1994.

124. **Li Z, Nicoll DA, Collins A, Hilgemann DW, Filoteo AG, Penniston JT, Weiss JN, Tomich JM and Philipson KD**. Identification of a peptide inhibitor of the cardiac sarcolemmal Na^+- Ca^{2+} exchanger. *J Biol Chem* 266: 1014-1020, 1991.

125. **Li ZP, Burke EP, Frank JS, Bennett V and Philipson KD**. The cardiac Na^+-Ca^{2+} exchanger binds to the cytoskeletal protein ankyrin. *J Biol Chem* 268: 11489-11491, 1993.

126. **Linck B, Qiu Z, He Z, Tong Q, Hilgemann DW and Philipson KD**. Functional comparison of the three isoforms of the Na^+/Ca^{2+} exchanger (NCX1, NCX2, NCX3). *Am J Physiol* 274: C415-C423, 1998.

127. **Litwin S, Kohmoto O, Levi AJ, Spitzer KW and Bridge JH**. Evidence that reverse Na-Ca exchange can trigger SR calcium release. *Ann N Y Acad Sci* 779: 451-463, 1996.

128. **Litwin SE and Bridge JH**. Enhanced Na^+-Ca^{2+} exchange in the infarcted heart. Implications for excitation-contraction coupling. *Circ Res* 81: 1083-1093, 1997.

129. **Litwin SE, Li J and Bridge JH**. Na-Ca exchange and the trigger for sarcoplasmic reticulum Ca release: studies in adult rabbit ventricular myocytes. *Biophys J* 75: 359-371, 1998.

130. **Liu XK, Engelman RM, Iyengar J, Cordis GA and Das DK**. Amiloride enhances postischemic ventricular recovery during cardioplegic arrest. A possible role of Na^+-Ca^{2+} exchange. *Ann N Y Acad Sci* 639: 471-474, 1991.

131. **Loo TW, Ho C and Clarke DM**. Expression of a functionally active human renal sodium-calcium exchanger lacking a signal sequence. *J Biol Chem* 270: 19345-19350, 1995.

132. **Lu HR, Yang P, Remeysen P, Saels A, Dai DZ and De Clerck F**. Ischemia/reperfusion-induced arrhythmias in anaesthetized rats: a role of Na^+ and Ca^{2+} influx. *Eur J Pharmacol* 365: 233-239, 1999.

133. **Lynch GS, Fary CJ and Williams DA**. Quantitative measurement of resting skeletal muscle [Ca2+]i following acute and long-term downhill running exercise in mice. *Cell Calcium* 22: 373-383, 1997.

134. **Lytton J**. Na^+/Ca^{2+} exchangers: three mammalian gene families control Ca^{2+} transport. *Biochem J* 406: 365-382, 2007.

135. **Maack C, Ganesan A, Sidor A and O'Rourke B**. Cardiac sodium-calcium exchanger is regulated by allosteric calcium and exchanger inhibitory peptide at distinct sites. *Circ Res* 96: 91-99, 2005.

136. **Magee WP, Deshmukh G, DeNinno MP, Sutt JC, Chapman JG and Tracey WR**. Differing cardioprotective efficacy of the Na^+-Ca^{2+} exchanger inhibitors, SEA0400 and KB-R7943. *Am J Physiol Heart Circ Physiol* 284: H903-H910, 2003.

137. **Marshall CR, Fox JA, Butland SL, Ouellette BF, Brinkman FS and Tibbits GF**. Phylogeny of Na^+/Ca^{2+} exchanger (NCX) genes from genomic data identifies new gene duplications and a new family member in fish species. *Physiol Genomics* 21: 161-173, 2005.

138. **Matsuda T, Arakawa N, Takuma K, Kishida Y, Kawasaki Y, Sakaue M, Takahashi K, Takahashi T, Suzuki T, Ota T, Hamano-Takahashi A, Onishi M, Tanaka Y, Kameo K and Baba A**. SEA0400, a novel and selective inhibitor of the Na^+- Ca^{2+} exchanger, attenuates reperfusion injury in the in vitro and in vivo cerebral ischemic models. *J Pharmacol Exp Ther* 298: 249-256, 2001.

139. **Matsumoto T, Miura T, Miki T, Genda S and Shimamoto K**. Blockade of the Na^+/Ca^{2+} exchanger is more efficient than blockade of the Na^+/H^+ exchanger for protection of the myocardium from lethal reperfusion injury. *Cardiovasc Drugs Ther* 16: 295-301, 2002.

140. **Matsuoka S**. Forefront of Na^+/Ca^{2+} exchanger studies: Regulation kinetics of Na^+/Ca^{2+} exchangers. *J Pharmacol Sci* 96: 12-14, 2004.

141. **Matsuoka S and Hilgemann DW**. Steady-state and dynamic properties of cardiac sodium-calcium exchange. Ion and voltage dependencies of the transport cycle. *J Gen Physiol* 100: 963-1001, 1992.

142. **Matsuoka S, Nicoll DA, He Z and Philipson KD**. Regulation of cardiac Na^+-Ca^{2+} exchanger by the endogenous XIP region. *J Gen Physiol* 109: 273-286, 1997.

143. **Matsuoka S, Nicoll DA, Hryshko LV, Levitsky DO, Weiss JN and Philipson KD**. Regulation of the cardiac Na^+-Ca^{2+} exchanger by Ca^{2+}. Mutational analysis of the Ca^{2+}-binding domain. *J Gen Physiol* 105: 403-420, 1995.

144. **Matsuoka S, Nicoll DA, Reilly RF, Hilgemann DW and Philipson KD**. Initial localization of regulatory regions of the cardiac sarcolemmal Na^+-Ca^{2+} exchanger. *Proc Natl Acad Sci U S A* 90: 3870-3874, 1993.

145. **Mattiello JA, Margulies KB, Jeevanandam V and Houser SR**. Contribution of reverse-mode sodium-calcium exchange to contractions in failing human left ventricular myocytes. *Cardiovasc Res* 37: 424-431, 1998.

146. **Menick DR, Renaud L, Buchholz A, Muller JG, Zhou H, Kappler CS, Kubalak SW, Conway SJ and Xu L**. Regulation of Ncx1 gene expression in the normal and hypertrophic heart. *Ann N Y Acad Sci* 1099: 195-203, 2007.

147. **Meyer M, Schillinger W, Pieske B, Holubarsch C, Heilmann C, Posival H, Kuwajima G, Mikoshiba K, Just H and Hasenfuss G**. Alterations of sarcoplasmic reticulum proteins in failing human dilated cardiomyopathy. *Circulation* 92: 778-784, 1995.

148. **Michaelis ML**. Drugs targeting Alzheimer's disease: some things old and some things new. *J Pharmacol Exp Ther* 304: 897-904, 2003.

149. **Milberg P, Pott C, Fink M, Frommeyer G, Matsuda T, Baba A, Osada N, Breithardt G, Noble D and Eckardt L**. Inhibition of the Na^+/Ca^{2+} exchanger suppresses torsades de pointes in an intact heart model of long QT syndrome-2 and long QT syndrome-3. *Heart Rhythm* 5: 1444-1452, 2008.

150. **Minelli A, Castaldo P, Gobbi P, Salucci S, Magi S and Amoroso S**. Cellular and subcellular localization of Na^+-Ca^{2+} exchanger protein isoforms, NCX1, NCX2, and NCX3 in cerebral cortex and hippocampus of adult rat. *Cell Calcium* 41: 221-234, 2007.

151. **Missan S and McDonald TF**. Cardiac Na^+-Ca^{2+} exchanger current induced by tyrphostin tyrosine kinase inhibitors. *Br J Pharmacol* epub: 2004.

152. **Mochizuki S and Jiang C**. Na^+/Ca^{++} exchanger and myocardial ischemia/reperfusion. *Jpn Heart J* 39: 707-714, 1998.

153. **Mochizuki S and MacLeod KT**. Effects of hypoxia and metabolic inhibition on increases in intracellular Ca^{2+} concentration induced by Na^+/Ca^{2+} exchange in isolated guinea-pig cardiac myocytes. *J Mol Cell Cardiol* 29: 2979-2987, 1997.

154. **Mohler PJ, Schott JJ, Gramolini AO, Dilly KW, Guatimosim S, duBell WH, Song LS, Haurogne K, Kyndt F, Ali ME, Rogers TB, Lederer WJ, Escande D, Le Marec H and Bennett V**. Ankyrin-B mutation causes type 4 long-QT cardiac arrhythmia and sudden cardiac death. *Nature* 421: 634-639, 2003.

155. **Molinaro P, Cuomo O, Pignataro G, Boscia F, Sirabella R, Pannaccione A, Secondo A, Scorziello A, Adornetto A, Gala R, Viggiano D, Sokolow S, Herchuelz A, Schurmans S, Di Renzo G and Annunziato L**. Targeted disruption of Na+/Ca2+ exchanger 3 (NCX3) gene leads to a worsening of ischemic brain damage. *J Neurosci* 28: 1179-1184, 2008.

156. **Murphy E, Cross H and Steenbergen C**. Sodium regulation during ischemia versus reperfusion and its role in injury. *Circ Res* 84: 1469-1470, 1999.

157. **Murphy E, Cross HR and Steenbergen C**. Is Na/Ca exchange during ischemia and reperfusion beneficial or detrimental? *Ann N Y Acad Sci* 976: 421-430, 2002.

158. **Murphy E, Wheeler DM, LeFurgey A, Jacob R, Lobaugh LA and Lieberman M**. Coupled sodium-calcium transport in cultured chick heart cells. *Am J Physiol* 250: C442-C452, 1986.

159. **Nicoll DA, Hryshko LV, Matsuoka S, Frank JS and Philipson KD**. Mutation of amino acid residues in the putative transmembrane segments of the cardiac sarcolemmal Na^+-Ca^{2+} exchanger. *J Biol Chem* 271: 13385-13391, 1996.

160. **Nicoll DA, Longoni S and Philipson KD**. Molecular cloning and functional expression of the cardiac sarcolemmal Na^+-Ca^{2+} exchanger. *Science* 250: 562-565, 1990.

161. **Nicoll DA, Ottolia M, Lu L, Lu Y and Philipson KD**. A new topological model of the cardiac sarcolemmal Na^+-Ca^{2+} exchanger. *J Biol Chem* 274: 910-917, 1999.

162. **Nicoll DA, Quednau BD, Qui Z, Xia YR, Lusis AJ and Philipson KD**. Cloning of a third mammalian Na^+-Ca^{2+} exchanger, NCX3. *J Biol Chem* 271: 24914-24921, 1996.

163. **Nicoll DA, Ren X, Ottolia M, Phillips M, Paredes AR, Abramson J and Philipson KD**. What we know about the structure of NCX1 and how it relates to its function. *Ann N Y Acad Sci* 1099: 1-6, 2007.

164. **Nicoll DA, Sawaya MR, Kwon S, Cascio D, Philipson KD and Abramson J**. The crystal structure of the primary Ca^{2+} sensor of the Na^+/Ca^{2+} exchanger reveals a novel Ca^{2+} binding motif. *J Biol Chem* 281: 21577-21581, 2006.

165. **O'Neil KT and DeGrado WF**. How calmodulin binds its targets: sequence independent recognition of amphiphilic alpha-helices. *Trends Biochem Sci* 15: 59-64, 1990.

166. **O'Rourke B, Kass DA, Tomaselli GF, Kaab S, Tunin R and Marban E**. Mechanisms of altered excitation-contraction coupling in canine tachycardia-induced heart failure, I: experimental studies. *Circ Res* 84: 562-570, 1999.

167. **Ogata M, Iwamoto T, Tazawa N, Nishikawa M, Yamashita J, Takaoka M and Matsumura Y**. A novel and selective Na^+/Ca^{2+} exchange inhibitor, SEA0400, improves ischemia/reperfusion-induced renal injury. *Eur J Pharmacol* 478: 187-198, 2003.

168. **Omelchenko A, Bouchard R, Le HD, Choptiany P, Visen N, Hnatowich M and Hryshko LV**. Inhibition of Canine (NCX1.1) and Drosophila (CALX1.1) Na^+-Ca^{2+} Exchangers by 7-Chloro-3,5-dihydro-5-phenyl-1H-4,1-benzothiazepine-2-one (CGP-37157). *J Pharmacol Exp Ther* 306: 1050-1057, 2003.

169. **Omelchenko A, Dyck C, Hnatowich M, Buchko J, Nicoll DA, Philipson KD and Hryshko LV**. Functional differences in ionic regulation between alternatively spliced isoforms of the Na^+-Ca^{2+} exchanger from *Drosophila melanogaster*. *J Gen Physiol* 111: 691-702, 1998.

170. **Omelchenko A, Le HD, Hnatowich M and Hryshko LV**. Effect of μ-calpain on CALX1.1, a Na^+-Ca^{2+} exchanger from *Drosophila melanogaster*. *Biophys J* 94: 85a, 2008.

171. **Omelchenko A, Le HD, Yurkov V, Hnatowich M and Hryshko LV**. Unique functional and pharmacological characteristics of NCX2. *Biophys J* January 2006: 512a, 2006.

172. **Ottolia M, John S, Xie Y, Ren X and Philipson KD**. Shedding light on the Na+/Ca2+ exchanger. *Ann N Y Acad Sci* 1099: 78-85, 2007.

173. **Ottolia M, Nicoll DA and Philipson KD**. Mutational analysis of the α-1 repeat of the cardiac Na^+-Ca^{2+} exchanger. *J Biol Chem* 280: 1061-1069, 2005.

174. **Ottolia M, Philipson KD and John S**. Conformational changes of the Ca^{2+} regulatory site of the Na^+-Ca^{2+} exchanger detected by FRET. *Biophys J* 87: 899-906, 2004.

175. **Pan Y, Iwamoto T, Uehara A, Nakamura TY, Imanaga I and Shigekawa M**. Physiological functions of the regulatory domains of the cardiac Na^+/Ca^{2+} exchanger NCX1. *Am J Physiol Cell Physiol* 279: C393-C402, 2000.

176. **Papa M, Canitano A, Boscia F, Castaldo P, Sellitti S, Porzig H, Taglialatela M and Annunziato L**. Differential expression of the Na^+-Ca^{2+} exchanger transcripts and proteins in rat brain regions. *J Comp Neurol* 461: 31-48, 2003.

177. **Philipson KD, Frank JS and Nishimoto AY**. Effects of phospholipase C on the Na^+-Ca^{2+} exchange and Ca^{2+} permeability of cardiac sarcolemmal vesicles. *J Biol Chem* 258: 5905-5910, 1983.

178. **Philipson KD, Longoni S and Ward R**. Purification of the cardiac Na^+-Ca^{2+} exchange protein. *Biochim Biophys Acta* 945: 298-306, 1988.

179. **Philipson KD, Nicoll DA, Ottolia M, Quednau BD, Reuter H, John S and Qiu Z**. The Na+/Ca2+ exchange molecule: an overview. *Ann N Y Acad Sci* 976: 1-10, 2002.

180. **Philipson KD and Nishimoto AY**. Stimulation of Na^+-Ca^{2+} exchange in cardiac sarcolemmal vesicles by phospholipase D. *J Biol Chem* 259: 16-19, 1984.

181. **Philipson KD and Ward R**. Effects of fatty acids on Na^+-Ca^{2+} exchange and Ca^{2+} permeability of cardiac sarcolemmal vesicles. *J Biol Chem* 260: 9666-9671, 1985.

182. **Pierce GN, Ward R and Philipson KD**. Role for sulfur-containing groups in the Na^+-Ca^{2+} exchange of cardiac sarcolemmal vesicles. *J Membr Biol* 94: 217-225, 1986.

183. **Pignataro G, Gala R, Cuomo O, Tortiglione A, Giaccio L, Castaldo P, Sirabella R, Matrone C, Canitano A, Amoroso S, Di RG and Annunziato L**. Two sodium/calcium exchanger gene products, NCX1 and NCX3, play a major role in the development of permanent focal cerebral ischemia. *Stroke* 35: 2566-2570, 2004.

184. **Pike MM, Kitakaze M and Marban E**. ^{23}Na-NMR measurements of intracellular sodium in intact perfused ferret hearts during ischemia and reperfusion. *Am J Physiol* 259: H1767-H1773, 1990.

185. **Pilitsis JG, Diaz FG, O'Regan MH and Phillis JW**. Inhibition of Na^+/Ca^{2+} exchange by KB-R7943, a novel selective antagonist, attenuates phosphoethanolamine and free fatty acid efflux in rat cerebral cortex during ischemia-reperfusion injury. *Brain Res* 916: 192-198, 2001.

186. **Pintado AJ, Herrero CJ, Garcia AG and Montiel C**. The novel Na^+/Ca^{2+} exchange inhibitor KB-R7943 also blocks native and expressed neuronal nicotinic receptors. *Br J Pharmacol* 130: 1893-1902, 2000.

187. **Pogwizd SM**. Clinical potential of sodium-calcium exchanger inhibitors as antiarrhythmic agents. *Drugs* 63: 439-452, 2003.

188. **Pogwizd SM, Qi M, Yuan W, Samarel AM and Bers DM**. Upregulation of Na^+/Ca^{2+} exchanger expression and function in an arrhythmogenic rabbit model of heart failure. *Circ Res* 85: 1009-1019, 1999.

189. **Pogwizd SM, Schlotthauer K, Li L, Yuan W and Bers DM**. Arrhythmogenesis and contractile dysfunction in heart failure: Roles of sodium-calcium exchange, inward rectifier potassium current, and residual β-adrenergic responsiveness. *Circ Res* 88: 1159-1167, 2001.

190. **Polumuri SK, Ruknudin A, McCarthy MM, Perrot-Sinal TS and Schulze DH**. Sodium-calcium exchanger NCX1, NCX2, and NCX3 transcripts in developing rat brain. *Ann N Y Acad Sci* 976: 60-63, 2002.

191. **Pott C, Goldhaber JI and Philipson KD**. Genetic manipulation of cardiac Na^+/Ca^{2+} exchange expression. *Biochem Biophys Res Commun* 322: 1336-1340, 2004.

192. **Pott C, Goldhaber JI and Philipson KD**. Homozygous overexpression of the Na+-Ca2+ exchanger in mice: evidence for increased transsarcolemmal Ca2+ fluxes. *Ann N Y Acad Sci* 1099: 310-314, 2007.

193. **Pott C, Philipson KD and Goldhaber JI**. Excitation-contraction coupling in Na^+-Ca^{2+} exchanger knockout mice: reduced transsarcolemmal Ca^{2+} flux. *Circ Res* 97: 1288-1295, 2005.

194. **Pott C, Ren X, Tran DX, Yang MJ, Henderson SA, Jordan MC, Roos KP, Garfinkel A, Philipson KD and Goldhaber J**. Mechanism of Shortened Action Potential Duration in Na^+-Ca^{2+} Exchanger Knockout Mice. *Am J Physiol Cell Physiol* 2006.

195. **Pott C, Yip M, Goldhaber JI and Philipson KD**. Regulation of cardiac L-type Ca^{2+} current in Na^+-Ca^{2+} exchanger knockout mice: functional coupling of the Ca^{2+} channel and the Na^+-Ca^{2+} exchanger. *Biophys J* 92: 1431-1437, 2007.

196. **Qiu Z, Nicoll DA and Philipson KD**. Helix packing of functionally important regions of the cardiac Na^{+}-Ca2+ exchanger. *J Biol Chem* 276: 194-199, 2001.

197. **Quednau BD, Nicoll DA and Philipson KD**. The sodium/calcium exchanger family-SLC8. *Pflugers Arch* 447: 543-548, 2004.

198. **Quednau BD, Nicoll DA and Philipson KD**. Tissue specificity and alternative splicing of the Na^+/Ca^{2+} exchanger isoforms NCX1, NCX2, and NCX3 in rat. *Am J Physiol* 272: C1250-C1261, 1997.

199. **Raizman JE, Komljenovic J, Chang R, Deng C, Bedosky KM, Rattan SG, Cunnington RH, Freed DH and Dixon IM**. The participation of the Na^+-Ca^{2+} exchanger in primary cardiac myofibroblast migration, contraction, and proliferation. *J Cell Physiol* 213: 540-551, 2007.

200. **Regehr WG**. Interplay between sodium and calcium dynamics in granule cell presynaptic terminals. *Biophys J* 73: 2476-2488, 1997.

201. **Ren X, Nicoll DA, Galang G and Philipson KD**. Intermolecular cross-linking of Na^+-Ca^{2+} exchanger proteins: evidence for dimer formation. *Biochemistry* 47: 6081-6087, 2008.

202. **Ren X, Nicoll DA and Philipson KD**. Helix packing of the cardiac Na^+-Ca^{2+} exchanger: proximity of transmembrane segments 1, 2, and 6. *J Biol Chem* 281: 22808-22814, 2006.

203. **Ren X, Nicoll DA and Philipson KD**. Transmembrane segments I, II, and VI of the canine cardiac Na^+/Ca^{2+} exchanger are in proximity. *Ann N Y Acad Sci* 1099: 40-42, 2007.

204. **Reuter H, Han T, Motter C, Philipson KD and Goldhaber JI**. Mice overexpressing the cardiac sodium-calcium exchanger: defects in excitation-contraction coupling. *J Physiol* 554: 779-789, 2004.

205. **Reuter H, Henderson SA, Han T, Matsuda T, Baba A, Ross RS, Goldhaber JI and Philipson KD**. Knockout mice for pharmacological screening: testing the specificity of Na^+-Ca^{2+} exchange inhibitors. *Circ Res* 91: 90-92, 2002.

206. **Reuter H, Henderson SA, Han T, Mottino GA, Frank JS, Ross RS, Goldhaber JI and Philipson KD**. Cardiac excitation-contraction coupling in the absence of Na^+ - Ca^{2+} exchange. *Cell Calcium* 34: 19-26, 2003.

207. **Reuter H and Porzig H**. Localization and functional significance of the Na^+/Ca^{2+} exchanger in presynaptic boutons of hippocampal cells in culture. *Neuron* 15: 1077-1084, 1995.

208. **Reuter H and Seitz N**. The dependence of calcium efflux from cardiac muscle on temperature and external ion composition. *J Physiol (Lond)* 195: 451-470, 1968.

209. **Ruiz-Meana M, Garcia-Dorado D, Hofstaetter B, Piper HM and Soler-Soler J**. Propagation of cardiomyocyte hypercontracture by passage of Na^+ through gap junctions. *Circ Res* 85: 280-287, 1999.

210. **Ruknudin A, Valdivia C, Kofuji P, Lederer WJ and Schulze DH**. Na^+/Ca^{2+} exchanger in *Drosophila*: cloning, expression, and transport differences. *Am J Physiol* 273: C257-C265, 1997.

211. **Ruknudin AM, Wei SK, Haigney MC, Lederer WJ and Schulze DH**. Phosphorylation and other conundrums of Na/Ca exchanger, NCX1. *Ann N Y Acad Sci* 1099: 103-118, 2007.

212. **Sahin-Toth M, Nicoll DA, Frank JS, Philipson KD and Friedlander M**. The cleaved N-terminal signal sequence of the cardiac Na^+-Ca^{2+} exchanger is not required for functional membrane integration. *Biochem Biophys Res Commun* 212: 968-974, 1995.

213. **Sakaue M, Nakamura H, Kaneko I, Kawasaki Y, Arakawa N, Hashimoto H, Koyama Y, Baba A and Matsuda T**. Na^+-Ca^{2+} exchanger isoforms in rat neuronal preparations: different changes in their expression during postnatal development. *Brain Res* 881: 212-216, 2000.

214. **Santacruz-Toloza L, Ottolia M, Nicoll DA and Philipson KD**. Functional analysis of a disulfide bond in the cardiac Na^+-Ca^{2+} exchanger. *J Biol Chem* 275: 182-188, 2000.

215. **Satoh H, Katoh H, Terada H and Hayashi H**. Involvement of Na^+/Ca^{2+} exchange in normal cardiac excitation-contraction coupling and in Ca^{2+} overload during ischemia and reperfusion. In: Miocardial ischemia and preconditioning, edited by Dhalla NS, Takeda N, Singh M and Lukas A. Boston: Kluwer Academic Publishers, 2003, p. 481-503.

216. **Satoh H, Mukai M, Urushida T, Katoh H, Terada H and Hayashi H**. Importance of Ca^{2+} influx by Na^+/Ca^{2+} exchange under normal and sodium-loaded conditions in mammalian ventricles *Mol Cell Biochem* 242: 11-17, 2003.

217. **Schafer C, Ladilov Y, Inserte J, Schafer M, Haffner S, Garcia-Dorado D and Piper HM**. Role of the reverse mode of the Na^+/Ca^{2+} exchanger in reoxygenation-induced cardiomyocyte injury. *Cardiovasc Res* 51: 241-250, 2001.

218. **Schillinger W, Fiolet JW, Schlotthauer K and Hasenfuss G**. Relevance of Na^+-Ca^{2+} exchange in heart failure. *Cardiovasc Res* 57: 921-933, 2003.

219. **Schouten VJ, Ter Keurs HE and Quaegebeur JM**. Influence of electrogenic Na/Ca exchange on the action potential in human heart muscle. *Cardiovasc Res* 24: 758-767, 1990.

220. **Schroder UH, Breder J, Sabelhaus CF and Reymann KG**. The novel Na^+/Ca^{2+} exchange inhibitor KB-R7943 protects CA1 neurons in rat hippocampal slices against hypoxic/hypoglycemic injury. *Neuropharmacology* 38: 319-321, 1999.

221. **Schulze DH, Muqhal M, Lederer WJ and Ruknudin AM**. Sodium/calcium exchanger (NCX1) macromolecular complex. *J Biol Chem* 278: 28849-28855, 2003.

222. **Schulze DH, Polumuri SK, Gille T and Ruknudin A**. Functional regulation of alternatively spliced Na+/Ca2+ exchanger (NCX1) isoforms. *Ann N Y Acad Sci* 976: 187-196, 2002.

223. **Schwarz EM and Benzer S**. *Calx*, a Na-Ca exchanger gene of *Drosophila melanogaster*. *Proc Natl Acad Sci U S A* 94: 10249-10254, 1997.

224. **Seki S, Taniguchi M, Takeda H, Nagai M, Taniguchi I and Mochizuki S**. Inhibition by KB-R7943 of the reverse mode of the Na^+/Ca^{2+} exchanger reduces Ca^{2+} overload in ischemic-reperfused rat hearts. *Circ J* 66: 390-396, 2002.

225. **Shannon TR, Hale CC and Milanick MA**. Interaction of cardiac Na-Ca exchanger and exchange inhibitory peptide with membrane phospholipids. *Am J Physiol* 266: C1350-C1356, 1994.

226. **Shieh BH, Xia Y, Sparkes RS, Klisak I, Lusis AJ, Nicoll DA and Philipson KD**. Mapping of the gene for the cardiac sarcolemmal Na^+-Ca^{2+} exchanger to human chromosome 2p21-p23. *Genomics* 12: 616-617, 1992.

227. **Shigekawa M, Katanosaka Y and Wakabayashi S**. Regulation of the cardiac Na^+/Ca^{2+} exchanger by calcineurin and protein kinase C. *Ann N Y Acad Sci* 1099: 53-63, 2007.

228. **Shiraga M, Tomiyama Y, Honda S, Suzuki H, Kosugi S, Tadokoro S, Kanakura Y, Tanoue K, Kurata Y and Matsuzawa Y**. Involvement of Na^+/Ca^{2+} exchanger in inside-out signaling through the platelet integrin αIIbβ3. *Blood* 92: 3710-3720, 1998.

229. **Sipido KR**. Calcium overload, spontaneous calcium release, and ventricular arrhythmias. *Heart Rhythm* 3: 977-979, 2006.

230. **Sipido KR, Bito V, Antoons G, Volders PG and Vos MA**. Na/Ca exchange and cardiac ventricular arrhythmias. *Ann N Y Acad Sci* 1099: 339-348, 2007.

231. **Sipido KR, Volders PG, de Groot SH, Verdonck F, Van De WF, Wellens HJ and Vos MA**. Enhanced Ca^{2+} release and Na/Ca exchange activity in hypertrophied canine ventricular myocytes : potential link between contractile adaptation and arrhythmogenesis. *Circulation* 102: 2137-2144, 2000.

232. **Sipido KR, Volders PG, Vos MA and Verdonck F**. Altered Na/Ca exchange activity in cardiac hypertrophy and heart failure: a new target for therapy? *Cardiovasc Res* 53: 782-805, 2002.

233. **Slodzinski MK, Juhaszova M and Blaustein MP**. Antisense inhibition of Na^+/Ca^{2+} exchange in primary cultured arterial myocytes. *Am J Physiol* 269: C1340-C1345, 1995.

234. **Sobolevsky AI and Khodorov BI**. Blockade of NMDA channels in acutely isolated rat hippocampal neurons by the Na^+/Ca^{2+} exchange inhibitor KB-R7943. *Neuropharmacology* 38: 1235-1242, 1999.

235. **Sokolow S, Manto M, Gailly P, Molgo J, Vandebrouck C, Vanderwinden JM, Herchuelz A and Schurmans S**. Impaired neuromuscular transmission and skeletal muscle fiber necrosis in mice lacking Na/Ca exchanger 3. *J Clin Invest* 113: 265-273, 2004.

236. **Spencer CI and Sham JS**. Effects of Na+/Ca2+ exchange induced by SR Ca2+ release on action potentials and afterdepolarizations in guinea pig ventricular myocytes. *Am J Physiol Heart Circ Physiol* 285: H2552-H2562, 2003.

237. **Szewczyk MM, Davis KA, Samson SE, Simpson F, Rangachari PK and Grover AK**. Ca^{2+}-pumps and Na^{+}-Ca^{2+}-exchangers in coronary artery endothelium versus smooth muscle. *J Cell Mol Med* 11: 129-138, 2007.

238. **Takahashi T, Takahashi K, Onishi M, Suzuki T, Tanaka Y, Ota T, Yoshida S, Nakaike S, Matsuda T and Baba A**. Effects of SEA0400, a novel inhibitor of the Na^{+}/Ca^{2+} exchanger, on myocardial stunning in anesthetized dogs. *European Journal of Pharmacology* 505: 163-168, 2004.

239. **Tanaka H, Nishimaru K, Aikawa T, Hirayama W, Tanaka Y and Shigenobu K**. Effect of SEA0400, a novel inhibitor of sodium-calcium exchanger, on myocardial ionic currents. *Br J Pharmacol* 135: 1096-1100, 2002.

240. **Tani M and Neely JR**. Na^{+} accumulation increases Ca^{2+} overload and impairs function in anoxic rat heart. *J Mol Cell Cardiol* 22: 57-72, 1990.

241. **Taniguchi S, Furukawa K, Sasamura S, Ohizumi Y, Seya K and Motomura S**. Gene expression and functional activity of sodium/calcium exchanger enhanced in vascular smooth muscle cells of spontaneously hypertensive rats. *J Cardiovasc Pharmacol* 43: 629-637, 2004.

242. **Thurneysen T, Nicoll DA, Philipson KD and Porzig H**. Sodium/calcium exchanger subtypes NCX1, NCX2 and NCX3 show cell-specific expression in rat hippocampus cultures. *Brain Res Mol Brain Res* 107: 145-156, 2002.

243. **Tortiglione A, Pignataro G, Minale M, Secondo A, Scorziello A, Di Renzo GF, Amoroso S, Caliendo G, Santagada V and Annunziato L**. Na+/Ca2+ exchanger in Na+ efflux-Ca2+ influx mode of operation exerts a neuroprotective role in cellular models of in vitro anoxia and in vivo cerebral ischemia. *Ann N Y Acad Sci* 976: 408-412, 2002.

244. **Trosper TL and Philipson KD**. Effects of divalent and trivalent cations on Na^{+}-Ca^{2+} exchange in cardiac sarcolemmal vesicles. *Biochim Biophys Acta* 731: 63-68, 1983.

245. **Venetucci LA, Trafford AW, O'Neill SC and Eisner DA**. Na/Ca exchange: regulator of intracellular calcium and source of arrhythmias in the heart. *Ann N Y Acad Sci* 1099: 315-325, 2007.

246. **Villa-Abrille MC, Sidor A and O'Rourke B**. Insulin effects on cardiac Na^{+}/Ca^{2+} exchanger activity: role of the cytoplasmic regulatory loop. *Journal of Biological Chemistry* 283: 16505-16513, 2008.

247. **Volders PG, Vos MA, Szabo B, Sipido KR, de Groot SH, Gorgels AP, Wellens HJ and Lazzara R**. Progress in the understanding of cardiac early afterdepolarizations and torsades de pointes: time to revise current concepts. *Cardiovasc Res* 46: 376-392, 2000.

248. **Wakabayashi S and Goshima K**. Kinetic studies on sodium-dependent calcium uptake by myocardial cells and neuroblastoma cells in culture. *Biochim Biophys Acta* 642: 158-172, 1981.

249. **Wakimoto K, Kobayashi K, Kuro O, Yao A, Iwamoto T, Yanaka N, Kita S, Nishida A, Azuma S, Toyoda Y, Omori K, Imahie H, Oka T, Kudoh S, Kohmoto O, Yazaki Y, Shigekawa M, Imai Y, Nabeshima Y and Komuro I**. Targeted Disruption of Na^+/Ca^{2+} Exchanger Gene Leads to Cardiomyocyte Apoptosis and Defects in Heartbeat. *J Biol Chem* 275: 36991-36998, 2000.

250. **Wang J, Zhang XQ, Ahlers BA, Carl LL, Song J, Rothblum LI, Stahl RC, Carey DJ and Cheung JY**. Cytoplasmic tail of phospholemman interacts with the intracellular loop of the cardiac Na^+/Ca^{2+} exchanger. *J Biol Chem* 281: 32004-32014, 2006.

251. **Watano T, Kimura J, Morita T and Nakanishi H**. A novel antagonist, No. 7943, of the Na^+/Ca^{2+} exchange current in guinea-pig cardiac ventricular cells. *Br J Pharmacol* 119: 555-563, 1996.

252. **Weber CR, Piacentino V, III, Ginsburg KS, Houser SR and Bers DM**. Na^+-Ca^{2+} exchange current and submembrane $[Ca^{2+}]$ during the cardiac action potential. *Circ Res* 90: 182-189, 2002.

253. **Weber CR, Piacentino V, III, Houser SR and Bers DM**. Dynamic regulation of sodium/calcium exchange function in human heart failure. *Circulation* 108: 2224-2229, 2003.

254. **Wei SK, Ruknudin A, Hanlon SU, McCurley JM, Schulze DH and Haigney MC**. Protein kinase A hyperphosphorylation increases basal current but decreases β-adrenergic responsiveness of the sarcolemmal Na^+-Ca^{2+} exchanger in failing pig myocytes. *Circ Res* 92: 897-903, 2003.

255. **Westerblad H, Lee JA, Lannergren J and Allen DG**. Cellular mechanisms of fatigue in skeletal muscle. *Am J Physiol* 261: C195-C209, 1991.

256. **Yamashita J, Itoh M, Kuro T, Kobayashi Y, Ogata M, Takaoka M and Matsumura Y**. Pre- or post-ischemic treatment with a novel Na^+/Ca^{2+} exchange inhibitor, KB-R7943, shows renal protective effects in rats with ischemic acute renal failure. *J Pharmacol Exp Ther* 296: 412-419, 2001.

257. **Yamashita J, Kita S, Iwamoto T, Ogata M, Takaoka M, Tazawa N, Nishikawa M, Wakimoto K, Shigekawa M, Komuro I and Matsumura Y**. Attenuation of ischemia/reperfusion-induced renal injury in mice deficient in Na^+/Ca^{2+} exchanger. *J Pharmacol Exp Ther* 304: 284-293, 2003.

258. **Yamashita J, Ogata M, Takaoka M and Matsumura Y**. KB-R7943, a selective Na^+/Ca^{2+} exchange inhibitor, protects against ischemic acute renal failure in mice by inhibiting renal endothelin-1 overproduction. *J Cardiovasc Pharmacol* 37: 271-279, 2001.

259. **Yang Z, Pascarel C, Steele DS, Komukai K, Brette F and Orchard CH**. Na+-Ca2+ exchange activity is localized in the T-tubules of rat ventricular myocytes. *Circ Res* 91: 315-322, 2002.

260. **Yoshiyama M, Nakamura Y, Omura T, Hayashi T, Takagi Y, Hasegawa T, Nishioka H, Takeuchi K, Iwao H and Yoshikawa J**. Cardioprotective effect of SEA0400, a selective inhibitor of the Na^+/Ca^{2+} exchanger, on myocardial ischemia-reperfusion injury in rats. *J Pharmacol Sci* 95: 196-202, 2004.

261. **Zhang S, Yuan JX, Barrett KE and Dong H**. Role of Na^+/Ca^{2+} exchange in regulating cytosolic Ca^{2+} in cultured human pulmonary artery smooth muscle cells. *Am J Physiol Cell Physiol* 288: C245-C252, 2005.